

FOR REFERENCE

NOT TO BE TAKEN FROM THIS ROOM

NONLINEAR FINITE ELEMENT ANALYSIS
OF
ALTINKAYA DAM

hepsi ustad pander

1985

ALI YAZICIOĞLU

Lacivort

November, 1985

Boğaziçi University

1985)

**NONLINEAR FINITE ELEMENT ANALYSIS
OF
ALTINKAYA DAM**

by

ALİ YAZICIOĞLU

B.Sc. in C.E., Karadeniz Technical University, 1982

Submitted to the Institute for Graduate Studies in
Science and Engineering in Partial Fulfillment of
the Requirements for the Degree of
Master of Science
in
Civil Engineering

Bogazici University Library



39001100314841

14


Boğaziçi University

November, 1985

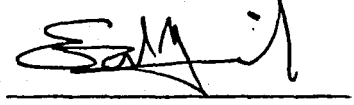
NONLINEAR FINITE ELEMENT ANALYSIS
OF
ALTINKAYA DAM

APPROVED BY :

Prof.Dr.H.Turan DURGUNOĞLU
(Thesis Supervisor)



Doç.Dr.Erol GÖLER



Doç.Dr.Vural ALTIN



Approval Date :

12. 11. 1985

ACKNOWLEDGEMENTS

I would like to express my sincere gratitude to those who have assisted me during the course of this study, especially to my thesis supervisor Prof.Dr.H.Turan Durgunođlu for his helpful suggestions, guidance and constructive criticism.

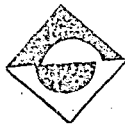
I am greatly indebted to the officials of the State Hydraulic Works (DSI) in charge of the Lower Kızılırmak Project and also to the staff of the consulting firm SU-IŞ for supplying data necessary for the analysis of Altınkaya Dam.

I would wish to thank to all Bođaziçi University Computer Center personnel for making facilities available to me.

I am also grateful to Miss Gül Tuncel for her patience, care and conscientiousness in typing the manuscript.

Istanbul, November 1985

Ali Yazıcıođlu



ABSTRACT

The behavior of earth and rockfill dams during construction is investigated in this study. In particular, attention is given to the prediction of stresses and deformations developed within Altınkaya Dam during construction.

For this purpose, the computer program developed for analyzing the earth and rockfill dams is employed. The analyses are performed by finite element methods with linear or nonlinear material properties and assuming plane strain, isotropic conditions. The real soil behavior is represented in the analysis by means of hyperbolic stress-strain parameters and the incremental analysis procedure is followed to simulate the actual construction sequence.

A parametric study is also conducted for determining the effects of the stress-strain parameters on the behavior of Altınkaya Dam and reasonable parameter ranges are established so as to minimize the stresses and displacements within the embankment .

ÖZET

Bu çalışmada, kaya ve toprak dolgu barajların inşa sırasındaki davranışları incelenmiştir. Özellikle, Altınkaya Barajı'nda inşa sırasında meydana gelebilecek gerilme ve deformasyonlar tahmin edilmeye çalışılmıştır.

Bu amaçla, kaya ve toprak barajların analizlerini yapmak üzere geliştirilmiş bir bilgisayar programından yararlanılmıştır. Analizlerde sonlu elemanlar yöntemi kullanılmış ve malzemenin izotropik ve düzlem şekil değiştirme yaptığı kabul edilmiştir. Ayrıca, malzemenin lineer veya lineer olmayan davranışı gözönüne alınmıştır. Zeminin gerçek davranışı, hiperbolik gerilme-şekil değiştirme parametreleri kullanılarak dikkate alınmış ve baraj gövdesinin inşa safhaları gövdenin tabakalar halinde inşa edildiğini kabul eden bir analiz prosedürü ile tanımlanmaya çalışılmıştır.

Bunlardan başka, malzemenin gerilme-şekil değiştirme parametrelerinin, Altınkaya Barajı'nın davranışı üzerindeki etkileri incelenmiş, gerilme ve deformasyonları en aza indirebilecek parametre aralıkları belirlenmiştir.

TABLE OF CONTENTS

	<u>Page</u>
Acknowledgements	iii
Abstract	iv
Özet	v
List of Figures	vi
List of Tables	vii
List of Symbols	viii
I. INTRODUCTION	1
2. METHOD OF ANALYSIS	
2.1 Introduction	7
2.2 Finite Element Method	8
2.3 Incremental Construction Procedure	10
2.4 Nonlinear Material Analysis	11
2.5 Types of Finite Element Procedure	12
2.6 Computer Program	13
2.7 Summary	14

	<u>Page</u>
3. HYPERBOLIC STRESS-STRAIN PARAMATERS	
3.1 Introduction	15
3.2 Hyperbolic Stress-Strain Relationships	16
3.2.1 Nonlinear Stress-Strain Relations	16
3.2.2 Effect of Confining Pressure on E_i and $(\sigma_1 - \sigma_3)_{ult}$	19
3.2.3 Relationship Between Tangent Deformation Modulus and the Stresses	22
3.2.4 Inelastic Material Behavior	22
3.2.5 Nonlinear Volume Change Behavior of Soils	24
3.2.6 Relationship between v_t and the stresses	26
3.3 Evaluation of Hyperbolic Stress-Strain Parameters from Laboratory Test Results	28
3.3.1 Selecting Data	28
3.3.2 Evaluation of C and ϕ for Cohesive Soils	28
3.3.3 Evaluation of ϕ_o and $\Delta\phi$ for Cohesionless Soils	30
3.3.4 Evaluation of K , n and R_f	33
3.3.5 Evaluation of K_{ur}	40
3.3.6 Evaluation of G , F and d	40
3.4 Factors Affecting the Hyperbolic Stress-Deformation Parameters	42
3.5 Summary	44
4. FINITE ELEMENT ANALYSES OF ALTINKAYA DAM	
4.1 Introduction	47
4.2 Description of Altinkaya Dam	48
4.3 Finite Element Idealization of Altinkaya Dam	53
4.4 Properties of the Materials in Altinkaya Dam	53
4.5 Nonlinear Finite Element Analysis of Altinkaya Dam	60
4.5.1 Settlements (Vertical Displacements) in Altinkaya Dam	60
4.5.2 Horizontal Displacements in Altinkaya Dam	63
4.5.3 Stresses in Altinkaya Dam	65

	<u>Page</u>
4.6 Build-up Analysis of Altinkaya Dam	71
4.7 Comparison of the Results of the Nonlinear and Build-up Analyses of Altinkaya Dam	72
4.8 Recommendations for Possible Instrument Locations	78
4.9 Summary and Conclusions	79
5. PARAMETRIC STUDY FOR STRESSES AND DEFORMATIONS OF ALTINKAYA DAM	
5.1 Introduction	80
5.2 The Values of Parameters Used in the Analyses	81
5.3 The Analyses Performed	81
5.4 Effect of Core Material	85
5.5 Effect of Shell Material	89
5.6 Reasonable Values of K and n for Altinkaya Dam	96
5.7 Summary	97
6. SUMMARY AND CONCLUSIONS	100
REFERENCES	104
APPENDICES	
. Appendix A	107
. Appendix B	111

LIST OF FIGURES

<u>Fig No</u>		<u>Page</u>
1.1	Cracking Patterns in Embankment Dams (Thomas, 1976)	3
1.2	Modes of Load Transfer (Squier, 1970)	5
3.1	Hyperbolic Representation of a Stress-Strain Curve (Kondner, 1963)	17
3.2	Variation of Initial Tangent Modulus With Confining Pressure (Duncan, Wong, 1974)	20
3.3	Variation of Strength With Confining Pressure (Duncan, Wong, 1974)	21
3.4	Unloading-Reloading Modulus	23
3.5	Hyperbolic Axial Strain-Radial Strain Curves (Duncan, Wong, 1974)	25
3.6	Variation of Initial Tangent Poisson's Ratio With Confining Pressure (Duncan, Wong, 1974)	27
3.7	Adjustment of Stress-Strain Curves (Duncan, Wong, 1974)	29
3.8	Mohr Envelopes For Oroville Dam Core Material (Duncan, Wong, 1974)	31
3.9	Modified Mohr Envelope For UU-Triaxial Tests on New Don Pedro Dam Core Material (Duncan, Wong, 1974)	32
3.10	Mohr Envelope For CD-Triaxial Tests On Oroville Dam Shell Material (Duncan, Wong, 1974)	34
3.11	Variation of Friction Angle With Confining Pressure For Oroville Dam Shell Material (Duncan, Wong, 1974)	35
3.12	Replotted Stress-Strain and Volume Change Curves For Oroville Dam (Duncan, Wong, 1974)	37
3.13	Transformed Stress-Strain Plot For Oroville Dam Shell Material (Duncan, Wong, 1974)	38

LIST OF FIGURES (cont'd)

<u>Fig No</u>		<u>Page</u>
3.14	Variation of Initial Tangent Modulus With Confining Pressure For Oroville Dam Shell Material (Duncan, Wong, 1974)	39
3.15	Variation of Poisson's Ratio With Radial Strain For Oroville Dam Shell Material (Duncan,Wong,1974)	41
3.16	Variation of Initial Poisson's Ratio With Confining Pressure For Oroville Dam Shell Material(Duncan,Wong, 1974)	43
4.1	Location Map of Altınkaya Dam	49
4.2	Plan View of Altınkaya Dam	50
4.3	Typical Design Section and Profile of Altınkaya Dam	51
4.4	Views Showing The Fill Placement in Altınkaya Dam	52
4.5	Finite Element Mesh For Altınkaya Dam	54
4.6	Major Zones of Altınkaya Dam Considered in FEM Analysis	55
4.7	Gradation Curves For the Materials Used in Altınkaya Dam (Data from State Hydraulic Works of Turkey, DSI)	57
4.8	Mohr Envelope for UU-Triaxial Tests on Altınkaya Dam Core Material. (Data from State Hydraulic Works of Turkey,DSI)	59
4.9	Contours of Settlement in Altınkaya Dam (Nonlinear Analysis)	62
4.10	Contours of Horizontal Displacement in Altınkaya Dam (Nonlinear Analysis)	64
4.11	Contours of Major Principal Stress in Altınkaya Dam (Nonlinear Analysis)	66
4.12	Contours of Minor Principal Stress in Altınkaya Dam (Nonlinear Analsis)	68
4.13	Contours of Maximum Shear Stress in Altınkaya Dam (Nonlinear Analysis)	69
4.14	Contours of Mobilized Strength in Altınkaya Dam (Nonlinear Analysis)	70
4.15	Contours of Settlement in Altınkaya Dam (Build-up Analysis)	73
4.16	Contours of Horizontal Displacement in Altınkaya Dam (Build-up Analysis)	74
4.17	Contours of Major Principal Stress in Altınkaya Dam (Build-up Analysis)	75

LIST OF FIGURES (cont'd)

<u>Fig No</u>		<u>Page</u>
4.18	Contours of Minor Principal Stress in Altınkaya Dam (Build-up Analysis)	76
4.19	Contours of Maximum Shear Stress in Altınkaya Dam (Build-up Analysis)	77
5.1	Variation of Modulus Number With Modulus Exponent For Core Material of Altınkaya Dam	83
5.2	Variation Of Modulus Number With Modulus Exponent For Shell Material of Altınkaya Dam	84
5.3	Plot of Maximum Settlement Versus Modulus Number of Core Material (Shell, GW-2)	87
5.4	Plot of Maximum Settlement Versus Modulus Number of Core Material (Shell, GW-1)	88
5.5	Plot of Maximum Settlement Versus Modulus Number of Shell Material (Core, CL-11D)	92
5.6	Plot of Maximum Settlement Versus Modulus Number of Shell Material (Core, CL-13E)	93
5.7	Plot of Maximum Settlement Versus Modulus Number of Shell Material (Core, CL-5B)	94
5.8	Maximum Stress and Displacement Locations in Altınkaya Dam	95
5.9	Variation of Modulus Number, K, in Granular Soils Under Drained Conditions (Kulhawy, 1969)	98

LIST OF TABLES

		<u>Page</u>
Table 3.1	Summary of the Hyperbolic Parameters	46
Table 4.1	Material Properties of Altınkaya Dam (Data From State Hydraulic Works of Turkey, DSI)	56
Table 4.2	Hyperbolic Stress-Strain Parameters Used in the Nonlinear FEM Analysis of Altınkaya Dam	61
Table 4.3	Values of E and ν used in the Build-up Analysis Altınkaya Dam	71
Table 5.1	Hyperbolic Stress-Strain Parameters for Various Core and Shell Materials	82
Table 5.2	Maximum Displacements and Stress Concentrations for Constant Shell Case	86
Table 5.3	Maximum Displacements and Stress Concentrations for Constant Core Case	90
Table A.1	Stress-Strain and Strength Parameters for Soils Tested Under Drained Conditions (Duncan, Wong, 1974)	108
Table A.2	Stress-Strain and Strength Parameters for Soils Tested Under Unconsolidated-Undrained Conditions (Duncan, Wong, 1974)	109

LIST OF SYMBOLS

<u>Symbol:</u>	<u>Meaning</u>
a	reciprocal of initial tangent modulus
b	reciprocal of hyperbolic deviator stress at failure
c	cohesion intercept
d	rate of change of initial tangent poisson ratio with strain
{ d }	nodal displacement matrix
D	grain size
D _r	relative density
E	deformation modulus
E'	modified deformation modulus
E _j	initial tangent modulus
E _t	tangent modulus
e ₀	initial void ratio
F	rate of change of initial tangent poisson ratio with confining pressure
{ F }	equivalent load matrix
G	initial tangent poisson ratio at one atmosphere
K	modulus number
K _{ur}	unloading-reloading modulus number
[K]	total stiffness matrix

LIST OF SYMBOLS - (cont'd)

<u>Symbol</u>	<u>Meaning</u>
n	modulus exponent
P_a	atmospheric pressure
PI	plasticity index
R_f	failure ratio
S_r	degree of saturation
W_L	liquid limit
W_{opt}	optimum water content
W_p	plastic limit
α	intercept of modified Mohr envelope
γ_d	dry unit weight
γ_{dmax}	maximum dry unit weight
$\Delta\epsilon_x, \Delta\epsilon_y, \Delta\gamma_{xy}$	change in strains
$\Delta\sigma_x, \Delta\sigma_y, \Delta\tau_{xy}$	increments of stresses during a step of the analysis
$\Delta\phi$	change in friction angle
ϵ_r	radial strain
ϵ_v	volumetric strain
ϵ_a	axial strain
ϕ	friction angle
ϕ_0	friction angle at one atmosphere
ψ	the slope angle of modified Mohr envelope
ν	Poisson ratio
ν'	modified Poisson ratio
ν_i	initial tangent Poisson ratio
ν_t	tangent Poisson ratio
σ_1	major principal stress
σ_3	minor principal stress

LIST OF SYMBOLS(cont'd)

<u>Symbol</u>	<u>Meaning</u>
$(\sigma_1 - \sigma_3)_f$	deviator stress at failure
$(\sigma_1 - \sigma_3)_{ult}$	ultimate deviator stress
τ_{max}	maximum shear stress

CHAPTER I

INTRODUCTION

Continuing advances in soil engineering and earth-moving equipments, and the easily available construction materials in the most of the dam sites have made the construction of earth and rockfill dams feasible and preferable throughout the world. Besides these and many other advantages of rockfill dams, there are some problems concerning the design and construction of earth and rockfill dams. These problems have been grouped by the ASCE Committee on Earth and Rockfill Dams (1967) as follows:

1. Strength and volume change characteristics of gravel and rockfill materials under high confining pressures.
2. Compaction methods in coarse gravels and rockfills.
3. Control of compaction in coarse gravels and rockfills.
4. Low-cost admixtures for improving characteristics of soils.
5. Slope protection of earth dams.
6. Factors to cause sliding of rockfill on foundation contact surfaces.
7. Prediction of pore pressures in compacted cohesive soils.
8. Dynamic behaviour of embankments in earthquake regions.
9. Stress and deformation measurements in embankments.
10. Cracking within embankments.

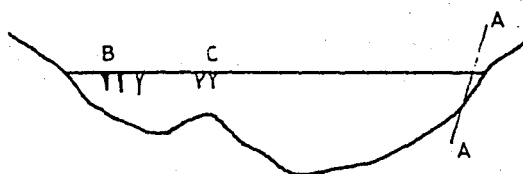
Among these problems, stresses deformations and cracking within embankments during construction are of special importance in this study.

According to Justo(1973) and also Thomas (1976), cracks which frequently occur in earthfill dams and in cores of rockfill dams during and after construction can be classified into four groups. Cracks normal to the axis usually appear in the crest of the dam as seen in Fig.1.1.A. These are primarily due to non-uniform settlement of the fill and may occur as tension failures(B) near the embankment or (C) over a rock prominence left in the foundation or as a shear failure (A-A) over a steep abutment or adjacent to a construction road. The extent of these cracks will depend upon the magnitude of non-uniform settlement of the dam and the tension cracks can be sometimes the most serious.

The second types of cracks are the cracks which occur parallel to the axis of the dam (Fig.1.1.B) and is often apparent in the transition zones on either side of the core. They usually result from differential settlement between the core and rockfill shells. Generally longitudinal cracks will not be dangerous, so long as they are discovered and properly backfilled.

Oblique cracking may also occur across the crest (Fig.1.1.C); it usually be associated with unsymmetrical sites and will be normal to the direction of maximum displacements. They are tension type cracks and should be considered seriously. Horizontal cracking which is the fourth group can occur in the core due to saturation of it and unequal settlement of the core and shells. This type of cracks may be serious because they don't usually appear on the surface.

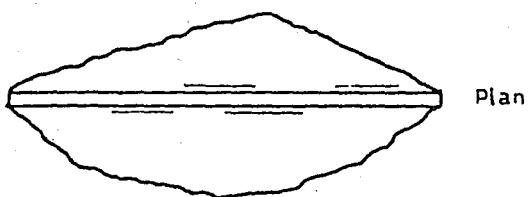
On the other hand, due to relative displacements of two zones , load may be transferred from one zone to another or from one location to



(A) Cracking normal to Dam axis

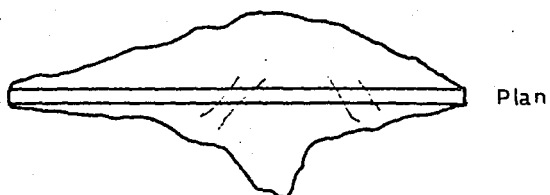
A-A Shear crack

B Tension cracks



Plan

(B) Cracking parallel to Dam axis



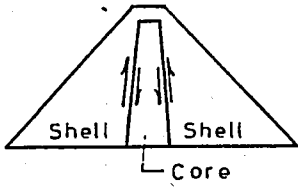
Plan

(C) Cracking oblique to Dam axis

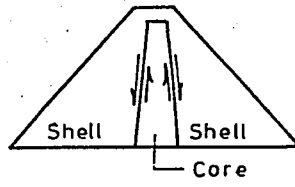
Fig. 1.1 Cracking Patterns in Embankment Dams (Thomas, 1976)

another in the embankment. Squier (1970) has described four modes of load transfer occurring in dams such as shown in Fig.1.2. In mode A, load is transferred from the core to the shells as a result of greater downward displacements of the core with respect to the shells. However, in mode B, transfer of load from the shells to the core occurs as a result of greater downward displacement of the shells with respect to the stiff core. While both of these load transfers may occur during construction, the load transfer may also be altered and immediate compressions may occur in the upstream rockfill with the reservoir filling. As a consequence of these compressions the saturated upstream shell may settle and move downward with respect to the core (Mode C). Load transfer mode D, as shown in Fig. 1.2, develops from differential settlements in the core and is most likely to occur at an abrupt change in slope of the embankment. The transfer of load to the abutments results in greater compressions and displacements of the core near the abutment slopes than those that would occur because of overburden pressures alone.

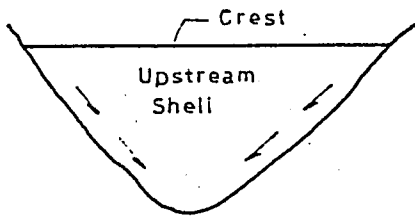
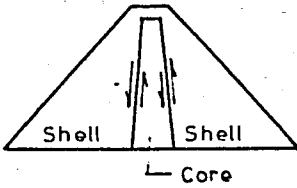
It is apparent that the stresses and movements within embankments have significant effects on the behaviour of embankments so the prediction of these values prior to construction becomes the engineer's main concern in the design of embankment dams. Therefore during the course of this study, the attention was focused on the behaviour of rockfill embankments during construction, i.e the prediction of stresses and movements within the embankments so that it might be shown whether cracking would occur, or whether the embankment would be safe during construction. For this purpose, the finite element method of analysis which is described in the following chapter was performed on Altinkaya Dam which was analyzed in this thesis. The real behaviour of soil such as nonlinearity, stress-dependency and inelasticity was introduced into



MODE A
 Modulus Core <
 Modulus Shell

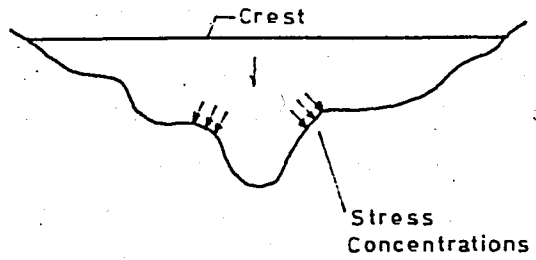


MODE B
 Modulus Core >
 Modulus Shell



Valley Cross Section

MODE C
 Saturation Of
 Upstream Shell



Valley Cross Section

MODE D
 Load Transfer
 To Abutment

Fig. 1.2 Modes of Load Transfer (Squier, 1970)

the analyses using the hyperbolic stress-strain parameters as described in Chapter 3. The computer program LSBUILD which is capable of performing analyses of both homogeneous and zoned embankments with linear and nonlinear material properties was used in the analyses and the results of two types of analyses which are namely the nonlinear and build - up analyses are presented in Chapter 4. Moreover, the effect of deformation modulus parameters on the behavior of Altinkaya Dam was investigated and for possible ranges for these parameters, the results are presented in Chapter 5.

CHAPTER 2

METHOD OF ANALYSIS

2.1. INTRODUCTION

Numbers of analytical methods such as infinite wedge analyses, photo-elastic analyses of gelatin models and the finite difference method have been used in practice to analyze the stresses and displacements in homogeneous embankments with the simple boundaries. As the problem of analysis becomes complex including in homogeneity, complex geometry, various loading conditions, and nonlinear soil behavior, the finite element method may be applicable due to its flexibility and generality. Some of the previous finite element analyses of embankments are presented below:

1. Clough and Woodward (1967) and Finn (1967) have performed the analyses of homogeneous embankments with linear and nonlinear material properties.
2. Kulhawy (1969) has performed the analyses of zoned and homogeneous embankments with nonlinear material properties.
3. Duncan and Wilson(1973) have performed the three dimensional finite element analyses of dams.
4. Walker and Duncan (1984) have analyzed the lateral bulging of earth dams.

In the following sections, the basic concepts of finite element method will be reviewed. In addition, types of analyses and procedures used in finite element method will be explained in detail and the computer program LSBUILD will be described.

2.2. FINITE ELEMENT METHOD

A general definition of the finite element method is an analysis method of a structural system which is represented as an assemblage of a finite number of nodal points. When this concept is applied to an elastic continuum, the number of possible elements and connections among them becomes infinite. There is thus a need for an idealization of the continuum into a structural system with finite discrete elements. This approach and approximation have shown to be acceptable.

The solution of finite element method depends on the accurate determination of the unknown nodal displacements. The basic equation which yields their solution is the one used in the stiffness matrix method of analysis.

$$\{F\} = [K]\{d\} \quad \dots (2.1)$$

where $\{F\}$ is the equivalent load matrix which is obtained by lumping the edge and element loads at the nodes, $\{d\}$ is the unknown nodal displacement matrix, and $[K]$ is the total stiffness matrix of the system. It is obtained by the superposition of the individual element stiffness matrices.

The finite element method have five major steps to perform to obtain a solution for the given problem. They can be obtained as follow;

1. The continuum is divided by imaginary lines or surfaces into

a number of elements. This requires the selection of the type and size of the finite elements to generate the mesh of the system.

2. Generation of the stiffness matrix quantities and the force matrix quantities for the elements.
3. Superposition of the element stiffness and force matrices to develop the stiffness and force matrices of the total structural system.
4. Determination of the unknown nodal displacements of the problem by the solution of the system of linear equations (Eq.2.1) obtained using the equilibrium conditions at the nodes.
5. Computations of all other required values such as stresses and strains associated with the problem.

Usually the accuracy and effectiveness of the finite element method will depend on the type and the number of elements used in the mesh generation. The proper mesh depends on the geometry and the nature of the problem.

In this study, a quadrilateral element consisting of two linear-strain triangular finite elements is chosen. The strain within this element varies linearly whereas the strains on the boundaries of the element are constant in order to secure the continuity of displacement across element boundaries. It has been proven that this type of element is more accurate and efficient for such problems involved in this study than constant strain triangles (Kulhawy 1969).

Moreover, the plane strain condition which assumes the stresses in a direction perpendicular to the x-y plane as nonzero is considered. For this case, the modulus of elasticity and the poisson's ratio values

are modified and are introduced as follow,

$$E = \frac{E}{1-\nu^2} \quad \dots(2.2)$$

$$\nu^1 = \frac{\nu}{1-\nu} \quad \dots(2.3)$$

2.3. INCREMENTAL CONSTRUCTION PROCEDURE

The finite element analysis can be adopted easily to take into account of the incremental construction procedure. The method of incremental construction analysis was first applied in the analysis of temperature and creep effects in the construction of concrete gravity dams. (King 1965), Raphael , Clough (1965) . In such analysis, it is necessary that the finite element idealization be arranged in horizontal layers corresponding to the construction lifts. The analysis then involves the evaluation of stresses and displacements in a succession of structures corresponding to the various stages of construction to be considered. For example, in the first step only the lowest layer of elements would be considered. The stiffness of these elements and the dead weight forces will be evaluated, and then the stresses, strains and the displacements developed in this lowest layer due to its own weight are computed. By repeating this procedure for each layer, the stresses, strains and the displacements developed throughout the embankment as a result of the new increments of load induced by placement of each new layer are calculated, these stress, strain and displacement are then added to those obtained for the preceding increment.

The accuracy of the results that are obtained will depend, of course, on the size of the increments considered, but experience has

indicated that relatively coarse construction increments will yield good results in the analysis of earth dams (Clough, Woodward 1967).

2.4 NONLINEAR MATERIAL ANALYSIS

Two different procedures have been used for approximating the nonlinear behaviour of soils in the past. These are namely the step-by-step (incremental) procedure and the iteration procedure.

In the iteration procedure, the initial values of E and ν are assumed and an analysis is performed. Then the stresses and strains corresponding to the values of E and ν obtained after the analysis are compared to those assumed. If they differ a new analysis is performed assuming new E and ν values. This procedure is repeated until the assumed E and ν values correspond with the calculated ones.

However, in the step-by-step (incremental) procedure as described earlier, a change in loading condition is approximated by a series of linear increments which successfully simulates the construction sequence. After each new lift is applied, the total stress state developed up to that time is determined. The stiffnesses of the elements must all be re-evaluated on the basis of soil properties appropriate to the new stress state before the next incremental analysis may be carried out. Therefore, when the incremental construction history is considered in the analysis, it is a relatively simple matter to account also for the effects of nonlinear material properties. In this study, the step-by-step procedure is used in the finite element analysis since any form of material nonlinearity can also be considered in this procedure.

2.5 TYPES OF FINITE ELEMENT PROCEDURES

Due to the generality and flexibility of the finite element method, it is easy to follow different types of procedures in the analyses of homogeneous and zoned embankments. These can be summarized as follows:

1. Gravity Turn-on Analysis: The construction sequence is ignored, gravity forces are applied throughout the embankment at the same time using constant values of modulus and the poisson ratio.
2. Build-up Analysis: The incremental construction procedure is followed by simulating the building of dam in layers and constant values of modulus and the poisson ratio are used.
3. The incremental construction procedure is followed but nonlinear values of modulus are used keeping the value of poisson ratio constant.
4. Nonlinear Analysis: The incremental construction procedure is again followed using both the nonlinear values of modulus and the poisson ratio.

Kulhawy (1969) has shown that, although the results of these analyses are somewhat different than each other, the values of displacements computed by using different finite element procedures will be approximately the same if the appropriate values of modulus and poisson ratio are introduced into the analysis and the stresses will also be approximately the same provided that the appropriate value of poisson ratio is used.

During the course of this study, two types of analyses which are namely, the nonlinear FEM analysis and the build-up analysis have been conducted on Altinkaya Dam and the results have been compared to each other.

2.6 COMPUTER PROGRAM

The computer program LSBUILD which is given in Appendix B has been developed by Kulhawy using the general programming concepts, the solution techniques of Wilson, and the incremental loading concepts of King which were subsequently modified by Woodward. The main purpose of this program is to compute the stresses, strains and displacements developed within homogeneous or zoned embankments during construction. It uses the finite element technique as described earlier and assumes plane strain and isotropic conditions.

The program LSBUILD which is capable of treating linear or non-linear hyperbolic material properties consists of six subroutines. The subroutine LAYOUT reads and prints the input data, computes the initial foundation stresses and the initial elastic properties for the elements. The subroutine LSSTIF develops the master stiffness matrix of the entire structure calling the subroutine LSQUAD for each quadrilateral element to set up the stiffness matrix of each element. It also modifies the stiffness matrix for given boundary conditions. The subroutine LST8 is called by LSQUAD for each quadrilateral element and sets up the stiffness matrix for an eight degrees of freedom linear strain triangular element. It is called twice, once for each of the two triangles comprising the quadrilateral element. The system of equations are solved by the subroutine BANSOL for the unknown nodal point displacements using Gaussian elimination technique. Finally, the subroutine LSRESUL computes and prints the stresses, strains and displacement in the structure at the end of each construction increment and evaluates the nonlinear material properties of each element for the next increment. LSQUAD is also called by LSRESUL for each quadrilateral element for the stress and strain computations.

2.7 SUMMARY

In this chapter, the basic concepts and the applicability of the finite element technique to stress-deformation problems has been summarized briefly. In particular, the attention was given to the analyses of embankment dams and two types of analyses procedures simulating the real construction sequence were discussed. It can be stated that the incremental analysis procedure can be used in the finite element analysis of embankments conveniently as any form of material nonlinearity can be easily incorporated in this procedure.

The computer program LSBUILD which has the capability of performing both the analyses of homogeneous and zoned embankments was also introduced. This program uses the finite element technique considering the plane strain condition, and follows the incremental construction procedure.

CHAPTER 3

HYPERBOLIC STRESS-STRAIN PARAMETERS

3.1 INTRODUCTION

In soil engineering, due to the availability of the powerful numerical analytical techniques such as the finite element method and with the development of high-speed, large capacity computers, it becomes feasible to perform analyses of stresses and deformations in earth and rockfill embankments. But, in order to perform these analyses reasonably, it is necessary to be able to describe the real behavior of soil, namely nonlinearity, inelasticity and stress-dependency in quantitative terms and to develop techniques for incorporating these into the analyses.

A simplified, practical hyperbolic stress-strain relationship for soils (first used by Duncan and Chang (1970)) which is convenient for use with the finite element method of analysis is described in this chapter. They are obtained using the data available from the standard laboratory test, and the soil characteristics can be represented reasonably. The hyperbolic parameters determined for about 135 different soils are also summarized in Appendix A (Duncan, Wong, 1974).

3.2 HYPERBOLIC STRESS-STRAIN RELATIONSHIPS

The incremental finite element analyses assume that the stress-strain variation is not linear throughout the analyses. Therefore such analyses could be done using hyperbolic relationship between stresses and strains treating the stress-strain behavior of the soil as being linear in each increment of the analyses. For plane strain conditions, assuming that the Hooke's Law is valid for the stress-strain relationship, it could be written as :

$$\begin{Bmatrix} \Delta\sigma_x \\ \Delta\sigma_y \\ \Delta\tau_{xy} \end{Bmatrix} = \frac{E_t}{(1+\nu_t)(1-\nu_t)} \begin{bmatrix} (1-\nu_t) & \nu_t & 0 \\ \nu_t & (1-\nu_t) & 0 \\ 0 & 0 & (1-2\nu_t)/2 \end{bmatrix} \begin{Bmatrix} \Delta\varepsilon_x \\ \Delta\varepsilon_y \\ \Delta\gamma_{xy} \end{Bmatrix} \quad \dots(3.1)$$

where $\Delta\sigma_x$, $\Delta\sigma_y$, $\Delta\tau_{xy}$: Increments of stresses during a step of the analysis.

E_t : Tangent value of deformation modulus.

ν_t : Tangent value of Poisson's ratio.

As the incremental procedure has been chosen for the analysis, the values of both E_t and ν_t appeared in equation (3.1) are re-evaluated in each element corresponding to the computed stress values in that element so that the behavior of soil such as nonlinearity, stress-dependency and inelasticity could be incorporated in the analysis.

3.2.1 NONLINEAR STRESS-STRAIN RELATIONS

Kondner (1963) and his colleagues have proposed the stress-strain curves represented by hyperbolas as shown in Fig.3.1. This hyperbola can be easily expressed by the hyperbolic formula given below :

$$(\sigma_1 - \sigma_3) = \frac{\varepsilon}{\frac{1}{E_i} + \frac{\varepsilon}{(\sigma_1 - \sigma_3)_{ult}}} \quad \dots(3.2)$$

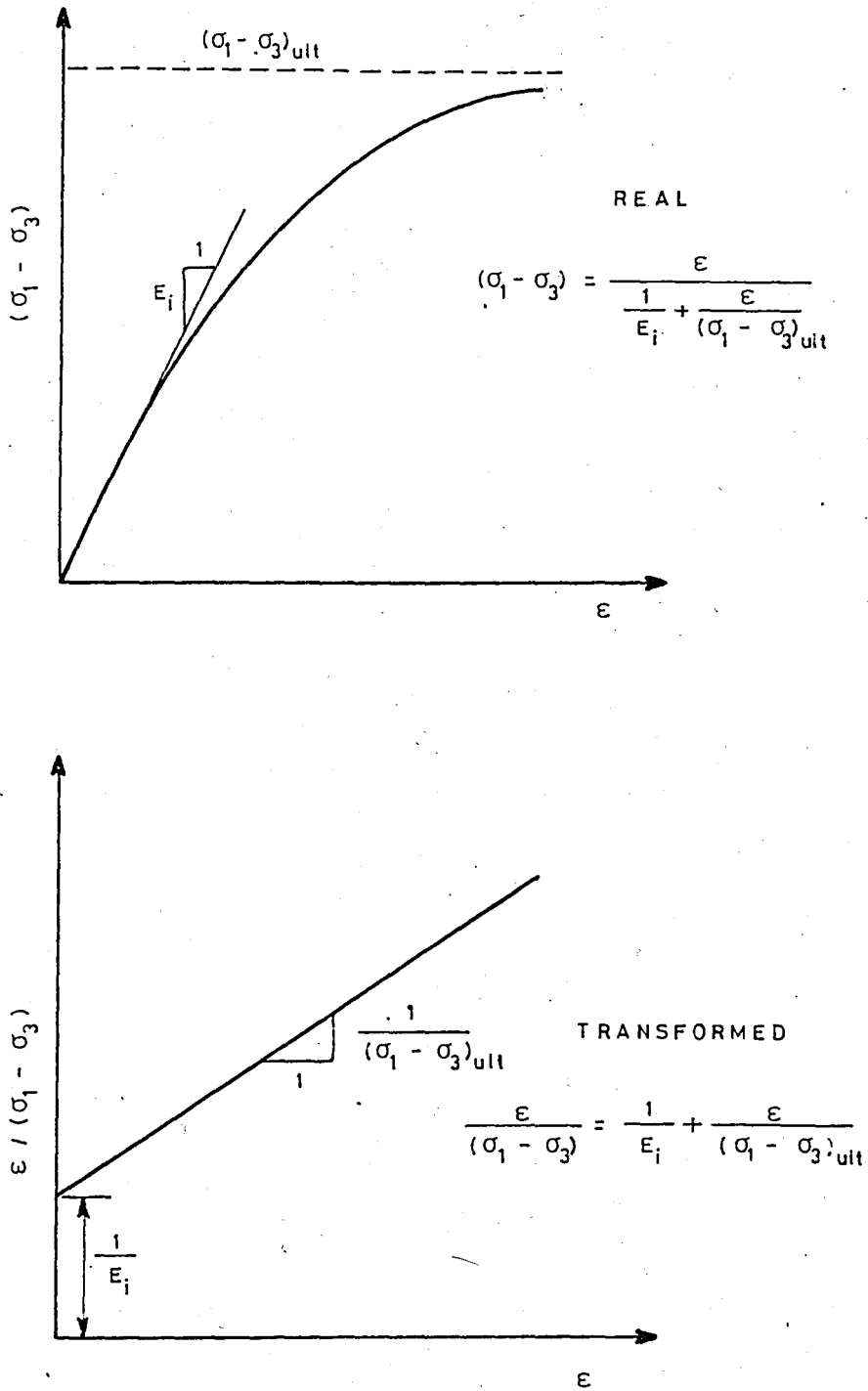


Fig. 3.1 Hyperbolic Representation of a Stress-Strain Curve
(Kondner, 1963)

in which σ_1, σ_3 : Major, minor principal stress
 ϵ : Axial strain
 $(\sigma_1 - \sigma_3)_{ult}$: Ultimate deviator stress
 E_i : Initial tangent modulus

If the value of $1/E_i$ is designated as a and the value of $1/(\sigma_1 - \sigma_3)_{ult}$ as b and both of them are introduced into the equation (3.2), the hyperbolic equation will have the following form:

$$\frac{\epsilon}{(\sigma_1 - \sigma_3)} = a + bc \quad \dots (3.3)$$

$$a = \frac{1}{E_i}, \quad b = \frac{1}{(\sigma_1 - \sigma_3)_{ult}}$$

There are two major advantages of representing the stress-strain relationship by a hyperbola although other types of curves may also be used.

1. The parameters which appear in equation (3.2) have physical significance. E_i is the initial tangent modulus and $(\sigma_1 - \sigma_3)_{ult}$ is the asymptotic value of stress difference which is always greater than the compressive strength of soil.
2. If the hyperbolic equation is transformed as shown in Fig.(3.1), it represents a linear relationship between $\epsilon/(\sigma_1 - \sigma_3)$ and ϵ . Therefore, it is easy to use this transformed plot in determining the best-fit hyperbola corresponding to the test data.

When the test results are plotted on the transformed plot, the points usually deviate from the straight line. In practice, it is recommended that a good match can be achieved by selecting the straight line such a way that it passes through the points where 70% and 95% of the strength are mobilized. (Duncan, Chang 1970).

3.2.2 EFFECT OF CONFINING PRESSURE ON E_i AND $(\sigma_1 - \sigma_3)_{ult}$

For all soils except fully saturated soils tested under unconsolidated-undrained conditions, the values of E_i and $(\sigma_1 - \sigma_3)_{ult}$ increase with increasing confining pressure since an increase in confining pressure will result in a steeper stress-strain curve and higher strength. This reveals that E_i and $(\sigma_1 - \sigma_3)_{ult}$ are stress-dependent.

Janbu has suggested the following empirical equation for the variation of E_i with σ_3 :

$$E_i = K \cdot P_a \left(\frac{\sigma_3}{P_a} \right)^n \quad \dots (3.4)$$

in which parameter K is the modulus number, n is the modulus exponent. P_a is the atmospheric pressure introduced into the equation in order to make conversion from one system of units to another more convenient. Both K and n are dimensionless numbers whereas E_i and P_a are of the same unit. Fig 3.2 shows the variation of E_i with σ_3 .

On the other hand, the variation of $(\sigma_1 - \sigma_3)_{ult}$ with σ_3 can be expressed, as shown in Fig 3.3, by relating $(\sigma_1 - \sigma_3)_{ult}$ to the compressive strength or the deviator stress at failure, $(\sigma_1 - \sigma_3)_f$, and considering the Mohr-Coulomb strength equation to relate $(\sigma_1 - \sigma_3)_f$ to σ_3 . The relationship between $(\sigma_1 - \sigma_3)_{ult}$ and $(\sigma_1 - \sigma_3)_f$ can be given as follows:

$$(\sigma_1 - \sigma_3)_f = R_f (\sigma_1 - \sigma_3)_{ult} \quad \dots (3.5)$$

where R_f is called failure ratio. Since $(\sigma_1 - \sigma_3)_f$ is always smaller than $(\sigma_1 - \sigma_3)_{ult}$, R_f is always smaller than 1 varying from 0.5 to 0.9 for most soils.

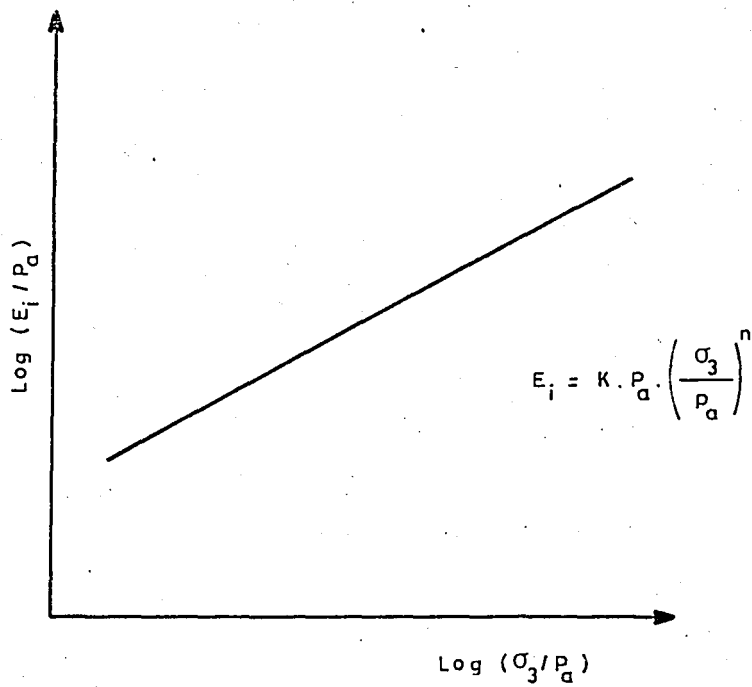
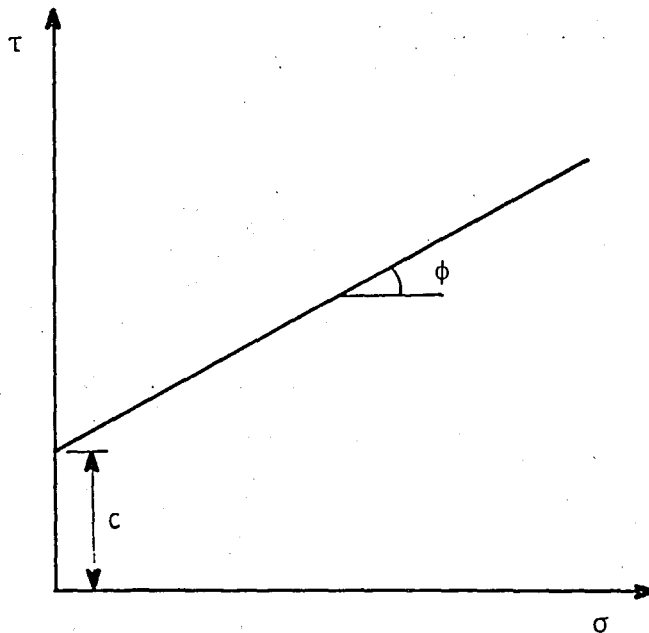


Fig. 3.2 Variation of Initial Tangent Modulus with Confining Pressure (Duncan, Wong, 1974)



$$(\sigma_1 - \sigma_3)_f = \frac{2c \cos \phi + 2\sigma_3 \sin \phi}{1 - \sin \phi}$$

$$(\sigma_1 - \sigma_3)_f = R_f (\sigma_1 - \sigma_3)_{ult}$$

*Fig. 3.3 Variation of Strength with Confining Pressure
(Duncan, Wong, 1974)*

Furthermore, the relationship between $(\sigma_1 - \sigma_3)_f$ and confining pressure, σ_3 can also be expressed by the wellknown Mohr-Coulomb strength equation as follows:

$$(\sigma_1 - \sigma_3)_f = \frac{2c \cdot \cos\phi + 2\sigma_3 \cdot \sin\phi}{1 - \sin\phi} \quad \dots(3.6)$$

where c and ϕ are cohesion intercept and the friction angle respectively.

3.2.3. RELATIONSHIP BETWEEN TANGENT DEFORMATION MODULUS AND THE STRESSES

The tangent deformation modulus E_t can be defined as the slope of the $\sigma - \epsilon$ curve at any point. If the equation (3.3) is differentiated with respect to ϵ and the equations (3.4), (3.5), (3.6) are substituted into the resulting equation, the following equation can be derived for E_t :

$$E_t = \left[1 - \frac{R_f(1-\sin\phi)(\sigma_1 - \sigma_3)}{2c \cdot \cos\phi + 2\sigma_3 \cdot \sin\phi} \right]^2 \cdot K \cdot P_a \left(\frac{\sigma_3}{P_a} \right)^n \quad \dots(3.7)$$

That means if the parameters K, n, c, ϕ and R_f are known, the value of E_t can be computed employing equation (3.7)

3.2.4. INELASTIC MATERIAL BEHAVIOR

If a triaxial specimen is loaded and then unloaded at some stage during a test, the stress-strain curve followed during unloading is steeper than the curve followed during loading. If it is reloaded after unloading, then the stress-strain curve will be steeper than the curve for primary loading and is quite similar in slope to the unloading curve as seen in Fig 3.4. This implies that the soil behavior is inelastic since the strains occurred during primary loading are partly recoverable on unloading.

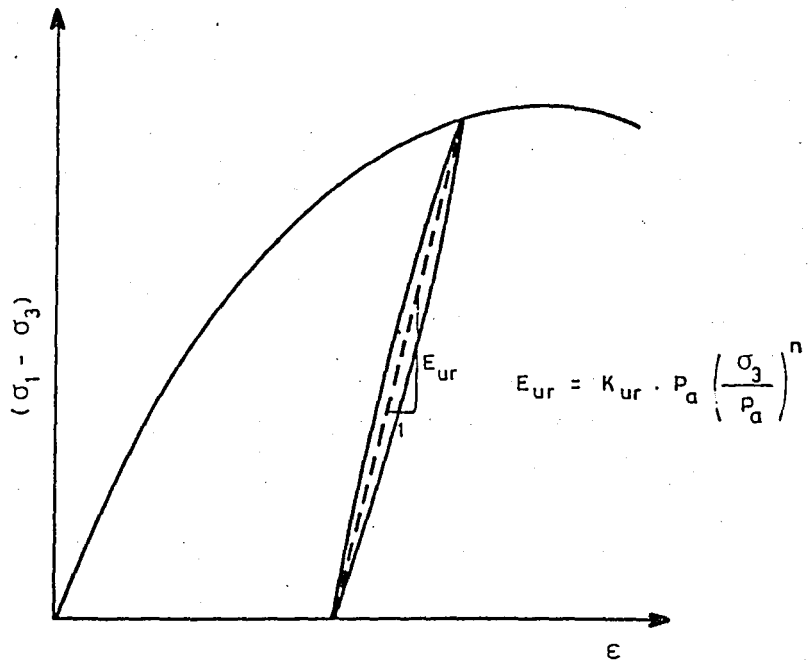


Fig. 3.4 Unloading-Reloading Modulus

In the hyperbolic stress-strain relationships, the same value of unloading-reloading modulus, E_{ur} , is used for both cases. The equation of E_{ur} related to σ_3 can be written as

$$E_{ur} = K_{ur} \cdot P_a \left(\frac{\sigma_3}{P_a} \right)^n \quad \dots (3.8)$$

where K_{ur} is the unloading-reloading modulus number which is always greater than the value of K (primary loading) by 20% for stiff soils and 300% for soft soils (Duncan, Wong 1974).

3.2.5. NONLINEAR VOLUME CHANGE BEHAVIOR OF SOILS

The value of tangent Poisson's ratio, v_t , may be determined by simply analyzing the volume changes occurred during a triaxial test. The volumetric strain ϵ_v and the axial strain ϵ_a are usually measured during a triaxial test, thus using these values the radial deformation can be expressed as

$$\epsilon_r = \frac{1}{2} (\epsilon_v - \epsilon_a) \quad \dots (3.9)$$

If the compressive strains are taken as positive, the value of ϵ_a becomes positive, then the value of ϵ_r is negative while the value of ϵ_v is either positive or negative. As the plot of ϵ_a versus ϵ_r is drawn as shown in Fig.3.5, it is seen that the resulting curve can be easily represented by a hyperbolic equation as follows:

$$\epsilon_a = \frac{-\epsilon_r}{v_i - d\epsilon_r} \quad \dots (3.10)$$

If a transformation is made to this equation, the following equation is obtained

$$\frac{-\epsilon_r}{\epsilon_a} = v_i - d\epsilon_r \quad \dots (3.11)$$

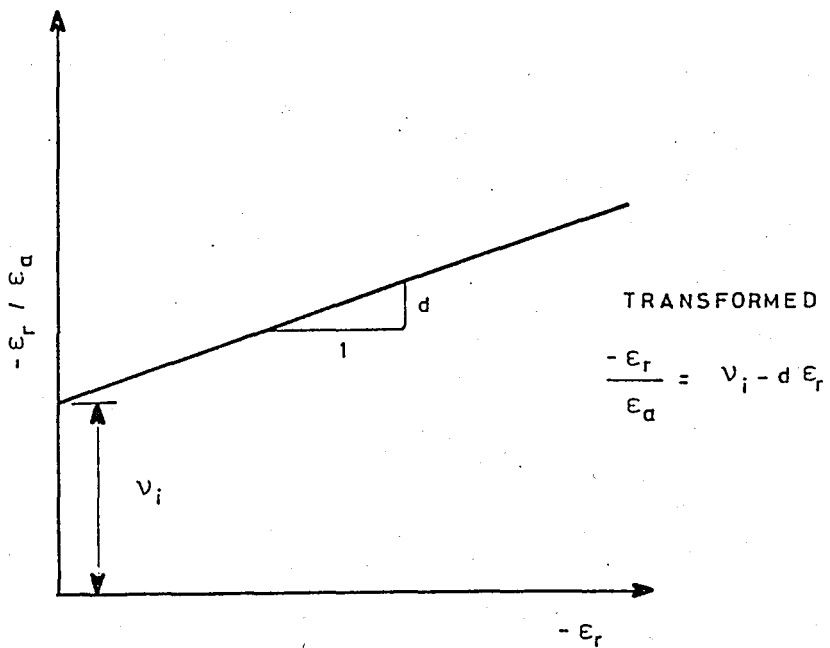
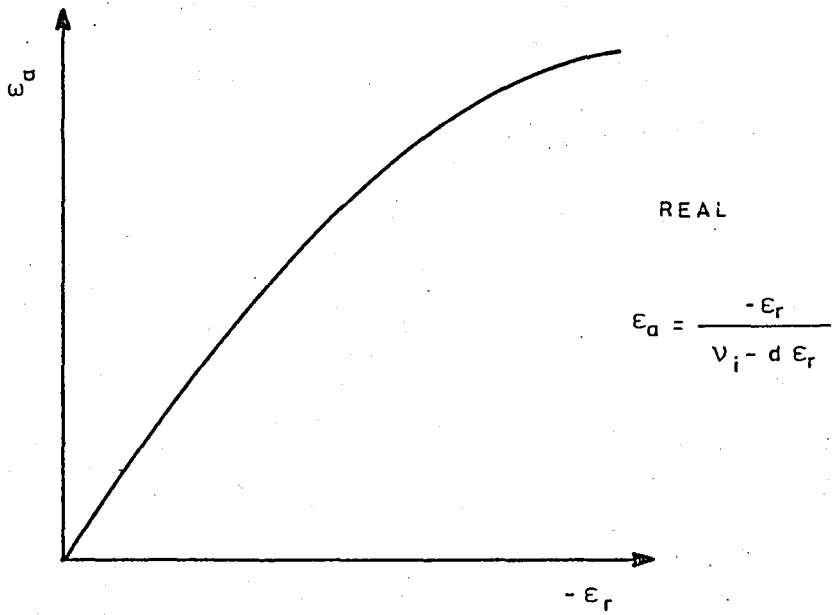


Fig. 3.5 Hyperbolic Axial Strain-Radial Strain Curves
(Duncan, Wong, 1974)

in which v_i is the initial Poisson's ratio at zero strain as seen in Fig.3.5 and d is a parameter representing the change in the value of Poisson's ratio with ϵ_r .

The variation of v_i with σ_3 , as shown in Fig.3.6 has also been given by Kulhawy (1969) and others as follows,

$$v_i = G - F \cdot \text{Log}_{10} \left(\frac{\sigma_3}{P_a} \right) \quad \dots (3.12)$$

where G is the value of v_i at σ_3 of one atmosphere and F is the reduction in v_i for ten-fold increase in σ_3 .

Although for saturated soils under undrained conditions there is no volume change hence v_i is equal to one half for any value of σ_3 , this equation implies that v_i decreases with σ_3 for most of other soils.

3.2.6. RELATIONSHIP BETWEEN v_t AND THE STRESSES

The negative value of tangent Poisson's ratio, $-v_t$, can be defined as the slope of the curve representing the variation of ϵ_a with ϵ_r as seen in Fig 3.5. By simply differentiating equation (3.10) with respect to ϵ and substituting the values of v_i , E_i , $(\sigma_1 - \sigma_3)_{ult}$, $(\sigma_1 - \sigma_3)_f$ into the equation, the value of v_t can be written in terms of the stresses as follows (Duncan and Wong 1974)

$$v_t = \frac{G - F \cdot \text{Log} \frac{\sigma_3}{P_a}}{\left[1 - \frac{d(\sigma_1 - \sigma_3)}{K \cdot P_a \left(\frac{\sigma_3}{P_a} \right)^n \cdot \left[1 - \frac{R_f(\sigma_1 - \sigma_3)(1 - \text{Sin}\phi)}{2c \cdot \text{Cos}\phi + 2\sigma_3 \cdot \text{Sin}\phi} \right]} \right]^2} \dots (3.13)$$

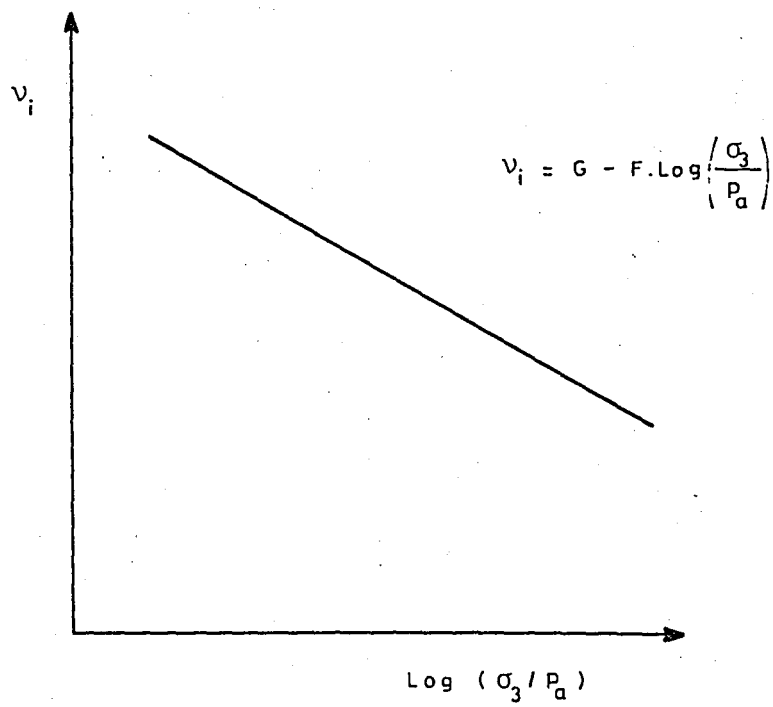


Fig. 3.6 Variation of Initial Tangent Poisson Ratio with Confining Pressure (Duncan, Wong, 1974)

3.3 EVALUATION OF HYPERBOLIC STRESS-STRAIN PARAMETERS FROM LABORATORY TEST RESULTS

The hyperbolic stress-strain parameters can be evaluated using the data from either drained or unconsolidated-undrained triaxial tests. The steps involved in the procedure for evaluating these parameters are presented in the following sections.

3.3.1 SELECTING DATA

The selection of data being appropriate to the problem is of great importance in evaluating the hyperbolic stress-strain parameters. In other words, the testing and soil conditions in the laboratory tests should conform to those in the problem being analyzed. Therefore, in the case of fill materials, the tests must be conducted using specimens compacted to the same density and water content as in the field while the laboratory tests must be performed on undisturbed specimens in the case of natural soils. The drainage conditions and the confining pressures applied during the tests should also correspond to those of interest in the problem.

Although most of the time, the data points do not exhibit smooth variations of stress and strain due to differences in the length of time, it is essential to draw smooth curves through the data points such as seen in Fig 3.7, using good judgement to make reasonable interpretations of all of the test data. Furthermore, inconsistent data deviating from the remaining data should also be eliminated.

3.3.2 EVALUATION OF c AND ϕ FOR COHESIVE SOILS

The parameters c and ϕ which are namely the cohesion intercept and friction angle can be determined by two different methods. In the first

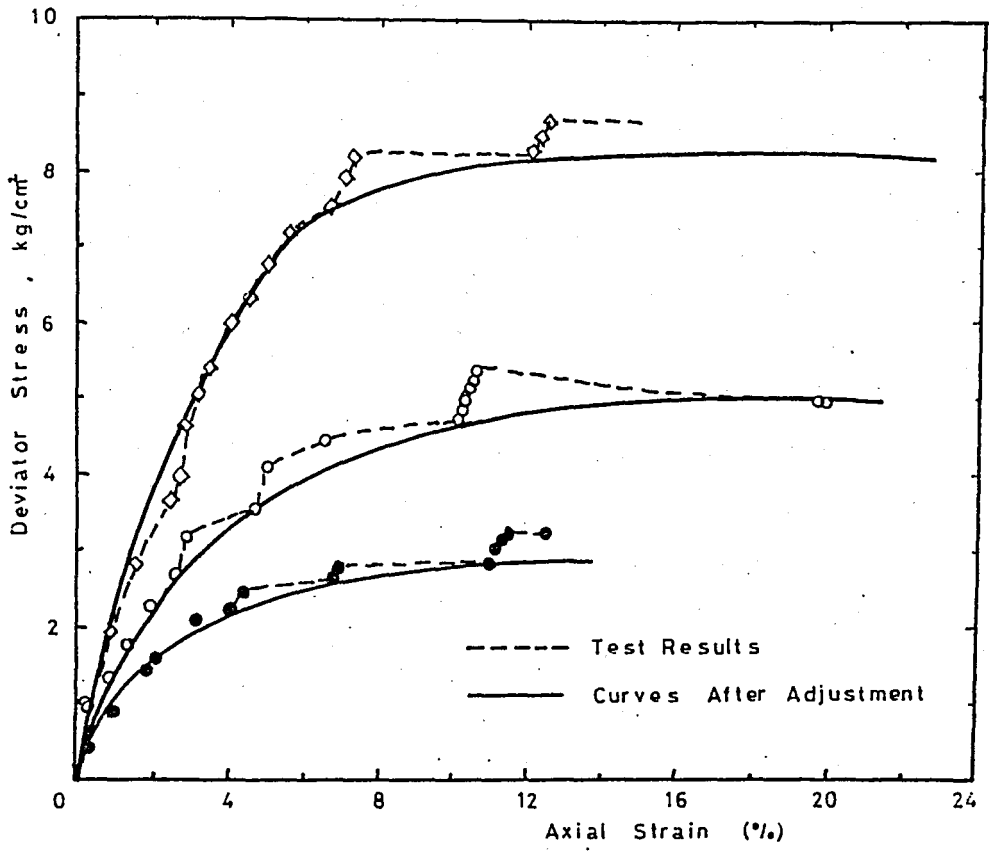


Fig. 3.7 Adjustment of Stress-Strain Curves (Duncan, Wong, 1974)

method, the Mohr's circles are drawn as shown in Fig 3.8 and the values of c and ϕ are determined by drawing the failure envelope and measuring the intercept and the slope angle.

The second method for evaluating the values of c and ϕ is to plot the values of $1/2 (\sigma_1 - \sigma_3)$ at failure against the values of $1/2 (\sigma_1 + \sigma_3)$ at failure, as shown in Fig 3.9, which is also known as Modified Mohr envelope. The advantage of this method is that it is simpler to fit best straight line through a series of points instead of drawing the best straight envelope for a series of circles which do not have a common tangent. On the other hand, it has a disadvantage since c and ϕ values can not be determined directly but using the following equations,

$$c = \alpha / \cos \phi \quad \dots (3.14)$$

$$\phi = \sin^{-1}(\tan \psi) \quad \dots (3.15)$$

where α = Intercept of Modified Mohr Envelope

ψ = The slope angle of Modified Mohr Envelope

3.3.3. EVALUATION OF ϕ_0 and $\Delta\phi$ FOR COHESIONLESS SOILS

The Mohr envelopes drawn for determining the value of ϕ are not mostly straight lines but curved to some extent. In case of cohesionless soils, since the curvature of the envelope is considerably large, it becomes difficult to select a single value of ϕ which is representative of the full range of the pressures. Especially in large rockfill dams, the value of ϕ is different in the bottom near the centre of the dam than near the surface of the slopes because of the different confining pressure conditions.

In order to get rid of such difficulties, the values of ϕ for the material which vary with confining pressure is used. The value of ϕ can

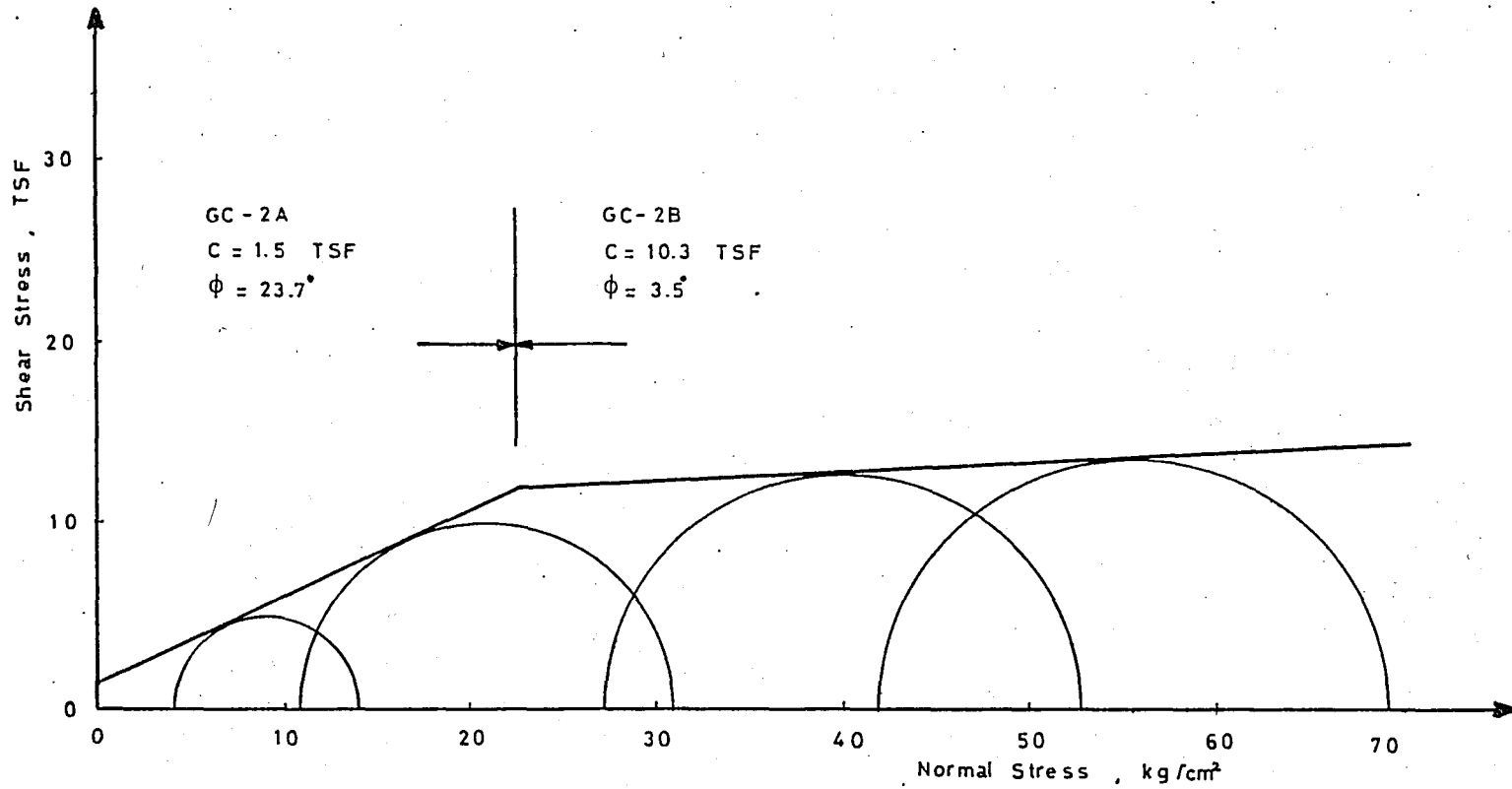


Fig. 3.8 Mohr Envelopes For Oroville Dam Core Material (Duncan, Wong, 1974)

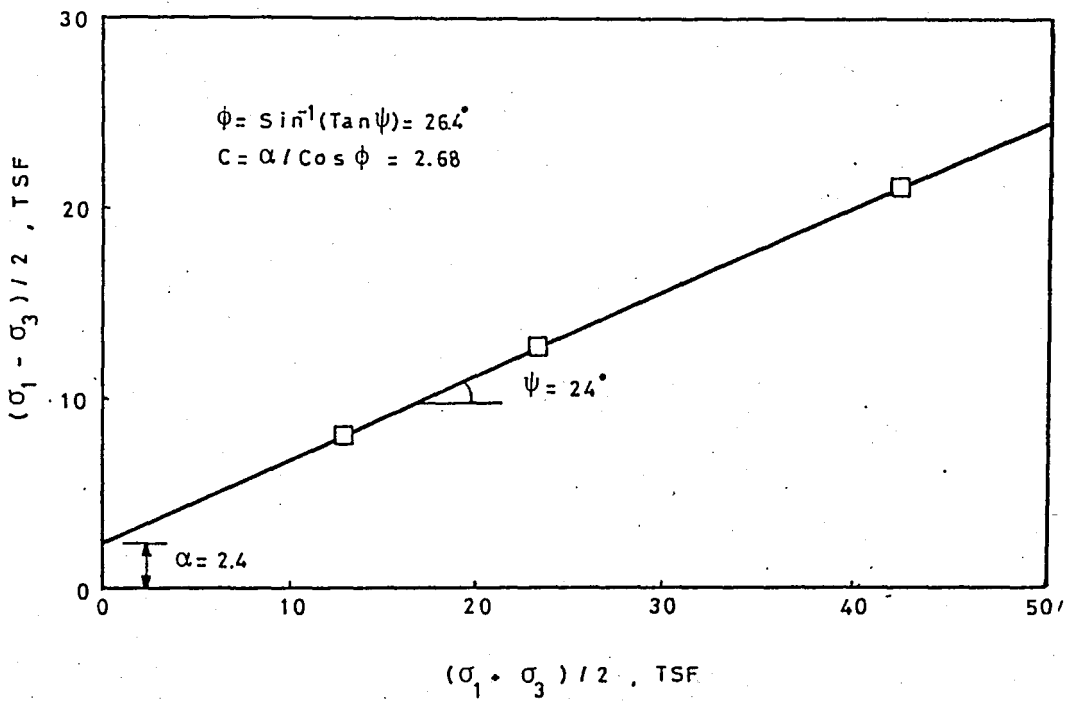


Fig. 3.9 Modified Mohr Envelope For UU-Triaxial Tests on
 New Don Pedro Dam Core Material (Duncan, Wong, 1974)

then be determined from each triaxial test, as shown in Fig 3.10, assuming the envelope for that circle passes through the origin of stress, by employing the following formula

$$\phi = \text{Sin}^{-1} \left(\frac{\sigma_1 - \sigma_3}{\sigma_1 + \sigma_3} \right) \quad \dots (3.16)$$

In addition, ϕ can also be evaluated by drawing separate envelopes for each circle passing through the origin. Hence it is found that the values of ϕ decrease being proportional to the logarithm of σ_3 as seen in Fig 3.11. Thus the values of ϕ can be computed as follows: (Duncan and Wong, 1974)

$$\phi = \phi_0 - \Delta\phi \text{Log}_{10} \left(\frac{\sigma_3}{P_a} \right) \quad \dots (3.17)$$

in which ϕ_0 = Value of ϕ for $\sigma_3 = P_a$

$\Delta\phi$ = Reduction in ϕ for ten-fold increase in σ_3

This equation can be used for evaluating the values of ϕ appropriate for any confining pressure within the range of pressures encompassed by the test results.

3.3.4 EVALUATION OF K, n AND R_f

There are two steps involved in evaluating the modulus number K and the modulus exponent n. The first step is to determine the values of E_i for each test conducted by using different confining pressure values. Then the second step is to plot these values against σ_3 on logarithmic scales for determining the values of K and n.

Since most real stress-strain curves are only approximately hyperbolic, some consideration must be given to the method of fitting a hyperbolic curve to the experimental data. As explained previously, Duncan and Chang (1970) have found that the best fit is usually achieved by

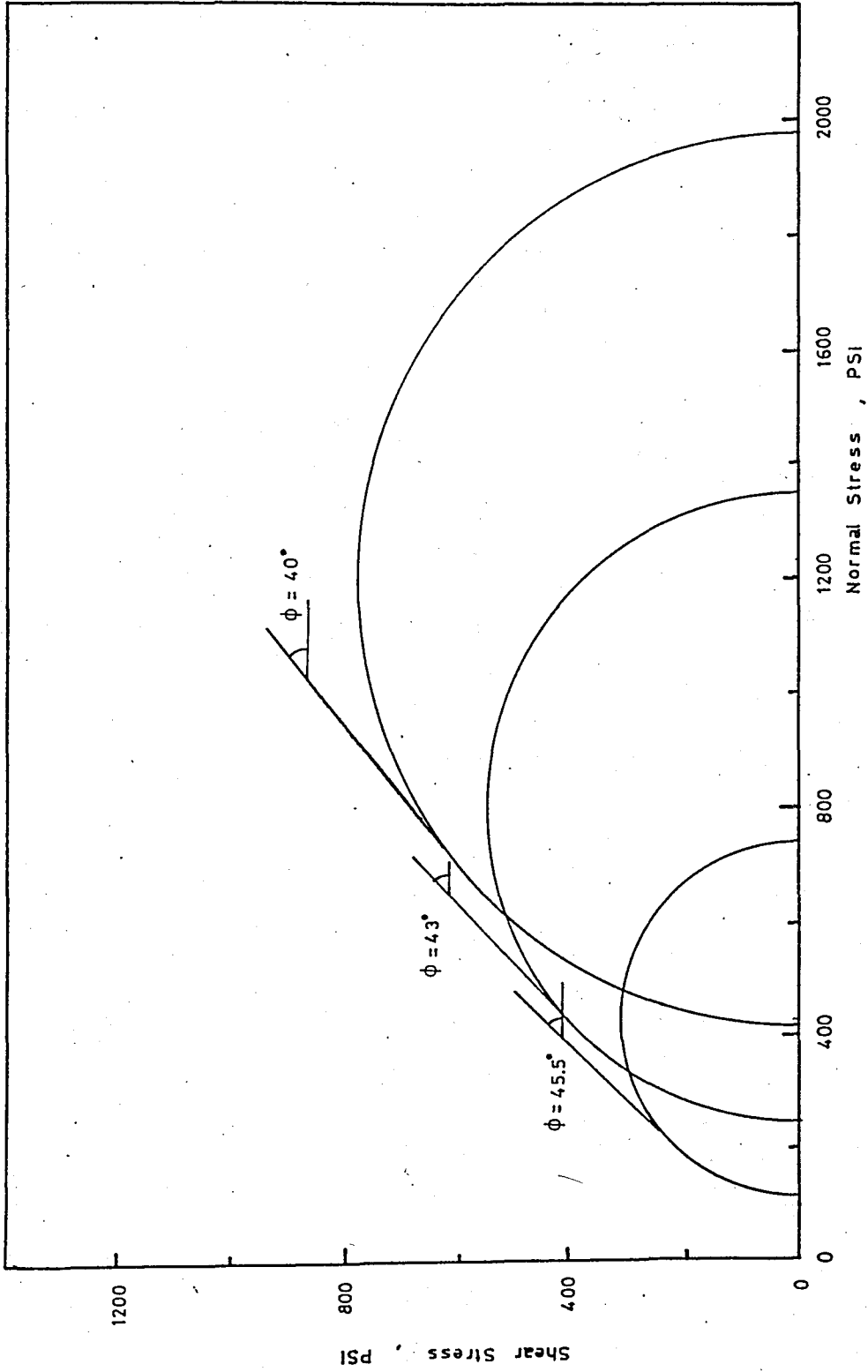


Fig. 3.10 Mohr Envelope For CD-Triaxial Tests on Oroville Dam Shell Material (Duncan, Mong, 1974)

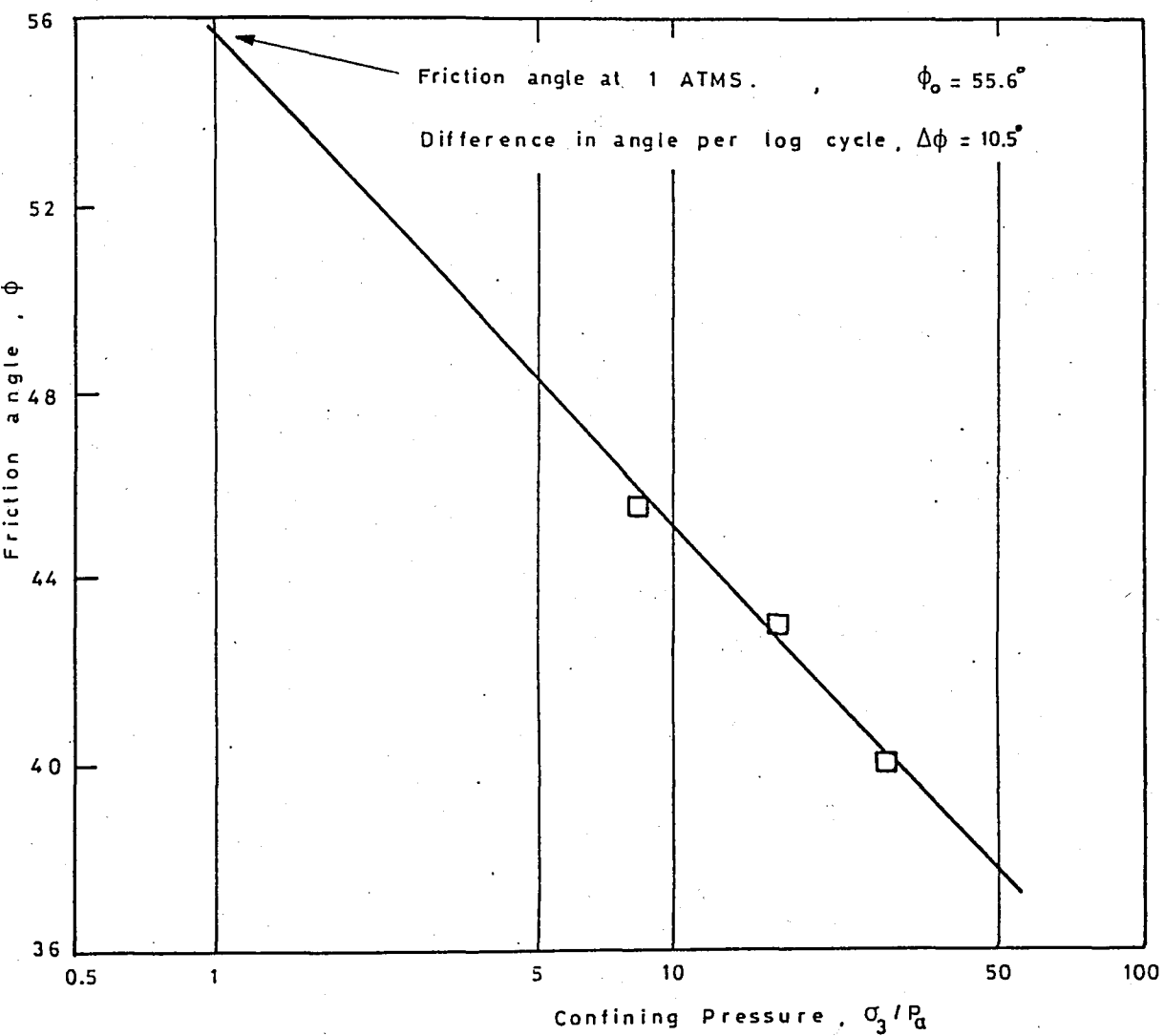


Fig. 3.11 Variation of Friction Angle with Confining Pressure For Oroville Dam Shell Material (Duncan, Wong, 1974)

matching the hyperbola to the experimental curve at the points where 70% and 95% of the strength are mobilized.

The curves of Oroville Dam shell material given by Duncan and Wong (1974) have been taken as an example here in order to show how to evaluate the values of K and n . As shown in Fig 3.12, the points corresponding to 70% and 95% of the strength are indicated by arrows for each of the three stress-strain curves. Once the hyperbola is matched to the data at 70% and 95% points, the transformed stress-strain plot can be easily drawn using only these two points as seen in Fig 3.13. Through each pair of points on this diagram a straight line is drawn corresponding to the hyperbola, then the values of E_i and $(\sigma_1 - \sigma_3)_{ult}$ are found to be reciprocals of the intercepts and the slopes of these lines as described earlier. After obtaining the values of $(\sigma_1 - \sigma_3)_{ult}$ and taking the values of $(\sigma_1 \sigma_3)_f$ from Fig 3.12, the values of R_f can be computed according to equation (3.5). The values of K and n can be determined by plotting the values of E_i / P_a against the values of σ_3 / P_a on logarithmic scales as illustrated in Fig. 3.14. The straight line shown in this figure can be expressed by equation (3.18) which is the same as equation (3.4).

$$\frac{E_i}{P_a} = K \left(\frac{\sigma_3}{P_a} \right)^n \quad \dots (3.18)$$

In this equation K is the value of (E_i / P_a) at the point where σ_3 is equal to P_a i.e. σ_3 / P_a equals to unity and n is the slope of the straight line in Fig 3.14. The values of n can also be determined numerically by using the following equation.

$$n = \frac{\Delta \text{Log}(E_i / P_a)}{\Delta \text{Log}(\sigma_3 / P_a)} \quad \dots (3.19)$$

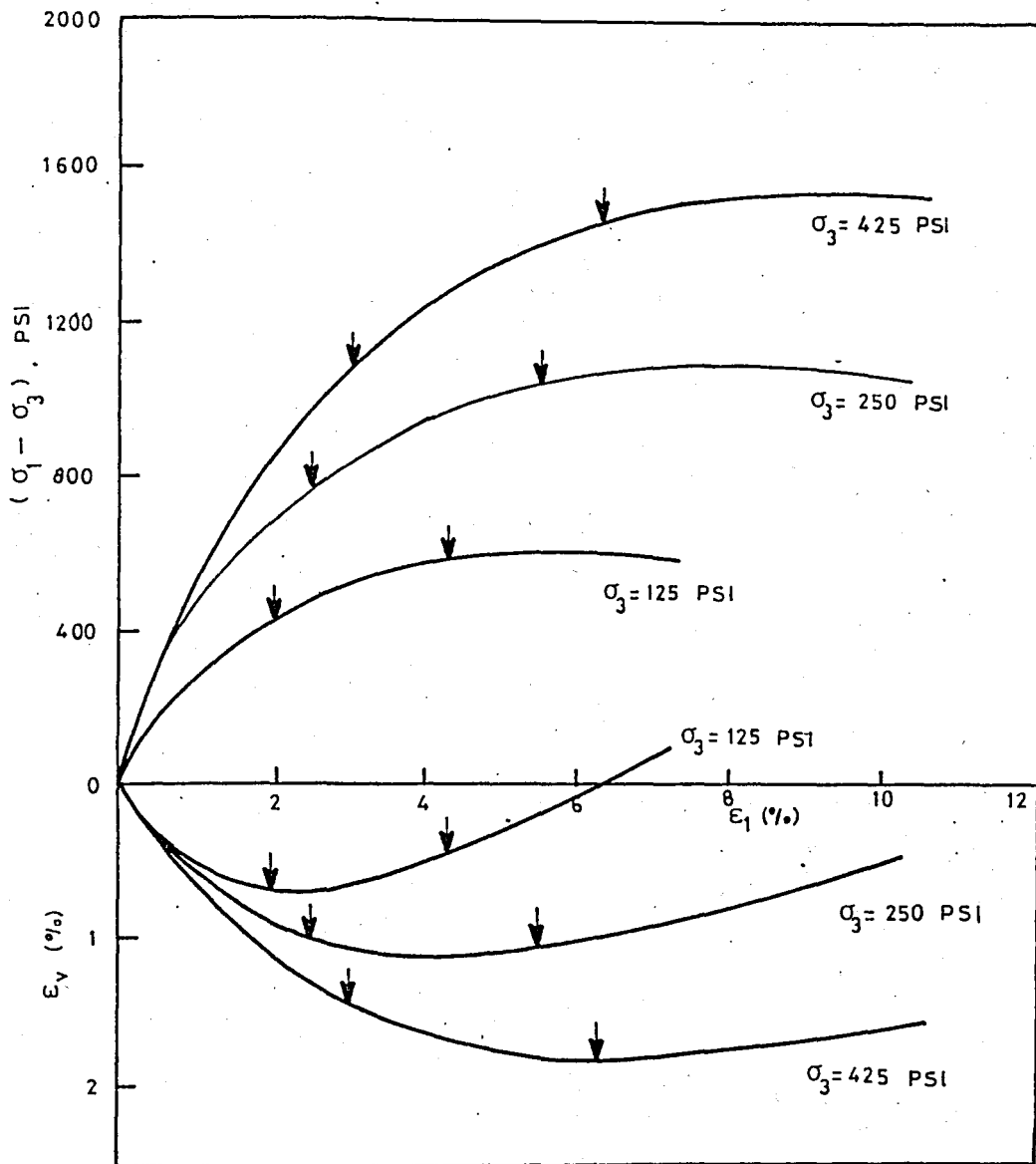


Fig. 3.12 Replotted Stress-Strain and Volume-Change Curves
For Oroville Dam (Duncan, Wong, 1974)

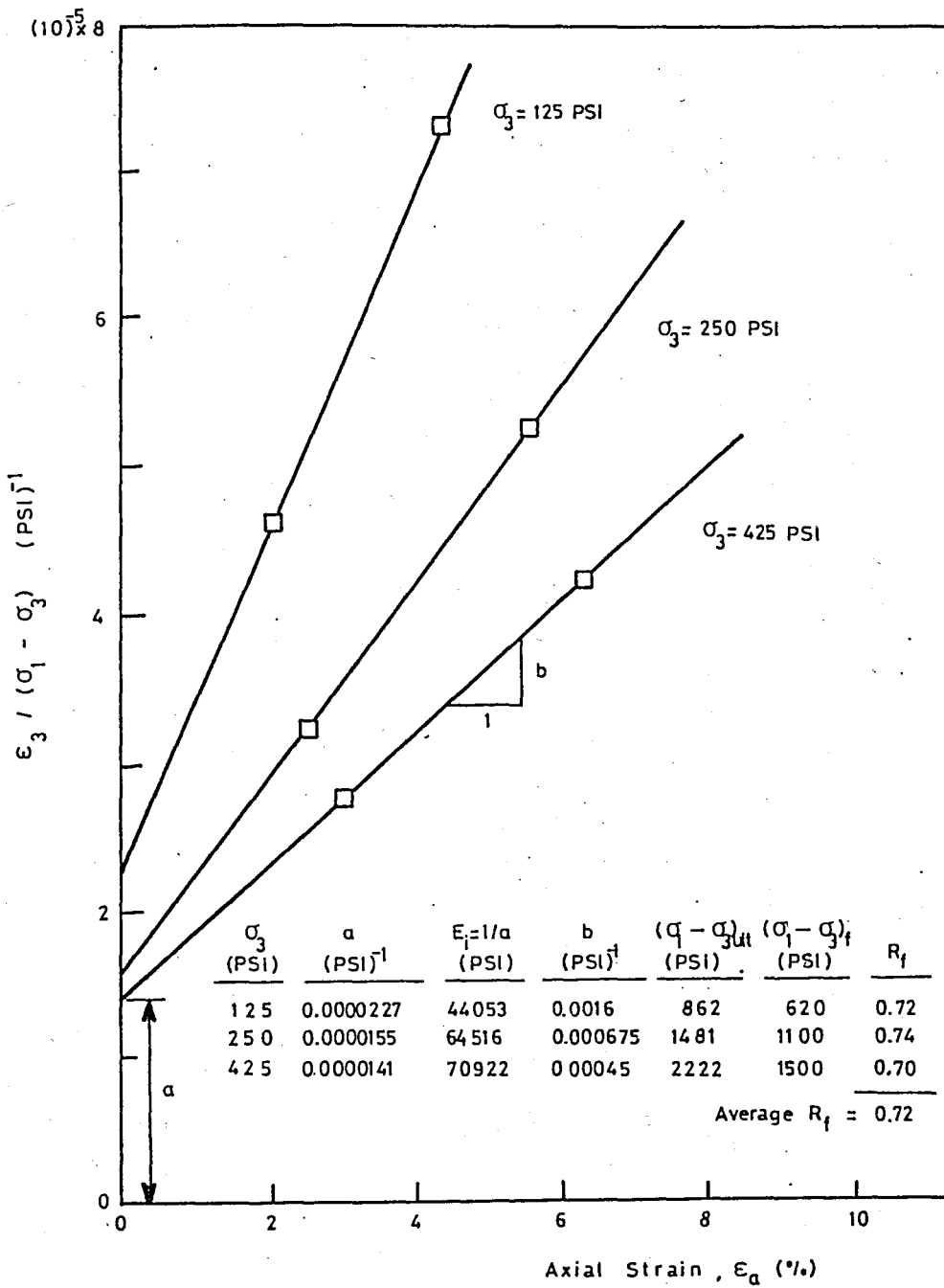


Fig. 3.13. Transformed Stress-Strain Plot For Oroville Dam Shell Material (Duncan, Wong, 1974)

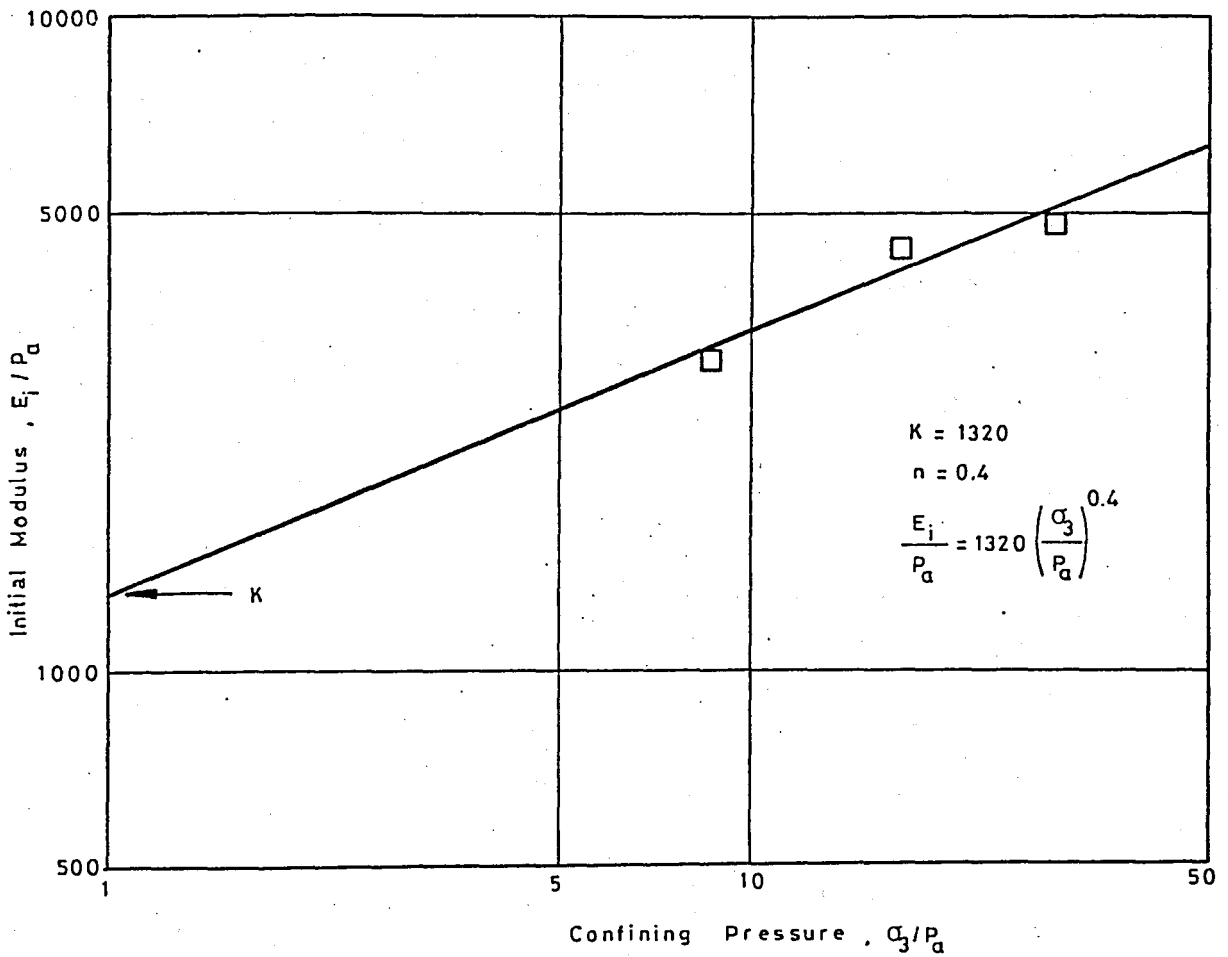


Fig. 3.14 Variation of Initial Tangent Modulus with Confining Pressure For Oroville Dam Shell Material (Duncan, Wong, 1974)

3.3.5 EVALUATION OF K_{ur}

Referring to the section 3.2.4, the value of K_{ur} is usually determined assuming that the value of n for unloading-reloading is same as the value of n for primary loading. Therefore, the value of K_{ur} may be evaluated using data from a single unloading curve, if the value of n has been determined. The best straight line is fitted to the unloading curve and the value of E_{ur} is evaluated. Once the value of E_{ur} is computed, the value of K_{ur} can be easily computed using equation (3.20)

$$K_{ur} = \frac{E_{ur}}{p_a \left(\frac{\sigma_3}{p_a} \right)^n} \quad \dots (3.20)$$

3.3.6 EVALUATION OF G, F AND d

There are two steps involved in evaluating the values of the Poisson's ratio parameters G , F and d . In the first step, the values of v_i and d for each test are determined. Then as a second step, the values of v_i are plotted against the logarithm of σ_3 and the values of G and F are evaluated.

As in the case of evaluating the modulus parameters, the hyperbolas are fitted to $\epsilon_r - \epsilon_a$ curves at the points where 70% and 95% of strength are mobilized and only these points are used for evaluating the parameters G , F and d . The values of ϵ_r can be determined employing equation (3.9) provided that the values of ϵ_a and ϵ_r are known. Then these values are plotted in a transformed ϵ_r vs. $-\epsilon_r / \epsilon_a$ diagram as shown in Fig 3.15.

In this diagram the values of v_i which are the Poisson's ratios at zero strain are intercepts of the straight lines while the values of d are the slopes of these lines. For practical purposes, a single value of d is

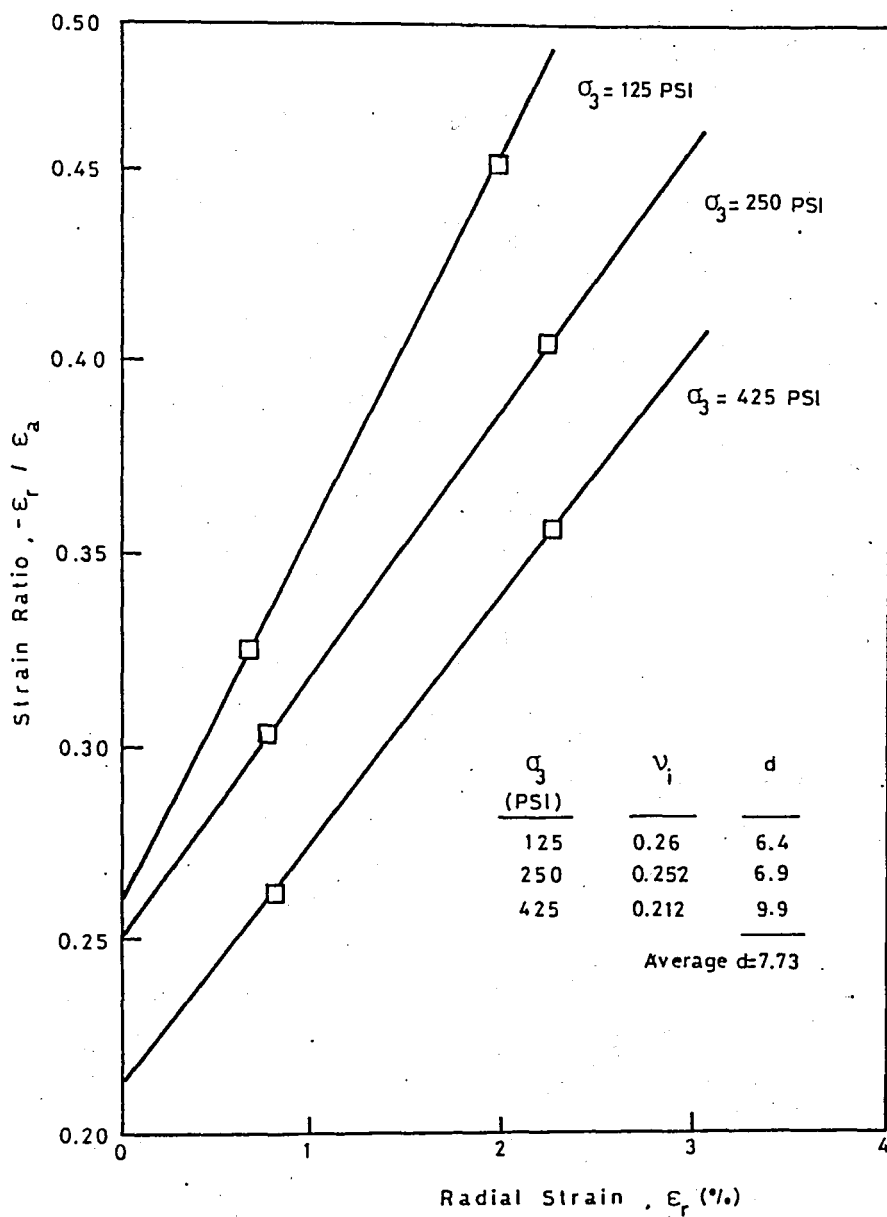


Fig. 3.15 Variation of Poisson Ratio with Radial Strain For Oroville Dam Shell Material (Duncan, Wong, 1974)

obtained by taking the average value of these three.

After determining the values of v_i they are plotted against the logarithm of σ_3/P_a , as shown in Fig 3.16. In this plot, the straight line can be expressed by the following equation

$$v_i = G - F \cdot \text{Log} \left(\frac{\sigma_3}{P_a} \right) \quad \dots (3.21)$$

As seen in this plot, the value of G is the intercept of v_i at the point where σ_3 is equal to atmospheric pressure and F is the decrease in v_i for ten-fold increase in σ_3 .

3.4 FACTORS AFFECTING THE HYPERBOLIC STRESS-DEFORMATION PARAMETERS

Duncan and Wong (1974) have been studied the most important factors affecting the hyperbolic stress-strain characteristics of soils. They have found that relative density, gradation, particle shape and mineral type are of great importance in determining the parameters of soils under drained conditions. Especially in cohesionless soils an increase in relative density will result in increased strength (higher value of ϕ), increased stiffness (higher value of K) and higher values of G and d . Moreover, it has been also shown that poorly graded soils generally have higher values of K, G and F than well-graded soils while $\phi_0, \Delta\phi, n$ and R_f do not appear to be affected by gradation.

On the other hand, the most important factors affecting the parameter values obtained under unconsolidated-undrained test conditions have been found to be soil structure, relative density and water content. These determine the pore pressures which develop during undrained loading, and they therefore control the stress-strain and strength behavior.

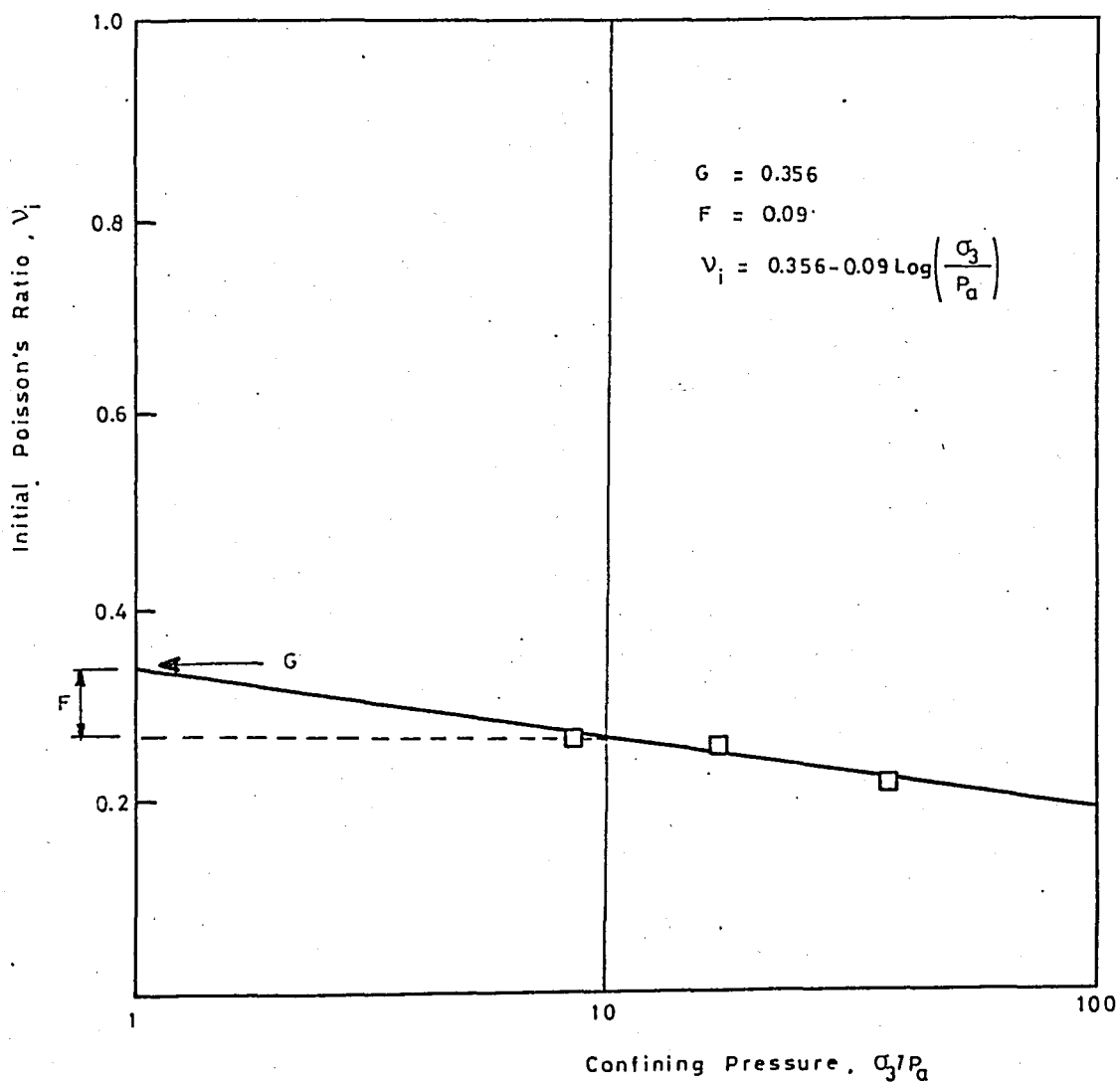


Fig. 3.16 Variation of Initial Poisson Ratio with Confining Pressure For Orville Dam Shell Material (Duncan, Wong, 1974)

The structure of compacted soils is determined by compaction procedure and the compaction water content in relation to optimum. Therefore, it is essential to compact the soil to the same density and water content as in the field.

The variations of the parameters with the soil properties and test conditions can also be seen in table A.1 and A.2 presented in Appendix A.

3.5 SUMMARY

There are nine hyperbolic stress-strain parameters representing three important characteristics of the behavior of soils namely: inelasticity, stress-dependency and nonlinearity and they are summarized in Table 3.1.

These parameters can be easily evaluated from the results of well-known triaxial compression tests. The values of parameters determined for about 135 different soils have been given by Duncan and Wong (1974), and they are presented in Appendix A. This information can help us in predicting the parameter values when there is not sufficient data available from triaxial compression tests or evaluating the reliability of parameters derived from laboratory test results.

Although it has been proven that these parameters are very useful in predicting the stresses and movements in soil masses, there are some limitations in using them:

1. The relationships are quite suitable for analysis of stresses and movements prior to failure. In other words, they are useful for predicting movements in stable soil masses.

2. The hyperbolic relationships do not include volume changes due to changes in shear stress. Therefore, they may be limited in accuracy with which they can be used to predict deformations in the dilatant soils such as dense sands under low confining pressures.
3. The values of parameters depend on relative density, water content, the range of pressures used in testing and drainage conditions. Therefore, the laboratory test conditions should correspond to the field conditions.

TABLE 3.1 Summary of the Hyperbolic Parameters

Parameter	Name	Function
K_i, K_{ur}	Modulus number	Relate E_i and E_{ur} to σ_3
n	Modulus exponent	
c	Cohesion intercept	Relate $(\sigma_1 - \sigma_3)_f$ to σ_3
ϕ	Friction angle	
R_f	Failure ratio	Relates $(\sigma_1 - \sigma_3)_{ult}$ to $(\sigma_1 - \sigma_3)_f$
G	Poisson's ratio parameter	Value of ν_i at $\sigma_3 = P_a$
F	Poisson's ratio parameter	Decrease in ν_i for ten-fold increase in σ_3
d	Poisson's ratio parameter	Rate of change of ν_t with strain

CHAPTER 4

FINITE ELEMENT ANALYSES OF ALTINKAYA DAM

4.1 INTRODUCTION

Engineers concerned with the design and construction of earth and rockfill dams have been interested in determining the stresses and deformations which develop in the dam during construction. Therefore, it is required to predict the stress distribution within the embankment prior to construction. In this chapter, attention is given to the prediction of stresses and movements occurred in Altinkaya Dam during construction, which is one of the highest rockfill dams being constructed in Turkey. This was done by employing the finite element method of analysis described previously, using the computer program LSBUILD. Two types of analyses were performed on the embankment; the nonlinear FEM analysis with nonlinear hyperbolic stress-strain parameters of the embankment materials and the build-up analysis with constant values of modulus and poisson's ratio of the materials. The accuracy and reliability of these analyses were later discussed. In addition, the factor of safety against local failure was computed from the values of stress levels obtained from the analyses. The possible instrument locations for measuring the stresses and deformations were also tried to be estimated using the results of the analyses.

4.2 DESCRIPTION OF ALTINKAYA DAM

Altinkaya Dam which is the main unit of the Lower Kızılırmak Project is being constructed (1985) by the State Hydraulic Works of Turkey (DSI) for producing electricity and flood control, Derbent Dam which is the second unit of the project will also be constructed for irrigation purposes.

Altinkaya Dam is located on the Kızılırmak river in approximately 27 km southwest of Bafra, as illustrated in Fig 4.1. It is a rockfill dam of which crest length is about 2030 ft (619m) while the base width at the original ground surface level is about 1850 ft as shown on the embankment plan (Fig 4.2) and its height is about 614 ft (187 m) at the axis of the embankment.

The dam body consists of 20.82 million cubic yards (15,92 million m^3) of soil and rock. Some of the embankment material is hauled from the borrow areas near the construction site, while the material excavated from the cut-off trench and spillway unit is also used as fill material.

As seen in the typical design section of the dam (Fig 4.3), the major zones are the impervious clay core, fine and coarse filters, inner and outer rockfills. A small zone of riprap is also placed on outer rockfill as a protection layer. The alluvial deposit under the impervious zone of dam was excavated down to the bedrock so that a cut-off trench could be provided. A thin layer of concrete was also poured just to have a smooth base upon which the impervious core was placed. On the other hand, the shell and a part of the filter zones were placed over the alluvial deposit. The bedrock was also found to be hard enough after conducting number of field tests so foundation deformations seen to be negligible.

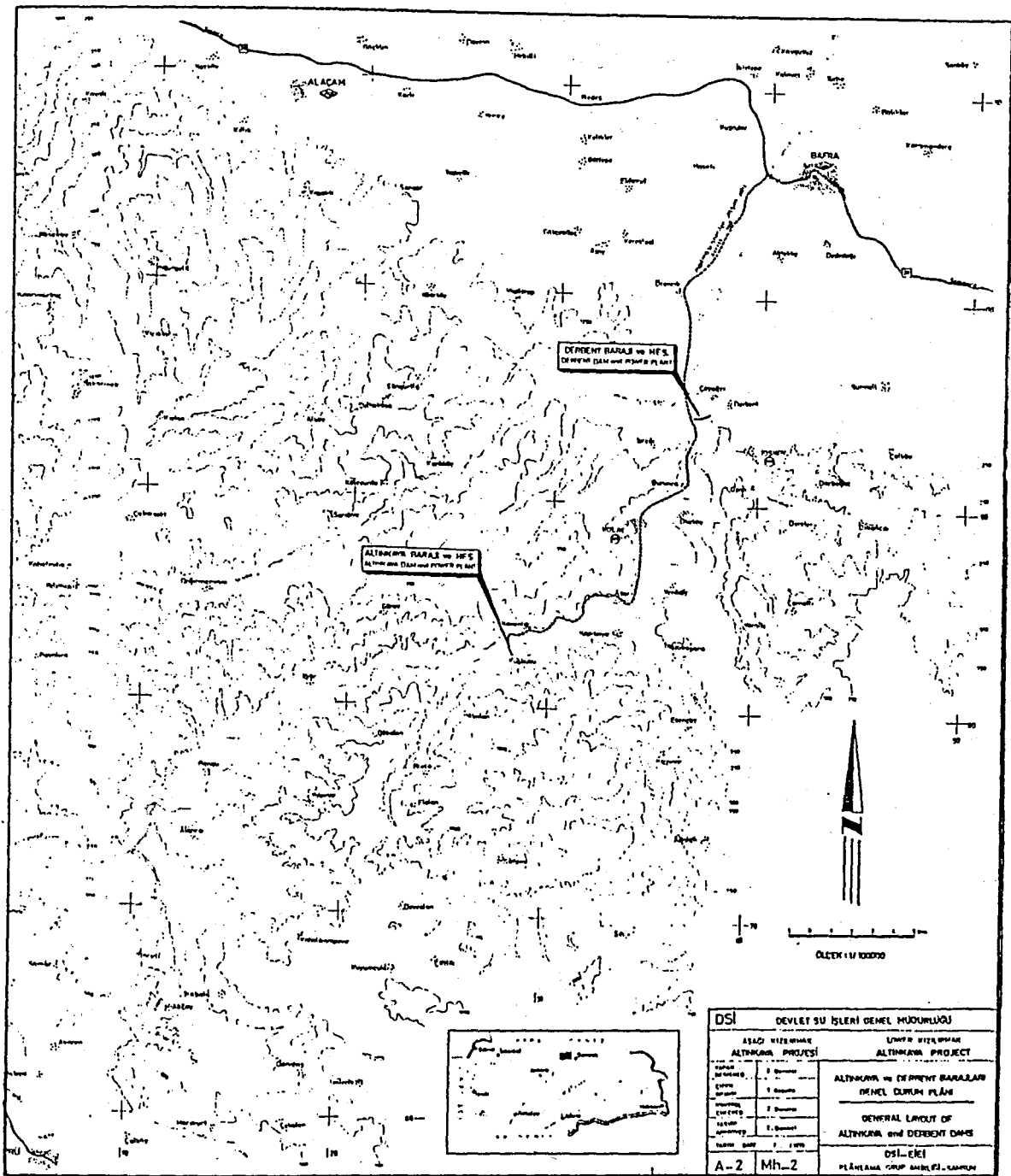


Fig. 4.1 Location Map of Altinkaya Dam

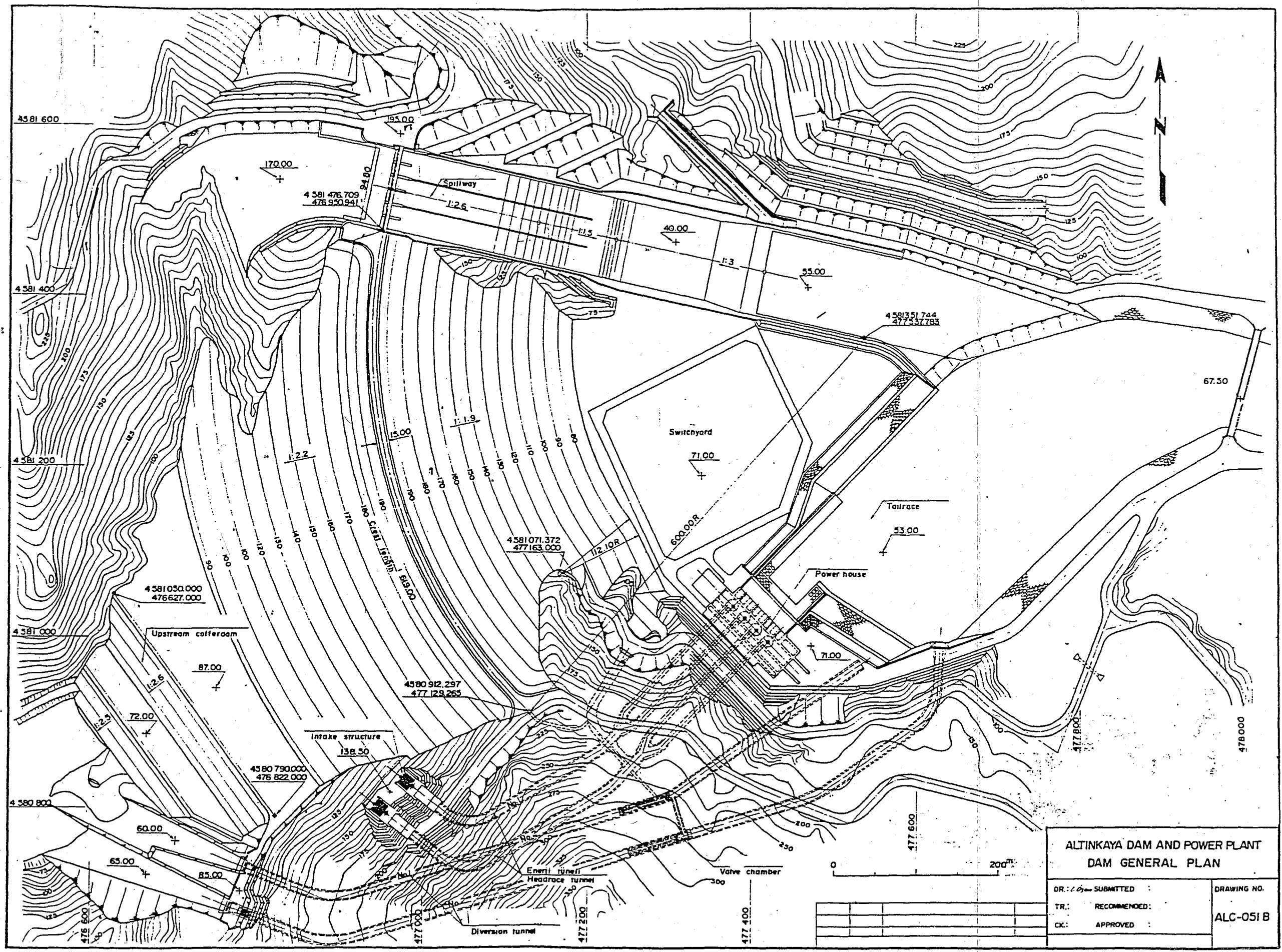


Fig. 4.2 Plan View of Altinkaya Dam

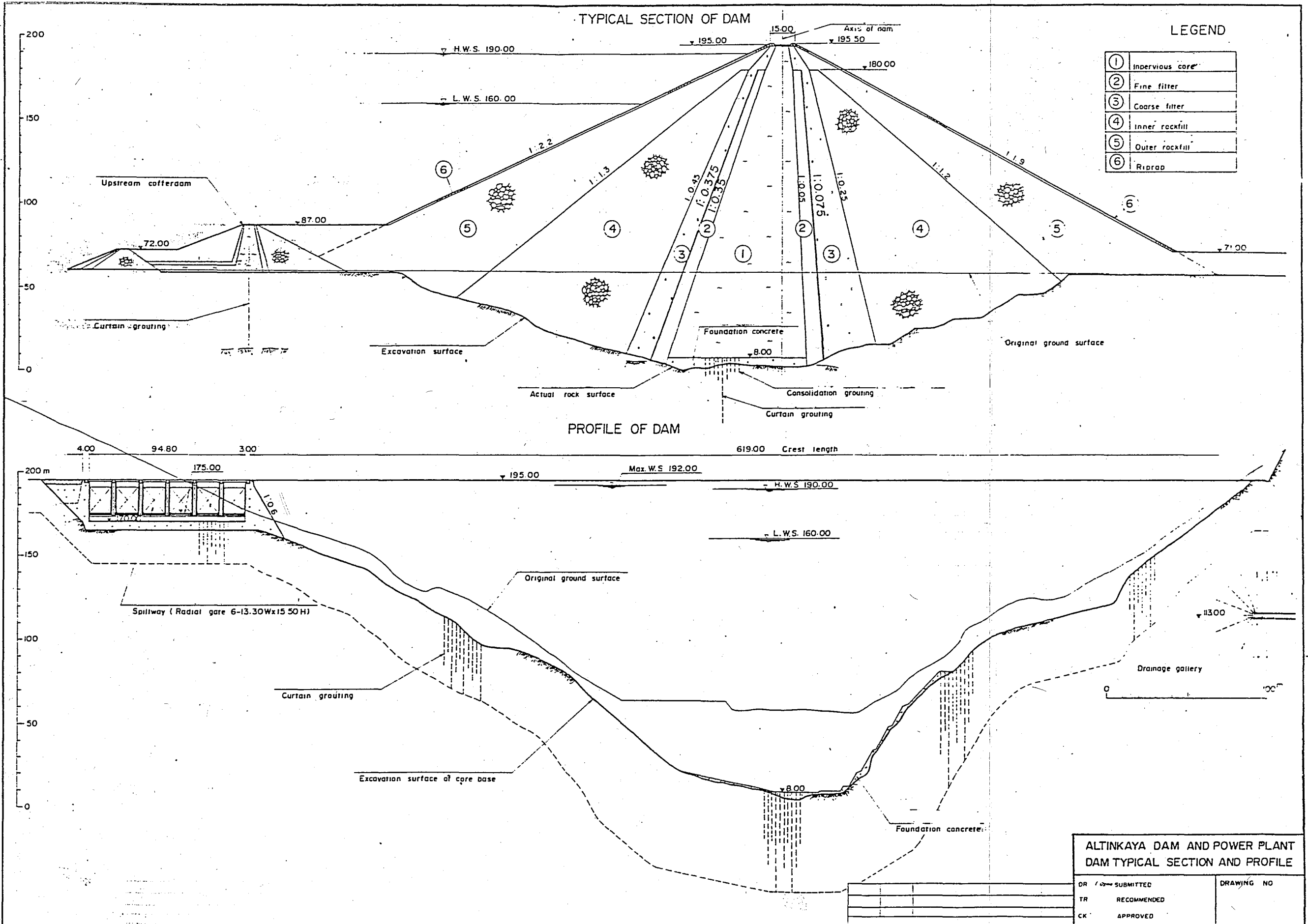


Fig. 4.3 Typical Design Section and Profile of Altinkaya Dam

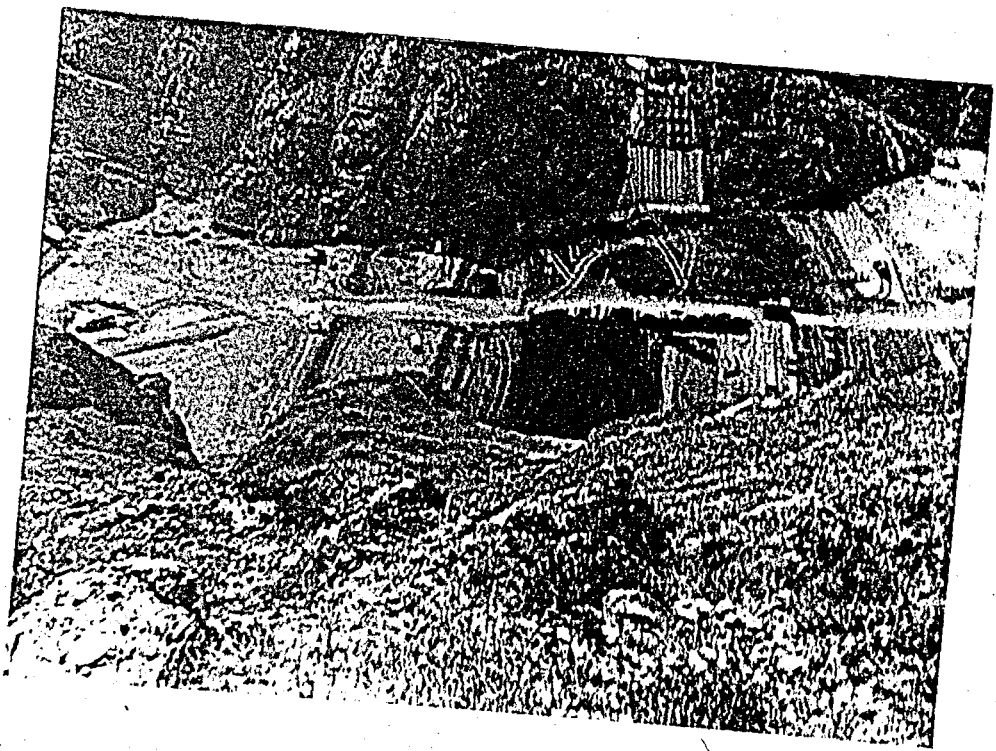
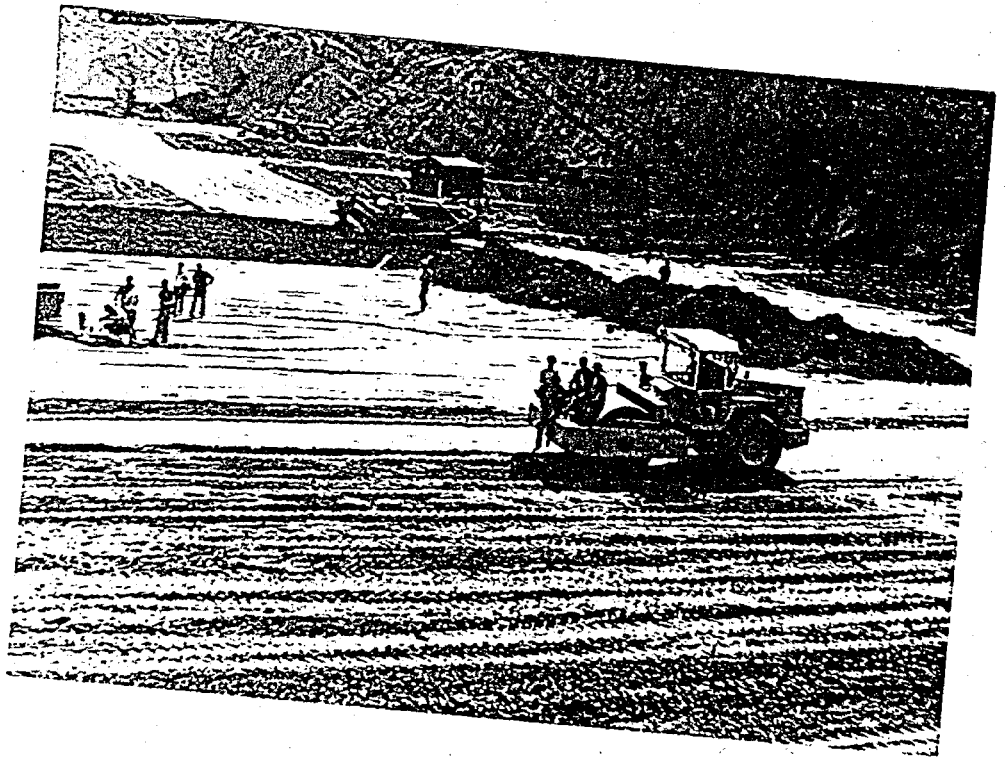


Fig 4.4 Views Showing The Fill Placement in Altinkaya Dam

4.3 FINITE ELEMENT IDEALIZATION OF ALTINKAYA DAM

The finite element idealization of Altinkaya Dam is illustrated in Fig 4.5. As seen in this figure, the discretization of the medium was undertaken by using 246 quadrilateral elements with a total of 283 nodal points. The analyses were performed using 11 layers and one cycle of iteration per layer, to insure the degree of correspondence between the computed values of stress and the values of the tangent modulus and the tangent poisson's ratio for each element. The nodal points through the bottom of the embankment were of constrained deformations assuming the foundation (bedrock) of the embankment to be rigid in the analyses.

Clough and Woodward (1967) have shown that the foundation deformations can have a significant effect on both the displacements and the stresses developed in earth embankments so the finite element analysis should include a portion of the foundation zone in the structural idealization. Therefore, the alluvial deposits underlying the upstream and downstream shell zones were included in the analyses. On the other hand, the main embankment contains a small portion of the upstream cofferdam. But this was not taken into consideration in the analyses as the effect of cofferdam deformations was appeared to be negligible.

4.4 PROPERTIES OF THE MATERIALS IN ALTINKAYA DAM

The major zones of the embankment are the shell, alluvial deposit, filters (transition) and impervious core as seen in Fig 4.6. The gradation curves for these materials obtained from the State Hydraulic Works of Turkey (DSI) are shown in Fig 4.7 and the material properties are presented in Table 4.1.

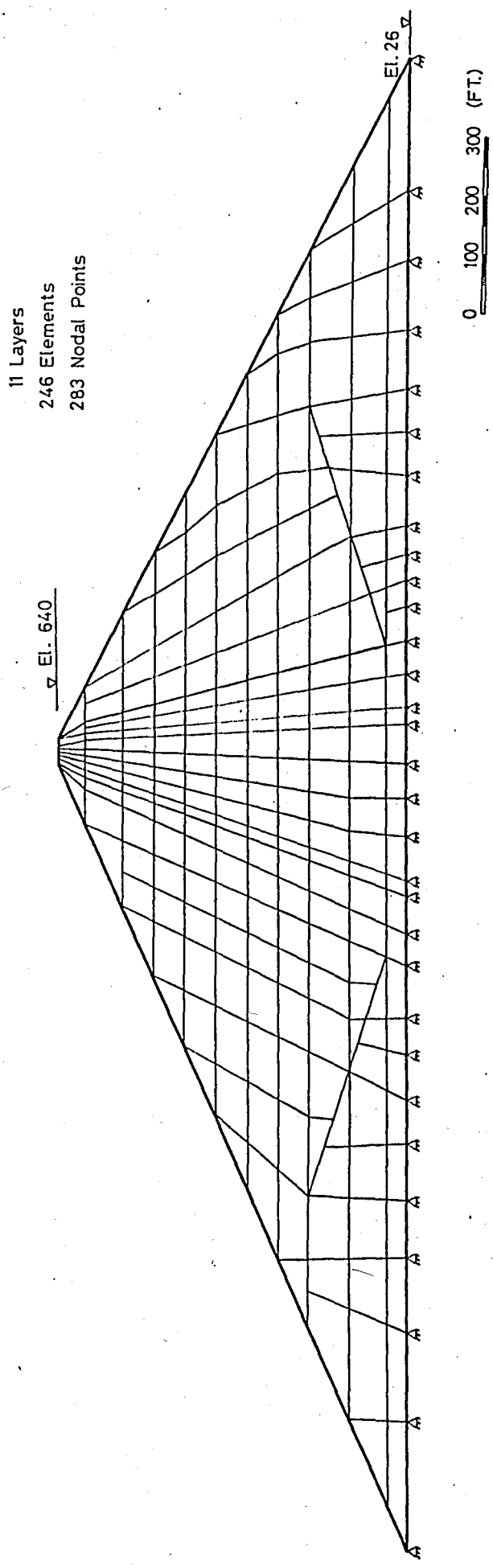


Fig. 4.5 Finite Element Mesh For Altunkaya Dam

LEGEND

①	Shell
②	Alluvial deposit
③	Filter
④	Impervious core

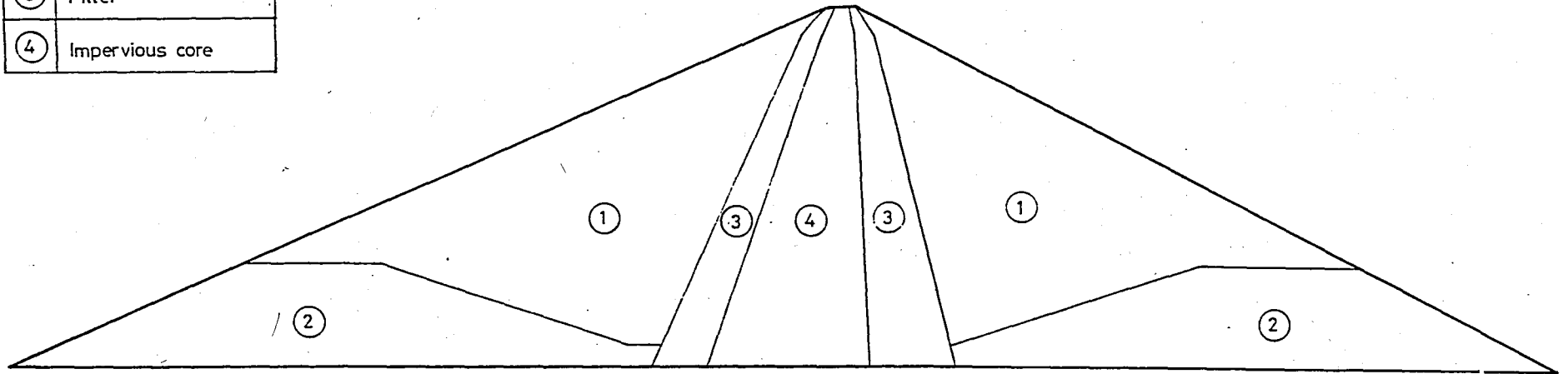


Fig. 4.6 Major Zones of Altinkaya Dam Considered in the Finite Element Analyses

TABLE 4.1 Material Properties of Altinkaya Dam, (Data From State Hydraulic Works of Turkey, DSI)

SOIL GROUP	SOIL DESCRIPTION	Grain Size (mm)			w_L (%)	PI (%)	γ_{dmax} (pcf)	w_{opt} (%)	γ_d (pcf)	e_o	D_r (%)	S_r (%)	Stress range (tsf)	No. of Tests	c (tsf)	ϕ
		D60	D30	D10												
CL	Clay Core	0.045	0.003	-	41.9	22.7	110	19.7	105	0.55	-	80.6	0.93-3.72	3	1.26	15.5
SP-GP	Fine Filter	8.5	1.1	0.3	-	-	140	5.3	133	-	81.5	-	-	-	-	-
SP-GP	Coarse Filter	16.0	3.0	0.4	-	-	148	4.1	142	-	86.2	-	-	-	-	-
GW-GP	Inner Rockfill	100.0	30.0	3.0	-	-	129	-	-	0.30	-	-	-	-	-	-

D60 = Grain size of 60% passing

w_L = Liquid limit

γ_{dmax} = Max. dry unit weight

e_o = Initial void ratio

ϕ = Friction angle

D30 = Grain size of 30% passing

PI = Plasticity index

γ_d = Dry unit weight

S_r = Degree of saturation

D10 = Grain size of 10% passing

w_{opt} = Optimum water content

D_r = Relative density

c = Cohesion intercept

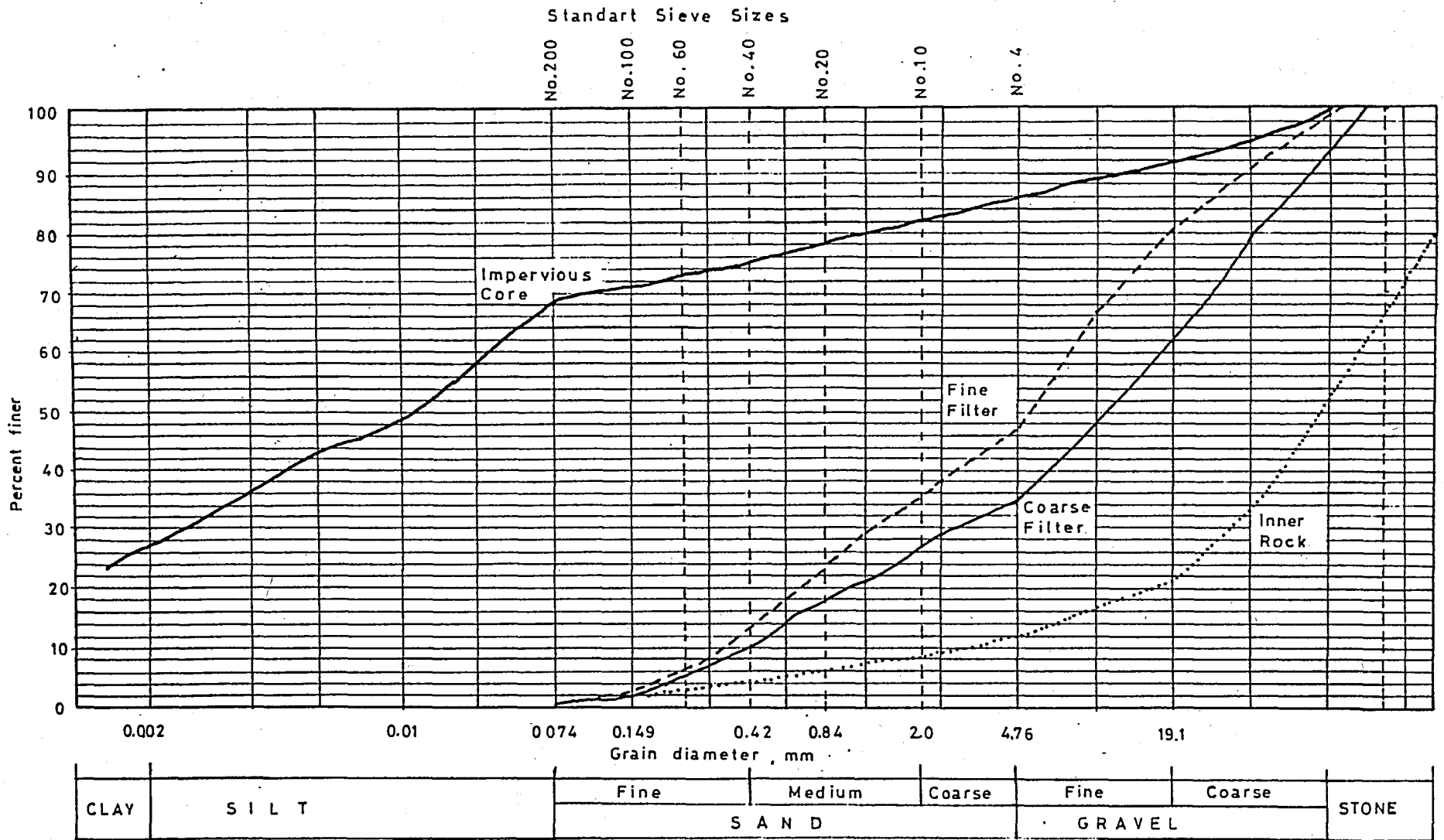


Fig. 4.7 Gradation Curves For the Materials Used in Altinkaya Dam (Data From State Hydraulic Works of Turkey, DSI)

The shell material is a kind of rock composed of tuff and breccia on the upstream face , and massive tuff, breccia and limestone on the downstream face of the embankment. Although there are two zones of rockfill namely: inner rockfill and outer rockfill, they differ from each other only in gradation in other words the properties of outer rockfill is quite similar to that of inner rockfill. In addition, there was not so much data available for the outer rockfill, therefore, the inner and outer rockfills were taken to be the same material for all practical purposes.

The fine filter and coarse filter materials are basically obtained from the alluvial material excavated from the river bed and they can be classified as silty sandy gravel or sandy gravel (GP) according to the Unified Soil Classification System. These filter materials could also be taken in the analysis as the same material even though they differ in gradation.

It should also be noted that the filter materials are somewhat finer than the alluvial soil, though they are basically the same material. In fact, the alluvial soil has been found to be poorly graded soil as required for a filter material.

The impervious core material, on the other hand, which is hauled from the borrow pits near the construction site, can be classified as sandy clay or lean clay (CL) according to the Unified Soil Classification System.

Although it has been desired to determine the hyperbolic stress - strain parameters of the materials of Altınkaya Dam from the results of triaxial tests conducted under appropriate drainage conditions, it became impossible as laboratory data regarding the embankment materials were unavailable except the triaxial test data for impervious core material. The data from the UU triaxial tests on the core material was the Mohr envelope

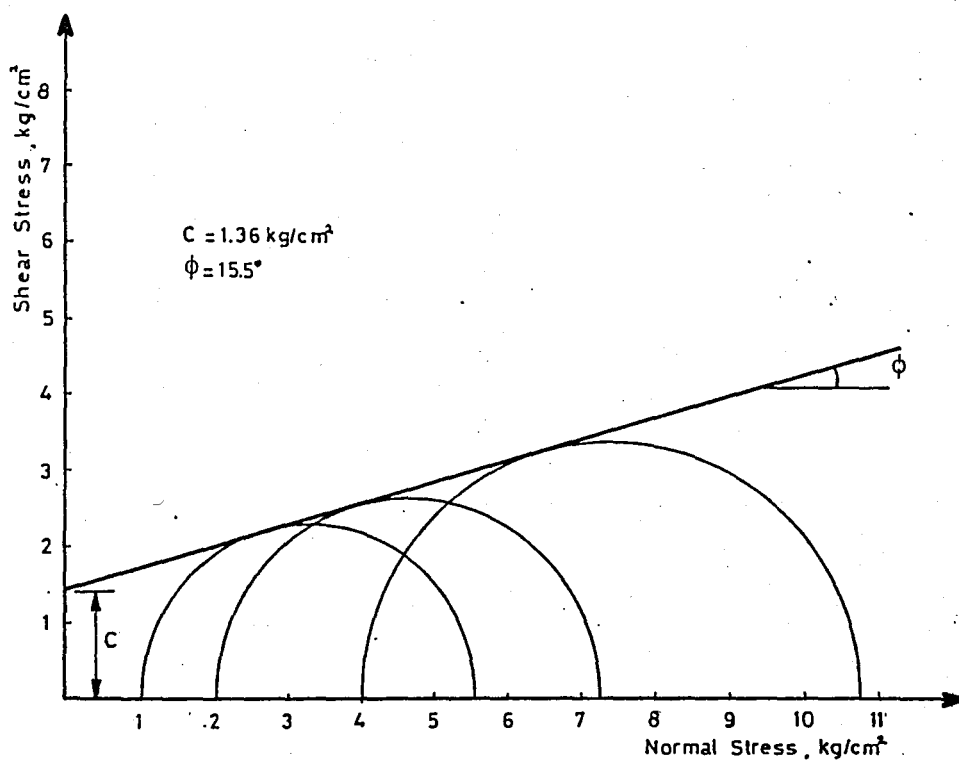


Fig. 4.8 Mohr Envelope For UU- Triaxial Tests on Altinkaya
 Dam Core Material (Data from State Hydraulic Works
 of Turkey, DSI)

and it was used for determining the cohesion intercept (c) and the friction angle (ϕ) of core material (Fig 4.8). The rest of the parameters of embankment materials for use in the finite element analysis of Altinkaya Dam were chosen from Table A.1 and A.2 considering the material properties.

The values of hyperbolic stress-strain parameters used in the analysis are summarized in Table 4.2. It is interesting to note that the parameter values for alluvial deposit have been chosen so that the value of K is greater than that of filter. This is because of the fact that the poorly graded soils have greater values of K than the well-graded soils as explained previously. Furthermore, the parameter values for shell, alluvial deposit and filter zones were chosen from the table for soils tested under drained conditions (Table A.1) whereas the parameter values for impervious core material were chosen from the table for soils tested under unconsolidated-undrained conditions (Table A.2).

4.5 NONLINEAR FINITE ELEMENT ANALYSIS OF ALTINKAYA DAM

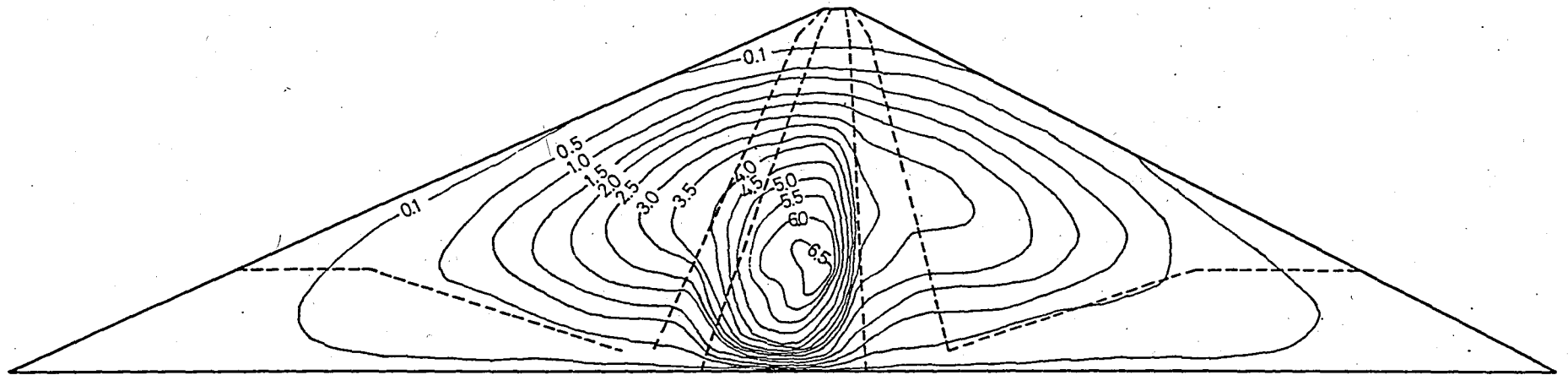
The behaviour of Altinkaya Dam during construction were investigated using the computer program LSBUILD and performing two different finite element analyses, namely: the nonlinear finite element analysis and the build-up analysis. The results of these analyses were also compared to each other for investigating the effect of different types of analyses on the stresses and movements of the embankment.

4.5.1 SETTLEMENTS (VERTICAL DISPLACEMENTS) IN ALTINKAYA DAM

After having performed the nonlinear finite element analysis of Altinkaya Dam during construction, the settlement contours have been drawn as shown in Fig 4.9. As there was no device installed for measuring the

TABLE 4.2 *Hyperbolic Stress-Strain Parameters Used in the Nonlinear FEM Analysis of Altinkaya Dam*

ZONE	SOIL GROUP	K	n	D	G	F	c (tsf)	ϕ	R _F
Shell (Rockfill)	GW-1	540	0.43	6.4	0.31	0.10	0	50	0.64
Alluvial deposit	GP-13	2500	0.21	14.6	0.35	0.17	0	58	0.75
Filter	GP-7	1500	0.34	15.5	0.40	0.15	0	51	0.54
Clay core	CL-13E	410	0.15	7.6	0.32	0.11	1.26	15.5	0.87



Settlement contours are in FT., Settlement is positive

Fig. 4.9 Contours of Settlement in Altinkaya Dam (Nonlinear Analysis)

deformations of dam body during construction, these results can be used to determine the behavior of Altinkaya Dam.

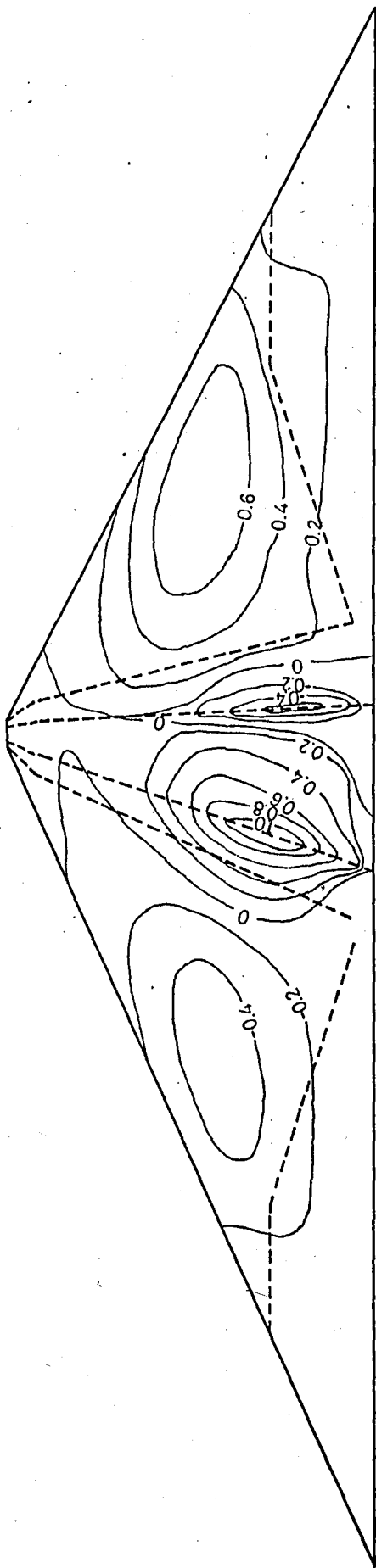
These contours show that the maximum settlement which is less than 7 ft. occurs in the impervious core at one third of the embankment height from the bottom close to the center line. It is interesting to note that the soft core settles with respect to the adjacent coarse zones resulting a load transfer from the core to the adjacent coarse zones. Moreover, it can be said that the settlement in the upstream shell is greater than in the downstream shell. This is because the upstream face of the impervious core is flatter than the downstream. A similar aspect can also be seen in this figure that the upstream filter zone settles more than the downstream one.

On the other hand, the settlement of impervious core seems to be decreased since it is partially restrained by the filter zones, which is clearly seen on the upstream face of impervious core. In addition, both of the shells settle with respect to the filter zones indicating that there exists a stress concentration in the filter zones.

The maximum settlements in the alluvial deposits are about 0.5 feet and they take place at the contact areas between shells and alluvial deposits. Therefore, it may be stated that both the settlements of impervious core and alluvial deposits result in the settlement of shells.

4.5.2 HORIZONTAL DISPLACEMENTS IN ALTINKAYA DAM

The contours of horizontal displacements obtained from the non-linear finite element analysis of Altinkaya Dam are shown in Fig. 4.10. As this figure indicates, the amount of maximum horizontal displacement is more than 1 ft occurring in downstream direction at the contact surface between



Horizontal displacement contours are in F.T., Downstream is positive (→)

Fig. 4.10 Contours of Horizontal Displacement in Altonkaya Dam (Nonlinear Analysis)

the upstream filter zone and the impervious core, as would be expected. In fact, the major horizontal movement in the embankment also seems to occur in the downstream direction.

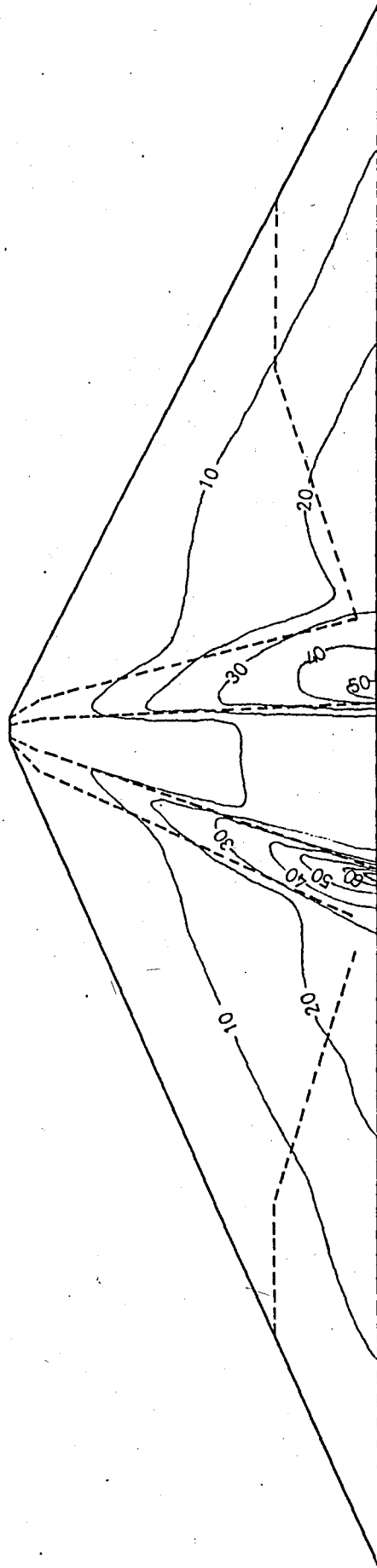
In the upstream shell, the movement of which maximum is about 0.5 ft is in the upstream direction while the upstream filter zone moves towards the centerline of the embankment. This is, of course, due to the fact that the soft core settles more than the adjacent zones and a part of upstream shell and the filter zone move into the core block. This is also the reason why the upper elevations of upstream shell moves slightly in a downstream direction.

Further, the downstream shell moves in a downstream direction and the amount of displacement in this zone varies 0.2 ft to 0.6 ft. However, there exists a small zone at the contact surface between downstream filter zone and core block in which the horizontal displacement is in upstream direction caused by core settlement.

4.5.3 STRESSES IN ALTINKAYA DAM

The finite element analysis also provides values of stresses developed within the embankment during construction and it is very useful in predicting what types of phenomena will occur in the embankment.

The contours of major principal stress, σ_1 , are shown in Fig.4.11 in Altinkaya Dam. It can be easily seen that there are load transfers from the soft core to the filter zones causing stress concentrations in the filter zones. This is again due to the settlement of core block with respect to the coarse zones as explained previously. The amount of maximum stress in transition zones reaches approximately $2.3\gamma H$. However, in the core block, a stress reduction is observed and the value of σ_1 is approximately equal to the half



Contours are in TSF.

Fig. 4.11 Contours of Major Principal Stress in Altunkaya Dam (Nonlinear Analysis)

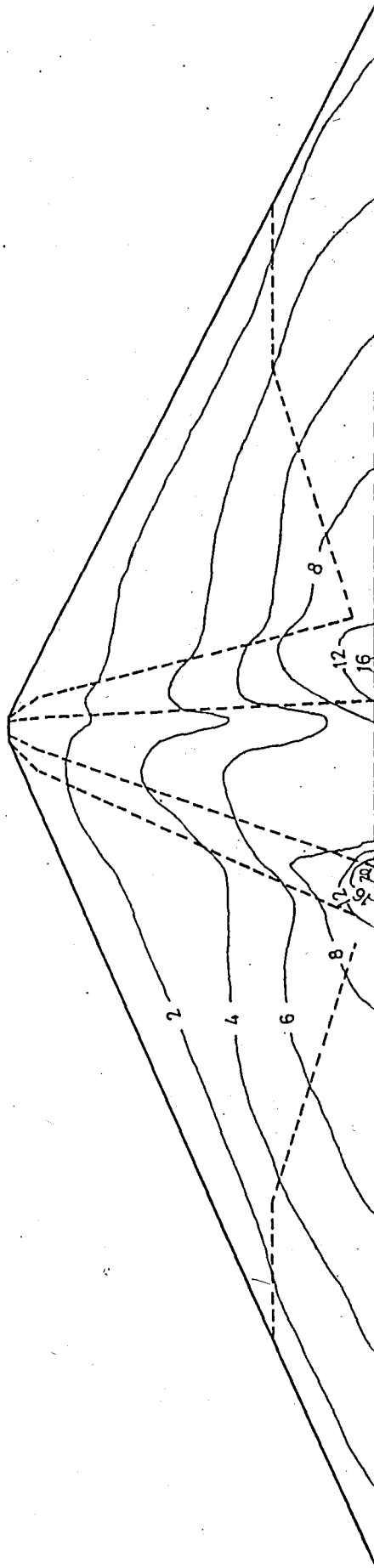
of the overburden pressure. A stress reduction as much as this has been measured in Gepatsch Dam in Austria (Schober, 1967).

The contours of minor principal stress, σ_3 , as illustrated in Fig 4.12, are similar to the contours of σ_1 . As seen in this figure, there exists a stress reduction in the core block while the transition zones are overstressed. It is also interesting to note that tensile stresses which might cause cracking don't exist throughout the embankment.

The contours of maximum shear stress, τ , are indicated in Fig 4.13. They are very similar to that of major principal stresses and shows that the shear stresses are small in the shells and core block than the transition zones. The maximum value of τ (>20 TSF) takes place in both of the transition zones in which stress concentrations exist.

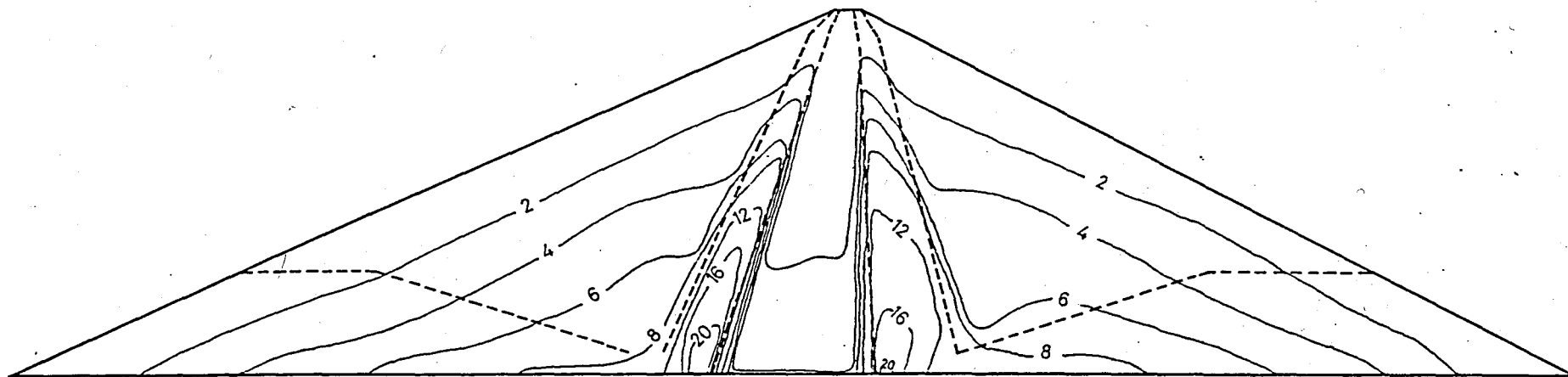
The values of mobilized strength which can be also used for predicting whether load transfers occur, are also shown in Fig 4.14. Furthermore, the mobilized strength defined as the ratio of mobilized deviator stress to the deviator stress at failure, provides information about the development of local failure in the embankment.

In Fig 4.14, the value of maximum mobilized strength is slightly greater than 80% which suggests that the factor of safety against local failure is about 1.25. The maximum mobilized strength occurs in the core near downstream transition zone where the minor principal stress, σ_3 , is considerably low. The settlement of core block with respect to adjacent filter zones results in a load transfer from the core to the adjacent zones, as stated previously. This becomes clear since the mobilized strength is increased in the filter zones, particularly in the upstream filter, and its value varies between 60% and 70%. As the critical failure surface for an overall stability analysis will pass through the center of the contours



Contours are in TSF.

Fig. 4.12 Contours of Minor Principal Stress in Altnkaya Dam (Nonlinear Analysis)



Contours are in TSF.

Fig. 4.13 Contours of Maximum Shear Stress in Altinkaya Dam (Nonlinear Analysis)

$$\text{Mobilized Strength} = \frac{(\sigma_1 - \sigma_3)_{\text{mobilized}}}{(\sigma_1 - \sigma_3)_{\text{failure}}}$$

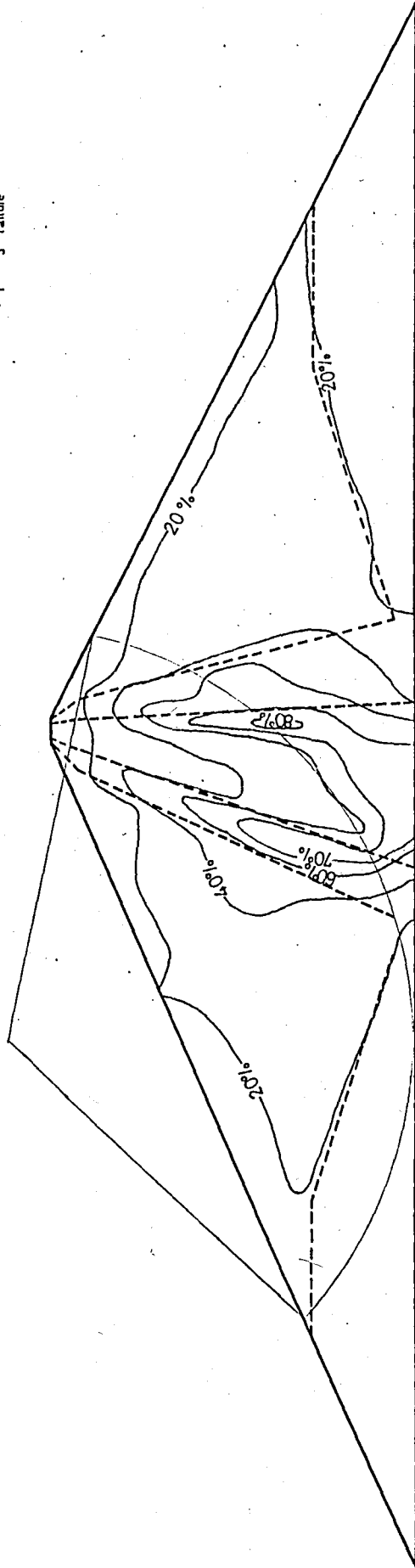


Fig. 4.14 Contours of Mobilised Strength in Altrunkaya Dam (NonLinear Analysis)

of maximum mobilized strength, it can be stated that the most critical failure surface for Altinkaya Dam will pass through the areas shown in Fig 4.14. It is obvious that the factor of safety against local failure will always be less than that of overall shear failure since the mobilized strength values at all the points along the critical failure surface are not as low as 80%.

4.6 BUILD-UP ANALYSIS OF ALTINKAYA DAM

The build-up analysis of Altinkaya Dam has also been conducted for comparison purposes. Since a build-up analysis assumes constant values of elasticity modulus and poisson's ratio following the construction sequence, it became necessary to determine the appropriate values of these parameters representing each zone. The best way of doing this was to take the average values of tangent modulus and poisson's ratio of each element in each zone obtained from the nonlinear analysis of the embankment. Thus, the build-up analysis was performed using the same mesh shown in Fig 4.5 and assigning these constant values of modulus and poisson's ratio as presented in Table 4.3.

Zone	E (tsf)	ν
Shell	612	0.300
Filter	2895	0.255
Alluvial Deposit	1381	0.424
Impervious Core	199	0.328

TABLE 4.3 Values of E and ν used in the build-up analysis of Altinkaya Dam

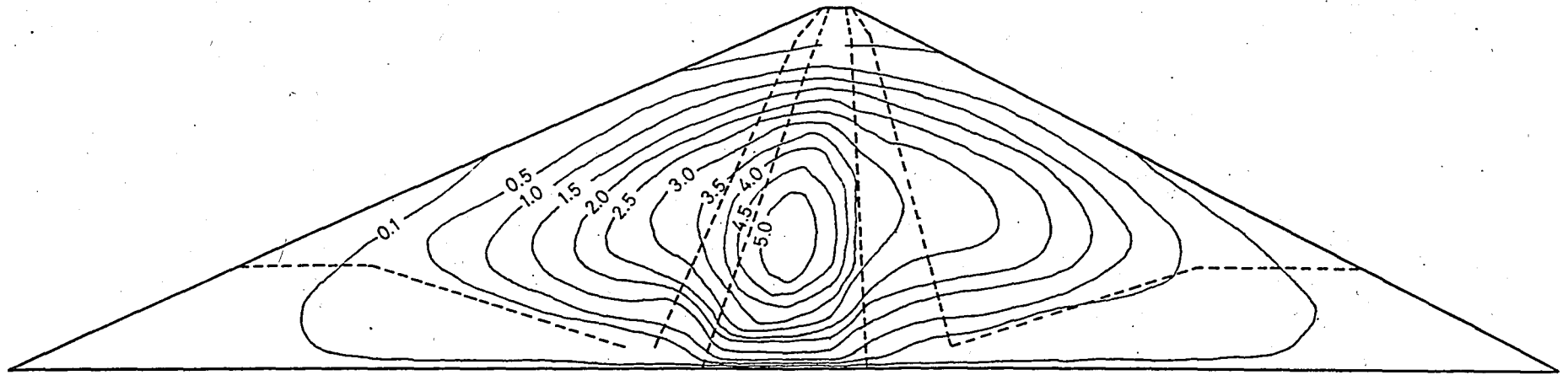
4.7 COMPARISON OF THE RESULTS OF THE NONLINEAR AND BUILD-UP ANALYSES OF ALTINKAYA DAM

The results of build-up analysis of Altinkaya Dam are presented as the contoured displacements and stresses so as to make the comparison conveniently, as illustrated in Fig 4.15 through 4.19.

Fig 4.15 shows the settlement contours obtained from build-up analysis. As this figure is compared to that of nonlinear analysis, it is apparent that the settlement contours of these analyses are almost identical but the settlement values calculated from build-up analysis seem to be underestimated being the maximum of about 5.2 ft.

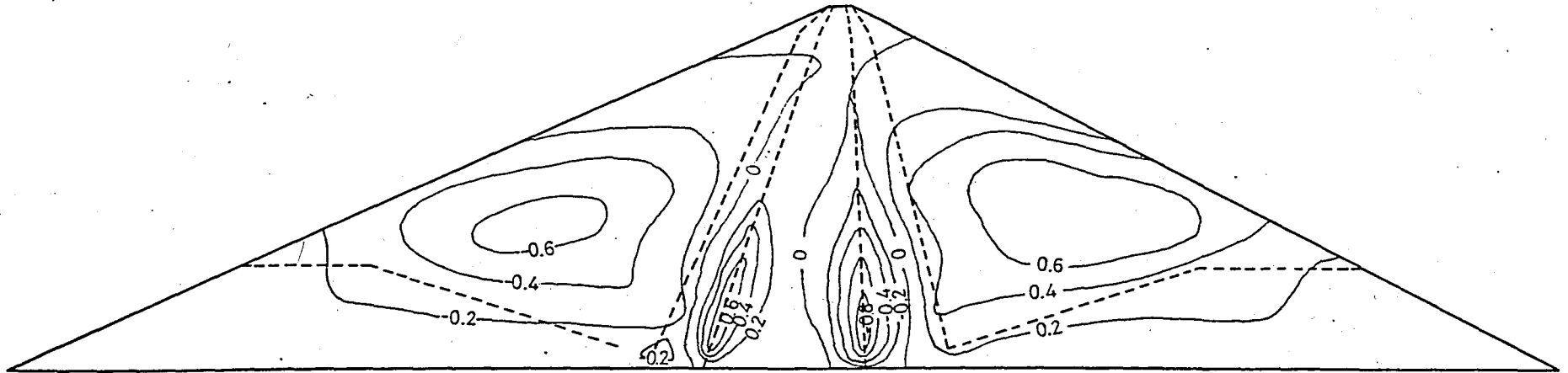
Horizontal displacement contours obtained from the build-up analysis are illustrated in Fig 4.16. Although these contours are also similar to those of the nonlinear analysis, there are small differences between them. For example, while a small decrease in horizontal displacements is observed on the upstream face of the impervious core, there exists a slight increase on the downstream face. Moreover, the horizontal displacements in the shells seem to be slightly increased as compared to the horizontal displacements calculated using nonlinear analysis.

The build-up analysis solution for the major principal stresses is shown in Fig 4.17. As seen in this figure, the major principal stresses are approximately the same as obtained from the nonlinear analysis. However, as shown in Fig 4.18, the minor principal stress values are found to be slightly greater than those of the nonlinear analysis. In addition, the maximum shear stress values seem to be almost the same in the embankment except a small decrease in the filter zones near the bottom of the embankment.



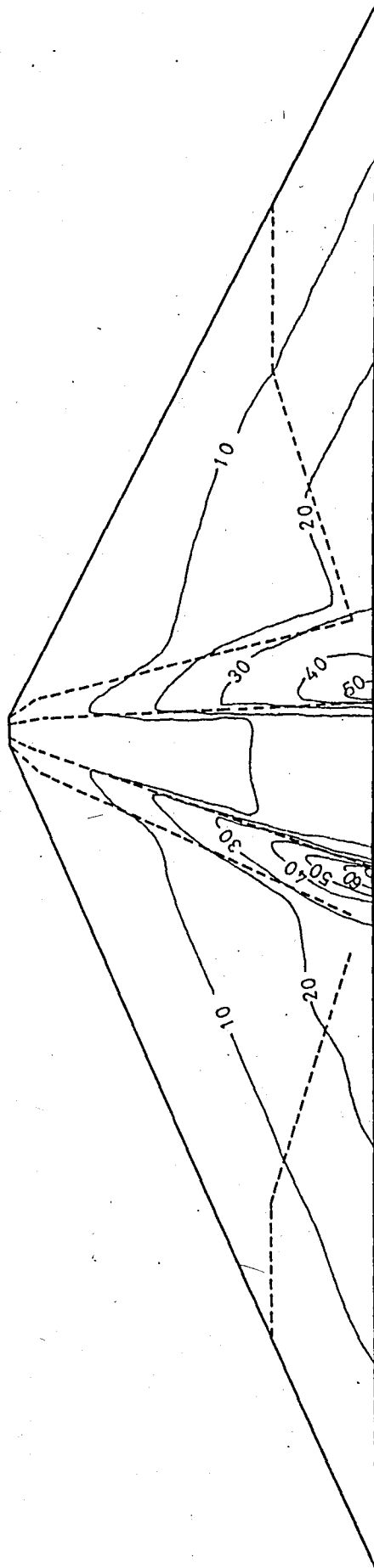
Settlement contours are in FT., Settlement is positive

Fig. 4.15 Contours of Settlement in Altinkaya Dam (Build-up Analysis)



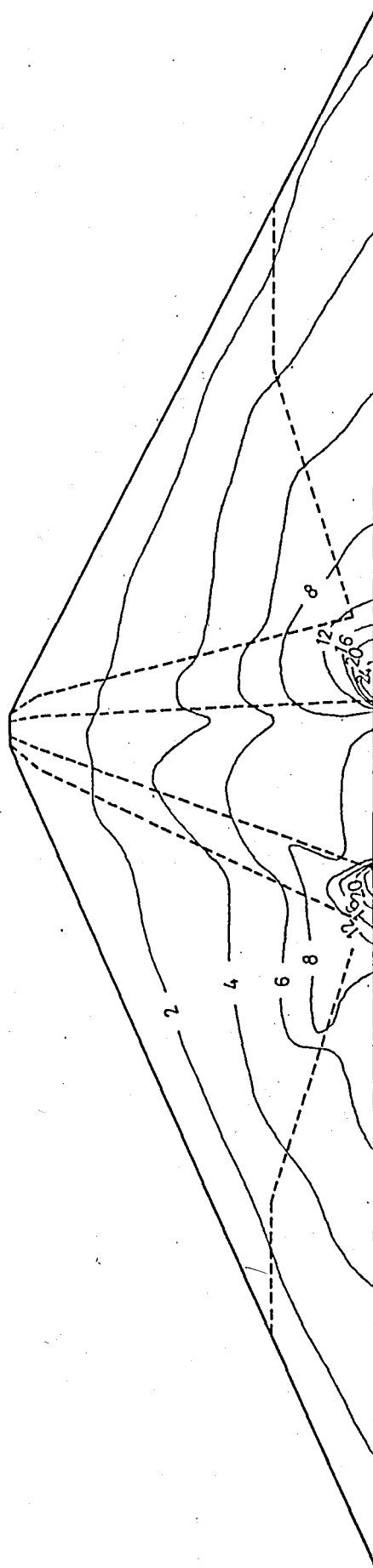
Horizontal displacement contours are in FT., Downstream is positive (→)

Fig. 4.16 Contours of Horizontal Displacement in Altinkaya Dam (Build-up Analysis)



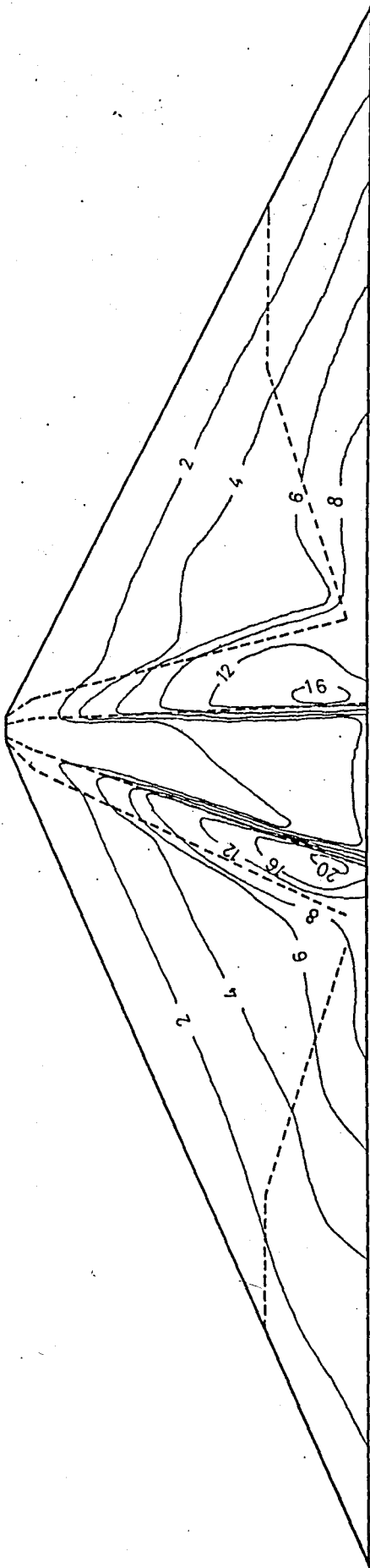
Contours are in TSF.

Fig. 4.17 Contours of Major Principal Stress in Altnkaya Dam (Build-up Analysis)



Contours are in TSF.

Fig. 4.18 Contours of Minor Principal Stress in Altinkaya Dam (Build-up Analysis)



Contours are in TSF.

Fig. 4.19 Contours of Maximum Shear Stress in Altunkaya Dam (Build-up Analysis)

Consequently, it can be stated that the differences in the results of two analyses seem to occur in the areas where a change in σ_3 takes place in build-up analysis. However, it is interesting to note that the build-up analysis can also predict the stresses and movements in embankments reasonably provided that the appropriate values of E and ν are introduced into the analysis.

4.8 RECOMMENDATIONS FOR POSSIBLE INSTRUMENT LOCATIONS

Instruments for measuring movements and pore pressures are needed to install in earth and rockfill dams. The main purpose of instruments is to furnish reliable information that the pore pressures and movements which actually develop in a given dam do not exceed appreciably to values assumed by the designer. Also, the measurements provide very useful information for the dams which will be designed in the future.

The results of finite element analysis are also helpful in interpreting the measurements and determining the possible instrument locations prior to construction. In the construction of Altinkaya Dam, the piezometers were installed for measuring the pore water pressures developed during and after construction whereas no device was installed for measuring movements and stresses. As the results of FEM analyses of Altinkaya Dam show, the most critical zones are the filters and the core. Therefore, if these analyses had been performed prior to construction and it had been decided to equip the dam with the instruments, the possible vertical settlement device locations would have been the core block, particularly near the centre of the core block along the crest, and/or the filter zones. The horizontal displacement measuring devices would have been located into the embankment at an elevation of about 250 ft since at these elevations the horizontal displacements are found to occur in great magnitudes. Moreover, the

the stress meters would also have been installed in filter zones in which stress concentrations seem to exist and in the core block in order to measure the stress reduction.

4.9 SUMMARY AND CONCLUSIONS

The studies presented in this chapter have revealed that the behaviour of Altınkaya Dam during construction can be predicted using the finite element method of analysis. Even though it is desirable to use the nonlinear parameter values determined under appropriate laboratory conditions, the parameter values have been chosen from Table A.1 and A.2 corresponding to the soil properties due to lack of appropriate laboratory data. If the laboratory test results were available, the results of the finite element analyses would of course be more accurate. But, since there was no device installed for measuring the stresses and movements in the embankment, these results are thought to be invaluable in guessing the behavior of the embankment. Results indicate maximum settlement developed in the embankment is less than 7 ft while the maximum horizontal displacement is more than 1 ft in the downstream direction. Even more, the stress concentrations exist in the filter zones and a stress reduction seems to occur in the core. It is also interesting to note that no tensile stresses would be expected to occur in the dam body. On the other hand, the embankment is found to be safe against local failure having a factor of safety of 1.25.

The comparison of the results of the nonlinear and build-up analyses has also shown that the behavior of the embankment could also be estimated using build-up analysis if the appropriate values of modulus and poisson's ratio parameters are introduced into the analysis.

CHAPTER 5
PARAMETRIC STUDY FOR STRESSES AND DEFORMATIONS
OF
ALTINKAYA DAM

5.1 INTRODUCTION

In the previous chapter, the finite element analyses of Altinkaya Dam during construction have been performed and the results have been discussed in detail. The values of parameters regarding the material properties are of special importance in the nonlinear analyses of embankments as explained in Chapter 3 therefore, it has been intended to conduct a parametric study for these parameters.

The studies presented in this chapter were performed so as to determine particularly the effect of modulus parameters K and n on the behavior of Altinkaya Dam during construction, since no comprehensive data was available regarding the material properties of the embankment. In order to do this, the nonlinear analyses of Altinkaya Dam were conducted with range of values of core and shell material parameters taken from Appendix A and the results were discussed in detail indicating the effects of range of these parameters. The ranges for the reasonable values of modulus parameters of core and shell to avoid large displacements were also determined and presented at the end of this chapter.

5.2 THE VALUES OF PARAMETERS USED IN THE ANALYSES

A series of nonlinear finite element analyses of Altınkaya Dam were performed in order to examine the effect of nonlinear parameters on the stresses and displacements of the embankment. In these analyses, attention was given to the parameters of core and shell materials, and particularly the effect of modulus parameters K and n were investigated. For this purpose, the parameters of filter and alluvial deposits were taken as constant with that of nonlinear analysis presented in Chapter 4 while the different parameters of core and shell material were chosen from Table A.1 and A.2, and these values are summarized in Table 5.1.

As seen in Table 5.1, three different groups of parameters were chosen for the core material corresponding to the material properties presented in Table 4.2. It is interesting to note that the values of K for core material vary 280 to 760 while the values of n vary 0.60 to 0.14 respectively as shown in Fig 5.1. Furthermore, it should also be pointed out here that for cohesive soils tested under undrained unconsolidated conditions, the values of n are large for low values of K . On the other hand, three different groups of nonlinear parameters were chosen for the shell material. The values of K for shell vary 210 to 540, and the values of n vary 0.51 to 0.37 as illustrated in Fig 5.2. They slightly differ each other in grain size, water content and dry density.

5.3 THE ANALYSES PERFORMED

Using the nonlinear parameters presented in Table 5.1 two groups of nonlinear analyses of Altınkaya Dam were performed. In the first group, keeping the parameters of shell constant, the analyses were conducted using three different core material parameters and this was repeated for two different shell material parameters as seen in Table 5.2.

TABLE 5.1 Hyperbolic Stress-Strain Parameters for Various Core and Shell Materials

ZONE	SOIL GROUP	K	n	D	G	F	c (tsf)	ϕ	R _f
Core	CL-11D	280	0.60	5.8	0.31	0.10	1.26	15.5	0.93
	CL-13E	410	0.15	7.6	0.32	0.11	1.26	15.5	0.87
	CL-5B	760	-0.14	3.1	0.31	0.09	1.26	15.5	0.97
Shell	GW-2	210	0.51	4.5	0.25	0.09	0	44	0.64
	GP-3	450	0.37	4.8	0.34	0.16	0	52	0.61
	GW-1	540	0.43	6.4	0.31	0.10	0	50	0.64

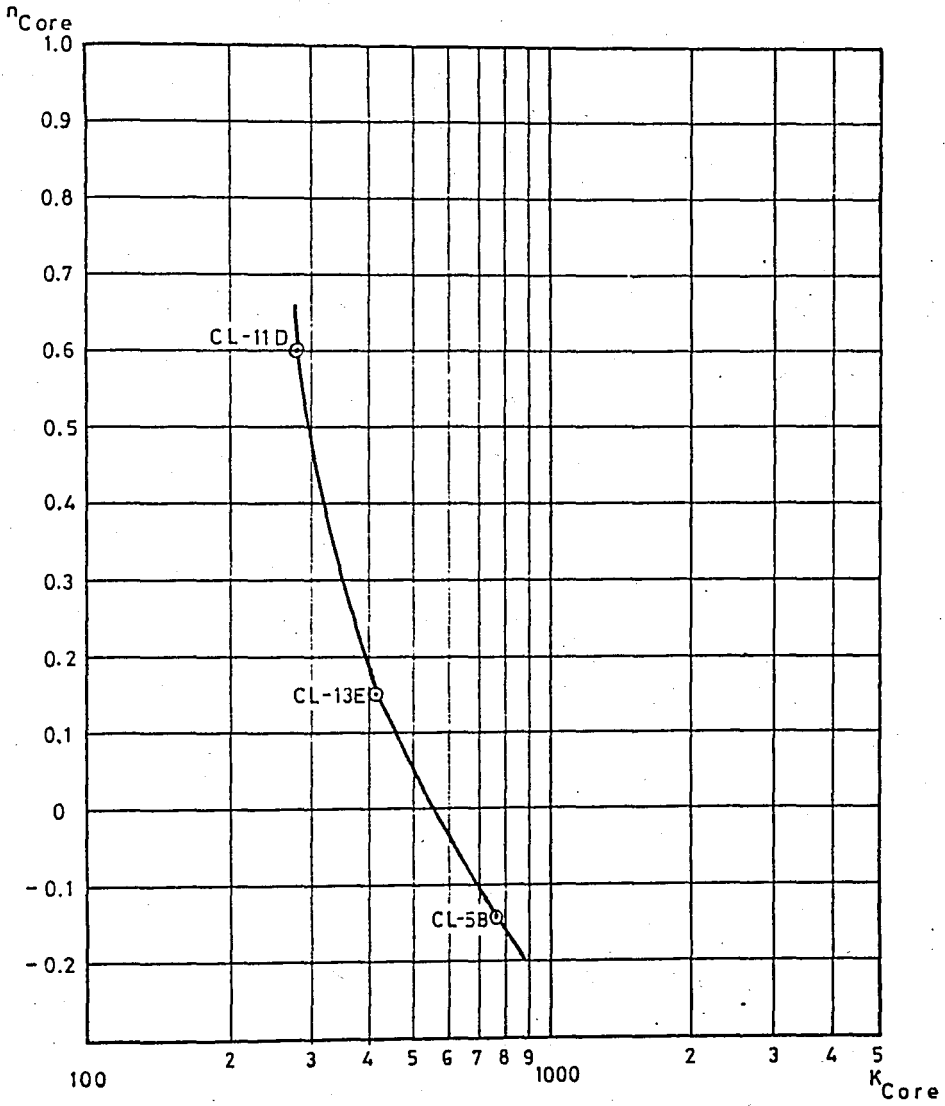


Fig. 5.1 Variation of Modulus Number, K , with Modulus Exponent, n ,
For Core Material of Altinkaya Dam

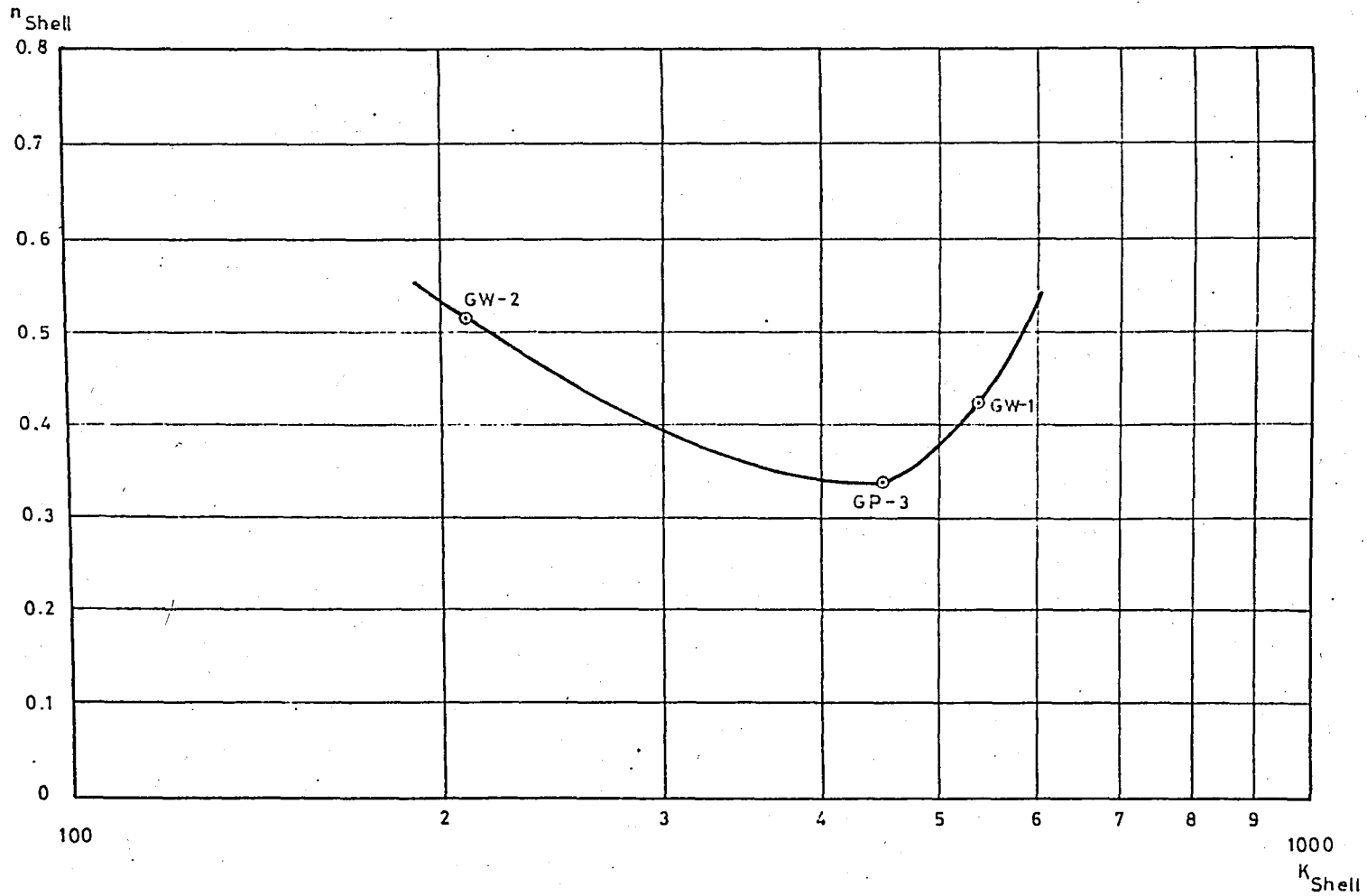


Fig. 5.2 Variation of Modulus Number, K , with Modulus Exponent, n , For Shell Material of Altinkaya Dam

In addition, utilizing the intermediate values of K and n taken from Fig 5.1 together with the poisson's ratio parameters of core CL-13E which have yielded reasonable settlement values, three other analyses were performed to establish the effect of K and n clearly.

In the second group of analyses, however, the analyses were performed using three different shell material parameters while keeping core material parameters constant. Again this was repeated for three different core material parameters as shown in Table 5.3. Further three intermediate values of K and n were also taken from Fig 5.2 and they were used in the analyses together with the poisson's ratio parameters of shell GW-1 which were used in the analyses presented in Chapter 4 and have yielded acceptable values of stresses and displacements. As it is evident, the purpose of the second group of analyses is to determine the effect of K and n of shell material on the behavior of the embankment.

5.4 EFFECT OF CORE MATERIAL

The results obtained from the first group of analyses have been summarized in Table 5.2. As far as the settlement is concerned, in case of stiff cores as compared to shell (Run 1 to 3), the settlement is found to be the largest for the most stiff core material (CL-5B), however, the minimum settlement is obtained for the core material CL-13E which is medium stiff among these three core materials. Similar trend can also be seen for the horizontal displacements. On the other hand, in case of shell GW-1 (Run 7 to 9) which is more stiff than the shell GW-2, maximum settlement also seems to occur for the most stiff core material and the minimum settlement is again obtained for the the core material CL-13E which is more softer than the shell. If the settlement values are plotted against the values of K for both shells as shown in Fig's 5.3 to 5.4 it can be seen

TABLE 5.2 Maximum Displacements and Stress Concentrations for Constant Shell Case

Z O N E			Modulus Parameters		Maximum Displacements				Maximum Stress Concentrations					
Shell	Run No.	Core	K	n	Settlement (ft)	Location (Node No.)	Horizontal disp. (ft)	Location (Node No.)	σ_1 (tsf)	Location (Ele.No.)	σ_3 (tsf)	Location (Ele.No.)	Mobilized Strength (%)	Location (Ele.No.)
GW-2	1	CL-11D	280	0.60	8.40	116	2.08	114	86.7	12	20.9	12	85	110-133
	2	CL-13E	410	0.15	7.16	116	1.57	114	85.9	12	20.8	12	81	110-133
	3	CL-5B	760	-0.14	11.39	116	3.22	114	103.5	12	24.8	12	94	110-133
	4		340	0.31	7.14	116	1.57	114	85.7	12	20.7	12	81	110-133
	5		550	0.01	6.95	116	1.47	114	83.1	12	20.6	12	83	110-133
	6		675	-0.07	7.18	116	1.46	114	83.1	12	19.9	12	87	110-133
GW-1	7	CL-11D	280	0.60	8.19	116	1.65	114	84.7	12	20.3	12	86	110-133
	8	CL-13E	410	0.15	6.96	116	1.23	114	79.5	12	19.2	12	80	110-133
	9	CL-5B	760	-0.14	10.51	116	2.33	114	92.7	12	22.0	12	93	110-133
	10		340	0.31	6.94	116	1.24	114	79.3	12	19.1	12	80	110-133
	11		550	0.01	6.66	116	1.13	114	78.7	12	19.1	12	83	110-133
	12		675	-0.07	6.43	116	1.06	114	78.0	12	19.0	12	84	110-133

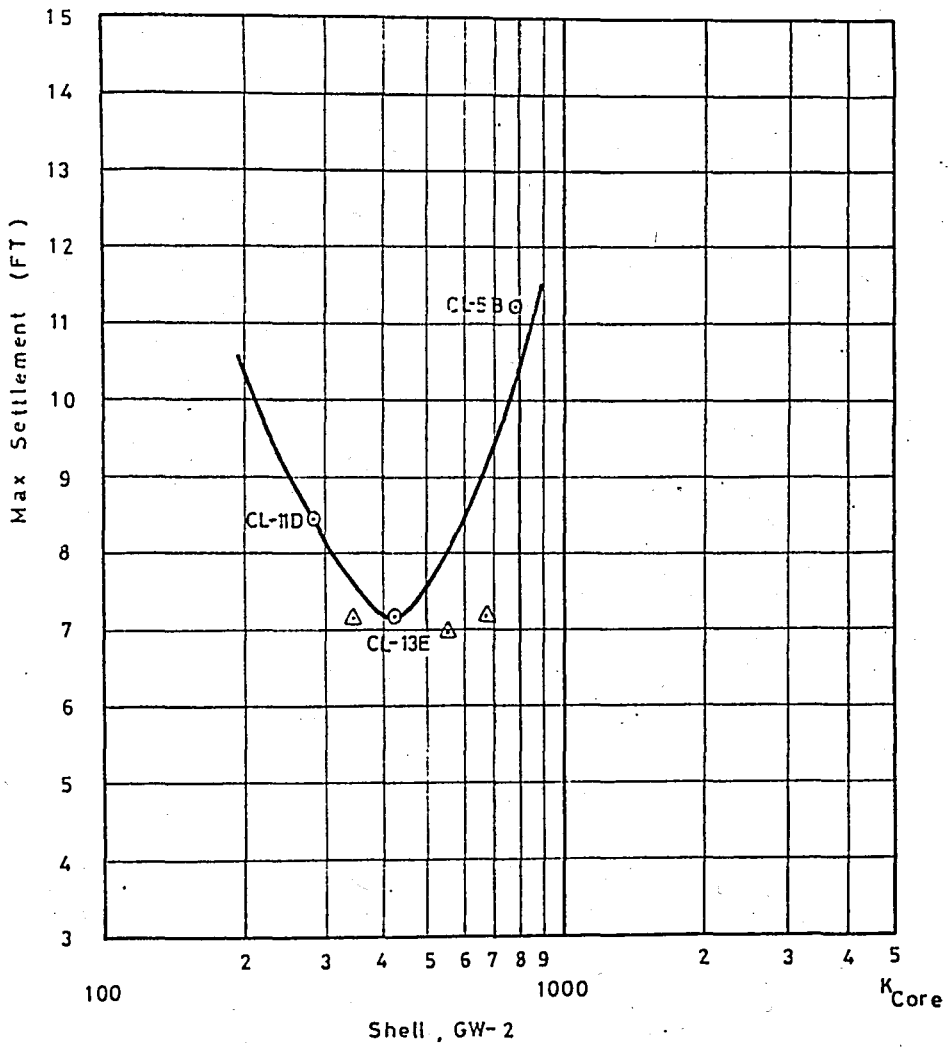


Fig. 5.3 Plot of Maximum Settlement versus Modulus Number K
For Core Material (Shell GW-2)

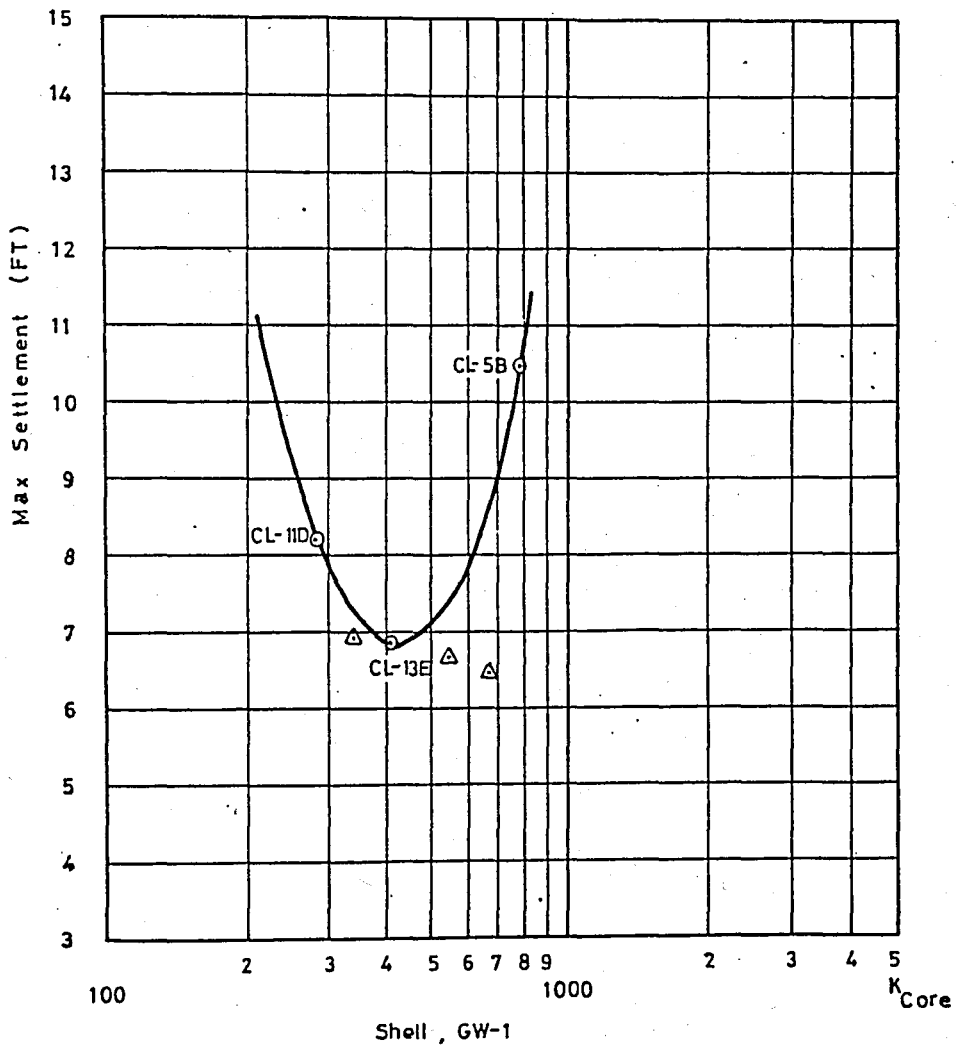


Fig. 5.4 Plot of Maximum Settlement versus Modulus Number K ,
For Core Material (Shell GW-1)

that the minimum settlement values may be obtained for the values of K between 280 and 760. Therefore, taking the intermediate values of K and corresponding values of n , three analyses were also performed for each shell. When the results of these analyses (Run 4-6 and Run 10-12) are compared to each other, it can be stated that, for the shell GW-1 which is more stiff than GW-2, the settlements appear to decrease gradually with increasing the stiffness of the core, however the settlements seem to decrease for the medium stiff core (Run 5) in case of shell GW-2 which is too soft. This indicates that though the change in settlement is not so significant, the settlement tends to decrease if the core material is not too stiff as compared to the shell material, in fact, the core is more softer than the shell. The same thing may be seen as well, if the results of Run 1-3 and Run 7-9 are compared to each other.

As far as the stresses are concerned, however, it may be said that the stresses don't seem to vary a great deal as compared to the displacements. For example, when the results of Run 7 and Run 8 are considered, the maximum settlement decreases by about 15% while the reduction in maximum principal stress is about 5% and the minimum principal stress is decreased by 4%. In addition, it may be pointed out that the mobilized strength values in case of the most stiff core (Run 3 and Run 9) are found to be about 94% yielding a factor of safety against local failure of about 1.06, which implies, for case of too stiff core, local failure may occur.

5.5 EFFECT OF SHELL MATERIAL

The second group of analyses are summarized in Table 5.3, which have been conducted to establish the effect of shell material. The variation of K with the maximum settlement for the core CL-11D could be followed in this table and as well in Fig 5.5. The maximum settlement decreases

TABLE 5.3 Maximum Displacements and Stress Concentrations for Constant Core Case

Z O N E			Modulus Parameters		Maximum Displacements				Maximum Stress Concentrations					
Core	Run No.	Shell	K	n	Settlement (ft)	Location (Node No.)	Horizontal disp. (ft)	Location (Node No.)	σ_1 (tsf)	Location (Ele.No.)	σ_3 (tsf)	Location (Ele.No.)	Mobilized Strength (%)	Location (Ele.No.)
CL-11D	13	GW-2	210	0.51	8.40	116	2.08	114	86.7	12	20.9	12	85	110-133
	14	GP-3	450	0.37	8.21	116	1.63	114	86.5	12	20.8	12	86	110-133
	15	GW-1	540	0.43	8.19	116	1.65	114	84.7	12	20.3	12	86	110-133
CL-13E	16	GW-2	210	0.51	7.16	116	1.57	114	85.9	12	20.8	12	81	110-133
	17	GP-3	450	0.37	7.01	116	1.22	114	81.3	12	19.7	12	80	110-133
	18	GW-1	540	0.43	6.96	116	1.23	114	79.5	12	19.2	12	80	110-133
	19		350	0.37	7.09	116	1.31	114	83.3	12	20.1	12	81	110-133
	20		500	0.39	6.99	116	1.27	114	80.6	12	19.5	12	80	110-133
	21		600	0.52	6.89	116	1.17	114	77.3	12	18.6	12	80	110-133
CL-5B	22	GW-2	210	0.51	11.39	116	3.22	114	103.5	12	24.8	12	94	110-133
	23	GP-3	450	0.37	10.66	116	2.35	114	94.9	12	22.6	12	93	110-133
	24	GW-1	540	0.43	10.51	116	2.33	114	92.7	12	22.0	12	93	110-133
	25		350	0.37	10.89	116	2.56	114	98.1	12	23.4	12	94	110-133
	26		500	0.39	10.59	116	2.43	114	94.3	12	22.5	12	93	110-133
	27		600	0.52	10.36	116	2.21	114	89.9	12	21.5	12	93	110-133

by an amount of 0.21 FT while the K values for shell vary 210 to 540, and for the core CL-5B, as seen in Fig 5.7, the change in the maximum settlement is about 0.88 FT, which may not seem to be important. In other words, the maximum settlement values are not influenced so much by the change of shell material parameters. Nevertheless, in order to show the effects of modulus parameters on the behavior of the dam clearly, three analyses were also conducted for each different core material using the intermediate values of K and n. Although a considerable change in settlement does not happen even the values of K vary 350 to 600 and the values of n vary 0.37 to 0.52, it is obvious that the maximum settlement decreases if the shell is of high values of K, or stiffness (Run 19-21 and Run 25-27). The similar trend is also seen for the horizontal displacements.

Furthermore, the stresses may not seem to be influenced by the change of shell material parameters considerably as seen in Table 5.3. But it should be noted here that the maximum principal stress equals to 103.5 TSF which is about 3 γ h and occurs in case of the most stiff core together with the most soft shell (Run 22), and the stresses tend to decrease with increasing stiffness of the shell relative to the core.

Moreover, it is also observed that the maximum displacement and the stress values appear to happen at the same locations throughout the analyses as shown in Fig 5.8.

Consequently, it may be deduced from the results of these analyses that the maximum displacements change with change of core material parameters significantly, however the shell material parameters don't appear to be as effective as the core material.

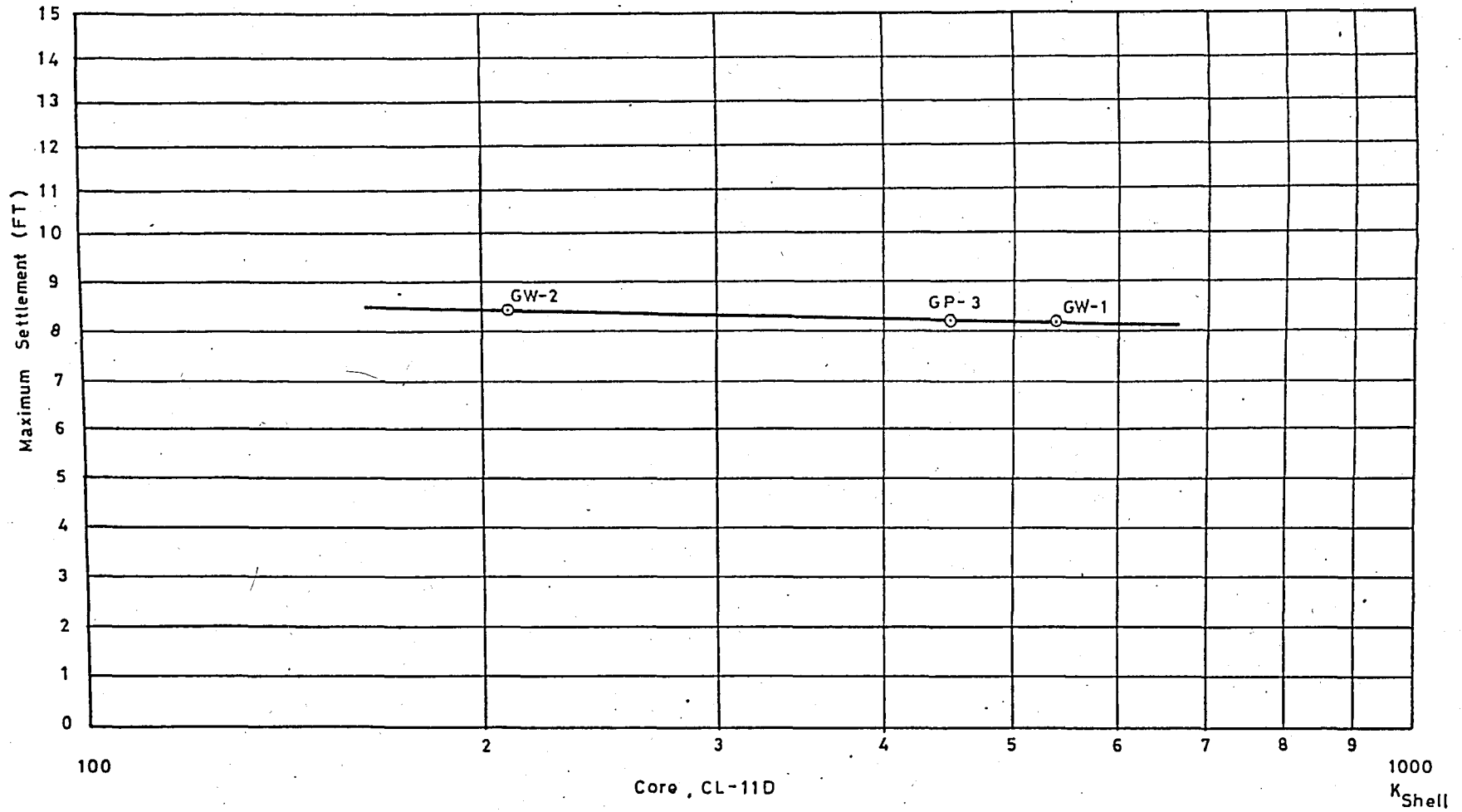


Fig. 5.5 Plot of Maximum Settlement versus Modulus Number, K, For Shell Material (Core CL-11D)

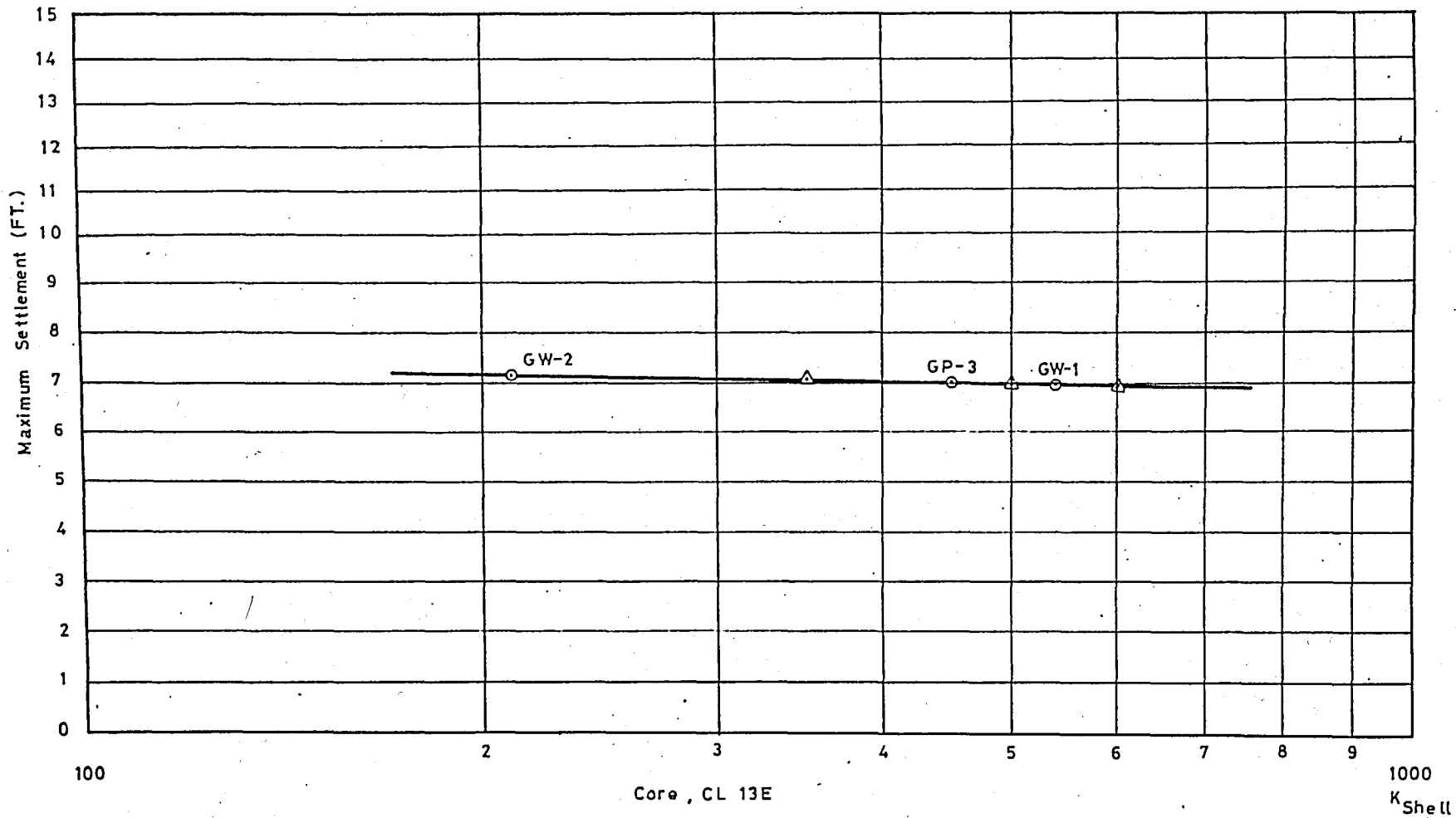


Fig. 5.6 Plot of Maximum Settlement versus Modulus Number, K, For Shell Material (Core CL-13E)

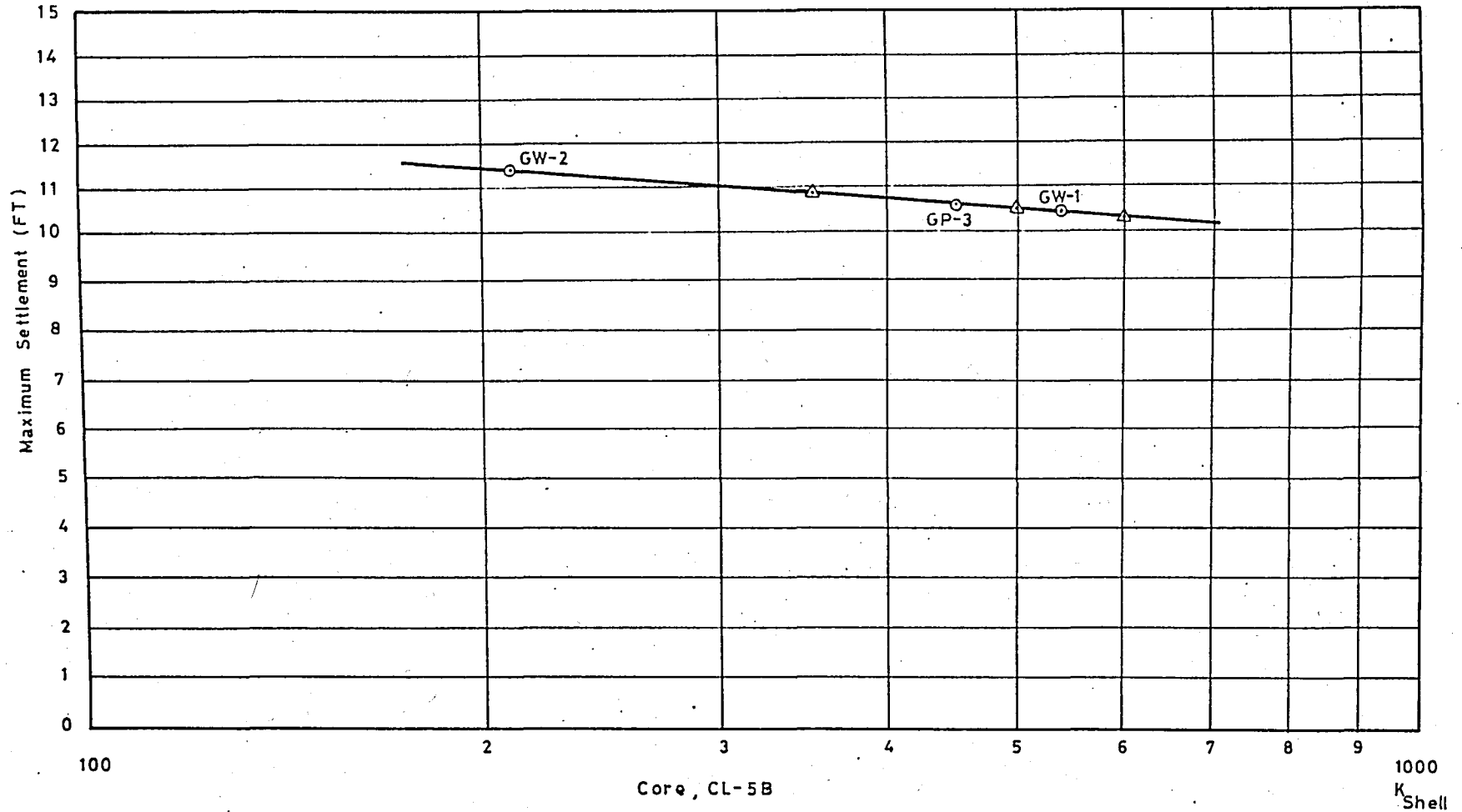


Fig. 5.7 Plot of Maximum Settlement versus Modulus Number, K, For Shell Material (Core CL-5B)

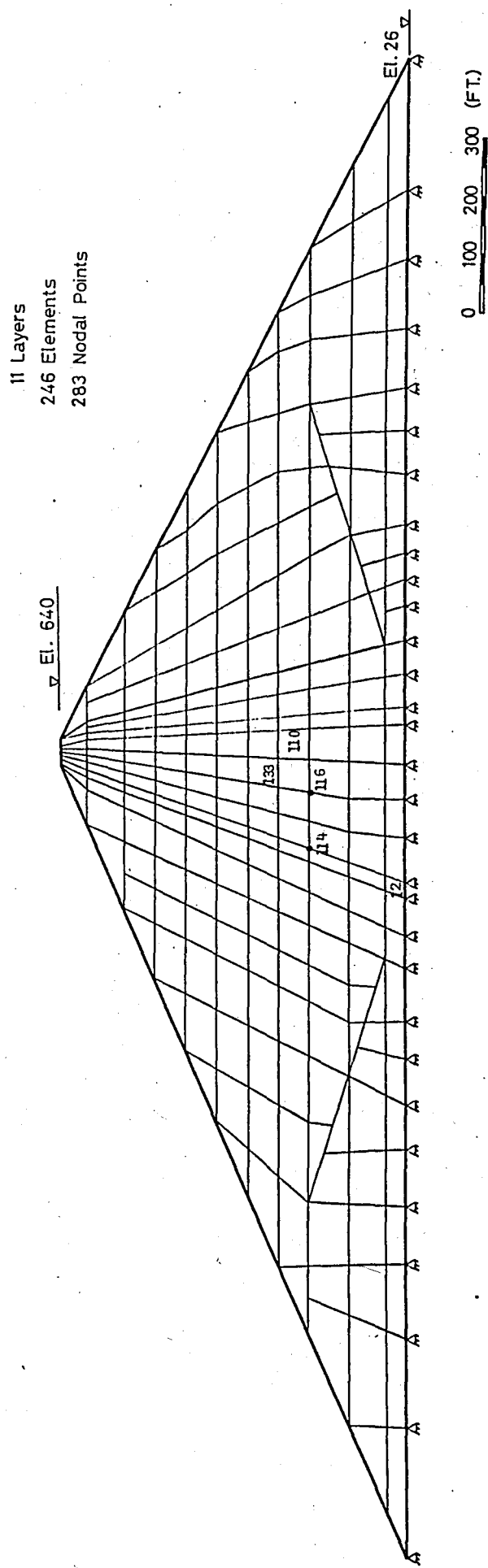


Fig. 5.8 Maximum Stress and Displacement Locations in Altrnkaya Dam

5.6 REASONABLE VALUES OF K and n FOR ALTINKAYA DAM

After having performed these analyses, it is interesting to review the results for the estimated reasonable values of modulus parameters K and n for the core and shell materials of Altinkaya Dam. As the values of stresses are not so much influenced by the change in the values of K and n, the reasonable values of these parameters are to be determined taking the maximum displacement occurred within the embankment into consideration.

As an engineer, it is always desirable to have the vertical and horizontal displacements developed in an embankment as small as possible. By conducting a series of analyses prior to construction, however, it is possible to determine the ranges of K and n in which they yield minimum displacement values. Hence, the soil properties such as water content, grain size, dry density etc. corresponding these values of K and n could be easily estimated during the design stage.

In this problem, considering the results of the analyses conducted the values of K for the core material may be approximately in the range of 350 to 650 while the corresponding n values vary approximately in the range of 0.30 to 0.05. On the other hand, as concluded previously, the shell material should be more stiff than the core material. Therefore, the values of K for shell material may be approximately varying from 500 to 700 or more, and the corresponding values of n are in the range of 0.39 to 0.52 as presented in Table 5.3.

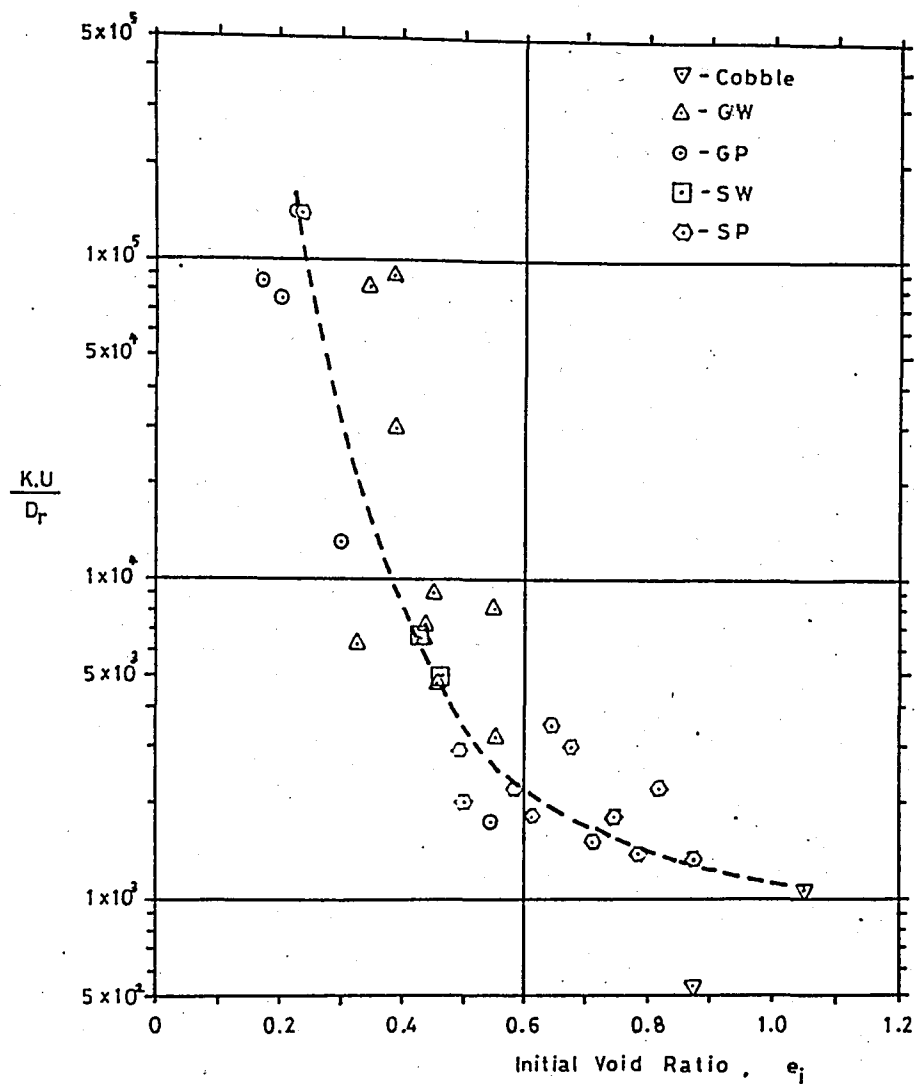
Although these ranges are determined being based on the maximum displacements, it should be noticed that the stress values corresponding to these displacements are small as well.

As explained in Chapter 3, the values of K for cohesive soils are considerably influenced by dry density, water content and void ratio. If these analyses had been conducted prior to construction, it would have been possible to obtain the reasonable values of K and n proposed for core material by simply modifying the water content or dry density and void ratio to be used in the construction of Altınkaya Dam. However, it is worthwhile to state here that the water content and void ratio might be decreased slightly, hence the dry density might be increased for the core material to have a more stiff core than as it is. But this might require extra passes during compaction of fill and result in additional cost.

On the other hand, Kulhawy (1969) has proposed the curve showing the variation of K in granular soils (Fig 5.9) depending on the uniformity coefficient, relative density and initial void ratio, and it can be used for estimating the values of K for shell material. In this problem, e_0 is equal to 0.30 and uniformity coefficient $U(D_{60}/D_{10})$ equals to 33.3 for the shell. Entering the curve with e_0 of 0.30, the value of KU/D_r is obtained as 3.7×10^4 , then, for K of 700, the relative density is found to be 0.63 which is too low. That means the uniformity coefficient might be increased i.e the grain size distribution for shell might be modified so as to have small displacements. In addition, the results indicates that it is essential to form a stiff shell for Altınkaya Dam.

5.7 SUMMARY

In this chapter, a parametric study has been conducted in order to establish the effects of material parameters, particularly the effects of modulus parameters of core and shell materials on the behavior of Altınkaya Dam during construction.



K = Modulus Factor (Range = 65 - 3780)
 U = Uniformity Coefficient, D_{60}/D_{10} (Range = 1.1 - 136.)
 D_r = Relative Density (Range = 0.38 - 1.00)

Fig. 5.9 Variation of Modulus Number, K , in Granular Soils Under Drained Conditions (Kulhawy, 1969)

As the results of two groups of analyses indicate, the maximum displacement values are considerably affected by the parameters of core material; however, the effects of shell material parameters do not seem to be as effective as the core parameters. On the other hand, the settlement values seem to decrease with increasing the stiffness of the shell and the core should be soft as compared to the shell in Altınkaya Dam.

The ranges of the values of K and n for both the core and shell were also determined and it might be suggested the water content and void ratio of the core might need to be decreased so as to increase the dry density to have smaller displacements. The grain size distribution of shell, on the other hand, might also be modified in order to have more stiff shell relative the core for Altınkaya Dam.

CHAPTER 6

SUMMARY AND CONCLUSIONS

The construction of earth and rockfill dams has become feasible due to the continuing developments in earth-moving equipments and also in geotechnical engineering throughout the world. This is because the construction of earth and rockfill dams is least expensive in certain dam sites where the rockfill and impervious material is easily available. However, there exist some problems concerning the design and construction of such dams. In particular, the prediction of stresses and deformations which develop during construction within the embankment is one of the main concerns of the designers, and it is the topic of this study.

If the analysis of stresses and deformations should be meaningful and realistic, it is essential that the real soil behavior such as non-linearity, inelasticity and stress-dependency, and the construction history need to be represented in the analysis in a reasonable way, therefore the analysis is an exceedingly complex problem. However, this problem can be attacked by using the finite element method which is explained in Chapter 2. This method is a powerful technique by which complex geometry of the embankment and nonlinear soil behavior can be easily involved in the analysis. The computer program LSBUILD given in Appendix B is capable of conducting the analyses of both earth and rockfill dams with either linear or nonlinear

material properties. Further, this program assumes plane strain condition and follows the incremental construction procedure.

The hyperbolic stress-strain parameters as described in Chapter 3 can be used for representing the real soil behavior within the embankment. They can be obtained from the results of conventional triaxial compression tests and the tables summarizing the parameters of about 135 different soils (Duncan and Wong, 1974) are given in Appendix A. These results may be used if there is no sufficient test data available. However, they are limited either in accuracy or in validity, and mostly depend on water content, relative density and range of pressures applied during the tests. The laboratory test conditions should conform to the field conditions as well.

Using the computer program LSBUILD, the nonlinear and build-up analyses of Altinkaya Dam which is one of the highest rockfill dams under construction in Turkey have been performed, as presented in Chapter 4. Since no comprehensive test data was available regarding the material properties, the hyperbolic stress-strain parameters required for the nonlinear finite element analysis of Altinkaya Dam have been estimated based on the results of tests on similar materials. It is evident that the results of the analyses would be more accurate if the laboratory test results were available. However, the results of the analyses performed during the course of this study may supply very valuable information on the behavior of the embankment during construction since no device had been installed for measuring the stresses and deformations within the embankment.

As the results of the nonlinear analysis indicate, the maximum settlement developed during construction is slightly less than 7 ft.

whereas the maximum horizontal displacement is found to be more than 1ft in the core in the downstream direction. Furthermore, the stress concentrations seem to occur in the filter zones while a stress reduction is observed in the core. It can also be noticed that the settlement of the core with respect to the adjacent coarse zones induces a load transfer from the core to the adjacent zones. Even more interesting thing is that no tensile stresses would be expected to occur in the embankment, which might cause serious cracking. On the other hand, the factor of safety against local failure which is the reciprocal of the maximum mobilized strength is found to be 1.25 for Altınkaya Dam.

The build-up analysis of Altınkaya Dam has been performed using constant values of modulus and poisson ratio as well. The comparison of these two analyses has shown that the results are almost the same except small differences in stresses and deformations in the zones where a change in σ_3 takes place. Consequently, it can be stated that the behavior of the embankment during construction could also be predicted by means of build-up analysis reasonably provided that the appropriate values of modulus and poisson's ratio are introduced into the analysis.

As presented in Chapter 5, the effects of material parameters, especially the effects of modulus parameters of core and shell materials on the behavior of Altınkaya Dam during construction have also been investigated. Results of two types of analyses performed reveal that the maximum displacements are affected by the parameters of core material significantly whereas the shell material parameters do not appear to be so effective. Besides these, the settlement values are found to decrease with increasing the stiffness of the shell. It is also shown, in order to minimize the settlements, the core should be more softer than the shell

for Altınkaya Dam.

The optimum ranges of the values of K and n , for both the core and shell of Altınkaya Dam are also presented in Chapter 5. In order to meet these values of K and n , it might be suggested to decrease the water content and void ratio of the core to some extent so that the dry density increases and smaller displacements are experienced. In addition, the grain size distribution of shell might also be adjusted so as to have more stiff shell relative to the core material for the embankment.

REFERENCES

1. Clough R.W. and Woodward R.J. (1967) "*Analysis of Embankment Stresses and Deformations*", Journal of the Soil Mechanics and Foundations Division, ASCE, Vol.93, No.SM4, July 1967
2. Duncan J.M. and Chang C.Y. (1970), "*Nonlinear Analysis of Stress and Strain in Soils*" Journal of the Soil Mechanics and Foundations Division, ASCE Vol.96, No.SM5, September 1970
3. Duncan J.M. and Wong K.S. (1974), "*Hyperbolic Stress-Strain Parameters For Nonlinear Finite Element Analyses of Stresses and Movements in Soil Masses*", Report No. TE-74-3, Office of Research Services, University of California, Berkeley, California
4. Justo J.L (1973), "*The Cracking of Earth and Rockfill Dams*", 11 th ICOLD Congresses, Madrid, 1973, Comm. C.11,IV
5. King I.P. (1965), "*Finite Element Analysis of Two Dimensional, Time - Dependent Stress Problems*", thesis presented to the University of California, at Berkeley, California in 1965, partial fulfillment of the requirements of the degree of Doctor of Philosophy.
6. Kondner R.L. (1963), "*Hyperbolic Stress-Strain Response : Cohesive Soils*", Journal of the Soil Mechanics and Foundations Division, ASCE, Vol. 89 , No.SM1, February 1963
7. Kulhawy H.F. (1969), "*Finite Element Analysis of the Behavior of Embankments*" Dissertation presented to the University of California, Berkeley, in 1969, in partial fulfillment of the requirements for the degree of Doctor Philosophy.
8. Lefebvre G., Duncan J.M. and Wilson L.E (1973), "*Three Dimensional Finite Element Analyses of Dams*", Journal of the Soil Mechanics and Foundations Division, ASCE, Vol.99, No.SM7, July 1973
9. Raphael J.M and Clough R.W. (1965), "*Construction Stresses in Dworkshak Dam*" Report No.65-3, Structural Engineering Laboratory, University of California, April 1965.

10. Résendiz D, and Romo P.M. (1972), "*Analysis of Embankment Deformations*", Proceedings of the Speciality Conference on Performance of Earth and Earth-Supported Structures, Purdue University, ASCE, Vol.1, Part 1, June 1972.
11. Schober W.(1967), "*Behavior of the Gepatsch Rockfill Dam*", Proceedings, 9th Congress on Large Dams, Vol.3, Istanbul, 1967
12. Sherard J.L., Woodward R.J., Gizienski S.F. and Clevenger W.A., "*Earth and Earth-Rock Dams ,Engineering Problems of Design and Construction*", John Wiley and Sons, New York, 1963
13. Squier L.R (1970), "*Load Transfer in Earth and Rockfill Dams*", Journal of the Soil Mechanics and Foundations Division, ASCE, Vol.96, No.SM 1, January 1970
14. Thomas H.H., "*The Engineering of Large Dams*", Part II, John Wiley and Sons, London, 1976
15. Ural O., "*The Finite Element Method*", Intertext Educ. Pub., New York, 1975
16. Walker W.L and Duncan J.M. (1984), "*Lateral Bulging of Earth Dams*" , Journal of Geotechnical Engineering, ASCE, Vol. 110, No.7, July 1984
17. Zienkiewicz O.C., "*The Finite Element Method in Engineering Science*", McGraw-Hill, London, 1977

A P P E N D I C E S

APPENDIX A

**STRESS-STRAIN AND STRENGTH
PARAMETERS FOR SOILS**

TABLE A.2 Continued

SOIL GROUP	SOIL DESCRIPTION	REFERENCES	GRAIN SIZE, MM					COMPACTION					INIT. VOID RATIO	RELATIVE DENSITY	DEGREE OF SATURATION	RATING	PARTICLE SHAPE	STRESS RANGE (TSF)	NUMBER OF TESTS	C (TSF)	FRICTION ANGLE	K	N	RF	G	F	D				
			GAO	D30	D10	LL	PI	TYPE	MAX. DRY UNIT WT. (PCF)	OPT. W/C	DRY U. WT. (PCF)	W/C																			
CL	CL-11C SANDY CLAY (ISOMERVILLE DAM)	CORPS OF ENGINEERS, FORT WORTH DIST. (1961)	0.06	0.002	-	25	12	STD. AASHO	107.5	16.8	102.6	19.3						87	*		.5 - 6.0	4	.74	6	23	.32	.61				
CL	CL-11D SANDY CLAY (ISOMERVILLE DAM)	CORPS OF ENGINEERS, FORT WORTH DIST. (1961)	0.06	0.002	-	25	12	STD. AASHO	107.5	16.8	106.7	16.7						85	*		.5 - 6.0	4	.91	18	280	.40	.93				
CL	CL-11E SANDY CLAY (ISOMERVILLE DAM)	CORPS OF ENGINEERS, FORT WORTH DIST. (1961)	0.06	0.002	-	25	12	STD. AASHO	107.5	16.8	101.5	16.3						72	*		.5 - 6.0	4	.66	20	220	.23	.90				
CL	CL-12A SANDY CLAY (ISOMERVILLE DAM)	CORPS OF ENGINEERS, FORT WORTH DIST. (1961)	0.065	0.0055	0.001	38	25	STD. AASHO	106.1	17.2	105.0	18.6						89	*		.5 - 6.0	4	1.30	8	140	.20	.84				
CL	CL-12C SANDY CLAY (ISOMERVILLE DAM)	CORPS OF ENGINEERS, FORT WORTH DIST. (1961)	0.065	0.0055	0.001	38	25	STD. AASHO	106.1	17.2	101.9	17.1						75	**		.5 - 6.0	4	1.00	13	120	.09	.83				
CL	CL-12D SANDY CLAY (ISOMERVILLE DAM)	CORPS OF ENGINEERS, FORT WORTH DIST. (1961)	0.065	0.0055	0.001	38	25	STD. AASHO	106.1	17.2	103.0	19.7						89	*		.5 - 6.0	4	.80	2	47	.33	.82				
CL	CL-12E SANDY CLAY (ISOMERVILLE DAM)	CORPS OF ENGINEERS, FORT WORTH DIST. (1961)	0.065	0.0055	0.001	38	25	STD. AASHO	106.1	17.2	104.5	13.9						70	**		.5 - 6.0	4	1.50	24	950	-.15	.90				
CL	CL-12F SANDY CLAY (ISOMERVILLE DAM)	CORPS OF ENGINEERS, FORT WORTH DIST. (1961)	0.065	0.0055	0.001	38	25	STD. AASHO	106.1	17.2	108.3	16.9						89	*		.5 - 6.0	4	1.50	8	470	0.	.95				
CL	CL-13A SANDY CLAY (ISOMERVILLE DAM)	CORPS OF ENGINEERS, FORT WORTH DIST. (1961)	0.066	0.0065	-	36	23	STD. AASHO	104.9	17.6	98.7	20.8						86	**		.5 - 6.0	4	.67	4	75	.44	.88				
CL	CL-13B SANDY CLAY (ISOMERVILLE DAM)	CORPS OF ENGINEERS, FORT WORTH DIST. (1961)	0.066	0.0065	-	36	23	STD. AASHO	104.9	17.6	104.9	16.8						72	*		.5 - 6.0	4	1.80	23	840	-.19	.84				
CL	CL-13C SANDY CLAY (ISOMERVILLE DAM)	CORPS OF ENGINEERS, FORT WORTH DIST. (1961)	0.066	0.0065	-	36	23	STD. AASHO	104.9	17.6	181.2	17.4						76	*		.5 - 6.0	4	1.20	12	270	.06	.87				
CL	CL-13D SANDY CLAY (ISOMERVILLE DAM)	CORPS OF ENGINEERS, FORT WORTH DIST. (1961)	0.066	0.0065	-	36	23	STD. AASHO	104.9	17.6	100.5	16.2						62	*		.5 - 6.0	4	1.40	29	1100	-.36	.83				
CL	CL-13E SANDY CLAY (ISOMERVILLE DAM)	CORPS OF ENGINEERS, FORT WORTH DIST. (1961)	0.066	0.0065	-	36	23	STD. AASHO	104.9	17.6	104.6	17.5						84	*		.5 - 6.0	3	1.40	13	410	.15	.87				
CL	CL-14 LEAN CLAY (CLINTON DAM)	CORPS OF ENGINEERS, KANSAS CITY DIST. (1966)	-	-	-	46	27	STD. AASHO	103.0	21.2	98.0	24.0						92	**		1.0 - 5.0	3	.77	2	97	.43	.86				
CL	CL-16C LEAN CLAY (CLINTON DAM)	CORPS OF ENGINEERS, KANSAS CITY DIST. (1966)	-	-	-	37	18	STD. AASHO	105.0	20.2	99.7	22.9						91	**		1.0 - 3.0	2	.97	1	110	.43	.90				
CL	CL-17A LEAN CLAY (CLINTON DAM)	CORPS OF ENGINEERS, KANSAS CITY DIST. (1966)	-	-	-	43	24	STD. AASHO	101.0	20.1	99.1	22.7						90	**		2.0 - 6.0	3	1.10	2	100	.27	.89				
CL	CL-17B LEAN CLAY (CLINTON DAM)	CORPS OF ENGINEERS, KANSAS CITY DIST. (1966)	-	-	-	43	24	STD. AASHO	101.0	20.1	98.1	23.9						90	**		2.0 - 6.0	3	.99	1	160	.54	.97				
CL	CL-17C LEAN CLAY (CLINTON DAM)	CORPS OF ENGINEERS, KANSAS CITY DIST. (1966)	-	-	-	43	24	STD. AASHO	101.0	20.1	98.9	22.7						90	**		2.0 - 6.0	3	1.10	3	130	.46	.91				
CL	CL-19A LEAN CLAY (CLINTON DAM)	CORPS OF ENGINEERS, KANSAS CITY DIST. (1966)	-	-	-	42	26	STD. AASHO	102.0	19.9	96.8	22.7						83	**		2.0 - 6.0	3	.78	2	93	.41	.85				
CL	CL-24A SANDY CLAY (CHATFIELD DAM)	CORPS OF ENGINEERS, OHAMA DIST. (1968)	0.016	-	-	43	26	STD. AASHO	104.0	19.3	97.6	23.4						90	*		6.0 - 10.0	2	1.20	0	240	0.	.95				
CL	CL-25A SANDY CLAY (CHATFIELD DAM)	CORPS OF ENGINEERS, OHAMA DIST. (1968)	0.09	0.007	-	34	18	STD. AASHO	113.0	15.1	107.6	18.1						86	*		6.0 - 10.0	2	.95	0	160	0.	.93				
CL	CL-28 SANDY CLAY (MCCORMICK DAM)	CORPS OF ENGINEERS, FORT WORTH DIST. (1961)	0.033	0.002	-	31	20	STD. AASHO	115.0	16.6	114.8	12.2						72	**		1.5 - 6.0	2	1.60	12	150	.16	.79				
CL	CL-29A SILTY CLAY (CANYON DAM)	CASAGRANDE ET AL (1962)	0.037	0.008	-	34	19	HARVARD	116.2	15.2	110.9	13.0						67	*		1.0 - 14.3	3	2.00	20	440	.17	.85				
CL	CL-29B SILTY CLAY (CANYON DAM)	CASAGRANDE ET AL (1962)	0.037	0.008	-	34	19	HARVARD	116.2	15.2	115.3	13.1						77	*		1.0 - 14.3	4	2.50	20	440	.34	.86				
CL	CL-30A SILTY CLAY (CANYON DAM)	CASAGRANDE ET AL (1962)	0.037	0.008	-	34	19	HARVARD	112.8	16.7	111.0	16.2						84	*		1.0 - 6.3	4	1.00	16	110	.94	.91				
CL	CL-30B SILTY CLAY (CANYON DAM)	CASAGRANDE ET AL (1962)	0.037	0.008	-	34	19	HARVARD	112.8	16.7	112.2	16.6						88	*		1.0 - 4.1	3	1.40	11	67	.71	.77				
CL	CL-100 SILTY CLAY (CANYON DAM)	CASAGRANDE ET AL (1962)	0.037	0.008	-	34	19	HARVARD	112.8	16.7	110.3	17.3						88	*		1.1 - 4.1	3	1.00	9	37	.37	.65				
CL	CL-33B SILTY CLAY (CANYON DAM)	CASAGRANDE ET AL (1962)	0.037	0.008	-	34	19	HARVARD	108.8	18.0	106.3	16.2						75	**		4.1 - 13.5	4	2.20	3	71	1.06	.98				
CH	CH-1 FAT CLAY (CLINTON DAM)	CORPS OF ENGINEERS, KANSAS CITY DIST. (1966)	-	-	-	60	38	STD. AASHO	96.0	26.5	90.0	23.8						90	**		1.0 - 3.0	2	.61	4	92	.21	.89				
CH	CH-1A FAT CLAY (MCHRAE DAM)	CORPS OF ENGINEERS, LOUISVILLE DIST. (1960)	0.0067	-	-	61	36	STD. AASHO	95.5	26.5	89.3	31.1						93	*		.7 - 2.9	2	.37	0	21	0.	.65				
CH	CH-3B FAT CLAY (MCHRAE DAM)	CORPS OF ENGINEERS, LOUISVILLE DIST. (1960)	0.0067	-	-	61	36	STD. AASHO	95.5	26.5	92.6	28.6						93	**		.7 - 2.9	3	.51	1	67	.02	.79				
CH	CH-4 FAT CLAY (MCHRAE DAM)	CORPS OF ENGINEERS, LOUISVILLE DIST. (1960)	0.018	-	-	69	45	STD. AASHO	100.0	22.7	96.4	26.5						94	**		1.1 - 2.9	2	.63	1	65	.14	.77				
CH	CH-1A FAT CLAY (CHATFIELD DAM)	CORPS OF ENGINEERS, OHAMA DIST. (1968)	0.0095	-	-	54	36	STD. AASHO	95.0	26.4	90.3	27.6						84	*		6.0 - 10.0	3	1.20	0	36	.72	.91				
CH	CH-5B FAT CLAY (CHATFIELD DAM)	CORPS OF ENGINEERS, OHAMA DIST. (1968)	0.0095	-	-	54	36	STD. AASHO	95.0	26.4	90.7	26.4						76	**		6.0 - 10.0	3	1.50	2	52	.66	.89				

APPENDIX B

USER'S MANUAL FOR PROGRAM LSBUILD

INPUT DATA INFORMATION

1. Control Cards (6 cards required)

a) Card 1 (12A6)

2-72 HED - Title card for program identification

b) Card 2 (6I4)

1-4 NUMELT - Total number of elements in the complete structure (Maximum = 275)

1-4 NUMNPT - Total number nodal points in the complete structure (Maximum = 300)

9-12 NFEL - Number of elements in the foundation portion (\leq NUMELT)

13-16 NFNP - Number of nodal points in the foundation portion (\leq NUMNPT)

17-20 NUMCEL - Number of elements in the cofferdam portion (Maximum = 100)

21-24 NUMCNP - Number of nodal points in the cofferdam portion (Maximum = 100)

c) Card 3 (7I4)

1-4 NUMBC - Number of nodal points in the structure with a constrained deformation (fixed in x, fixed in y, fixed in x and y) (Maximum = 100)

- 5-8 NZONES - Number of different material types (Maximum =10)
- 9-12 NLAY - Number of construction layers desired
(Maximum =25)
- 13-16 NUMIT - Number of solution cycles per construction layer
(e.g. - for 1 cycle of iteration per layer, NUMIT=2)
- 17-20 NONLIN - Code for linear or nonlinear material properties
(0 for all linear material, 1 for some or all nonlinear materials)
- 21-24 NWATER - Code for additional loads (e.g.-water forces) to be placed on the structure after the usual construction sequence is completed (0 for no added loads, 1 if are to be added)
- 25-28 NPUNCH - Code for punching out stresses etc., after last layer
(0=no, 1= yes)

d) Card 4 (2F10.0)

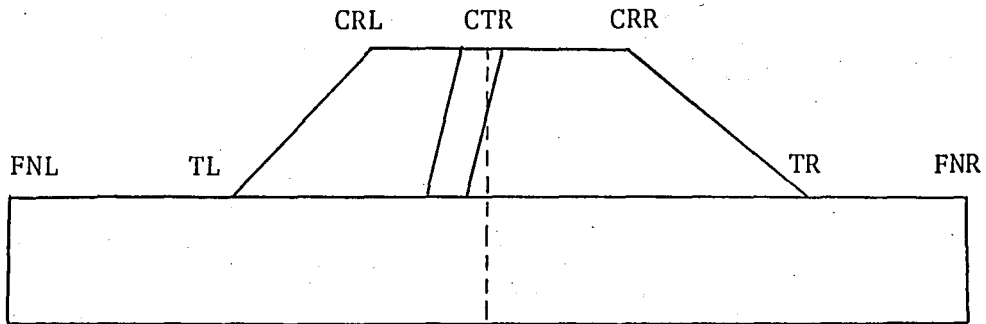
- 1-10 AKO - Initial earth pressure coefficient in the foundation
- 11-20 REDMOD - Factor used in simulating construction sequences.
(0.00001 yields good results)

e) Card 5 (7F10.0) (See following figure for details)

- 1-10 FNL - X coordinate of foundation surface to the left of the embankment
- 11-20 TL - X coordinate of embankment toe to the left
- 21-30 CRL - X coordinate of embankment crest to the left
- 31-40 CTR - X coordinate of embankment centerline
- 41-50 CRR - X coordinate of embankment crest to the right
- 51-60 TR - X coordinate of embankment toe to the right
- 61-70 FNR - X coordinate of foundation surface to the right of the embankment

f) Card 6 (7F10.0)

Same as Card 5 for the Y coordinates



If the X-coordinates of the following are equal:

$$FNL = TL \text{ and } FNR = TR$$

then the embankment is considered to be on a rigid foundation.

If only the half-section of a symmetrical embankment is being analyzed, the full section geometry must still be read in above.

2. Material Property Cards (See description following input procedure)

a) Units conversion card (F10.0)

1-10 CONS - Units conversion constant

b) Weight and elastic constant cards (I4, 6F10.4)

(number of cards required = NZONES)

1-4 N - Material type number

5-14 GAM - Unit weight

15-24 COEF } - Tangent modulus constants

25-34 EXP

35-44 DD

45-54 GG } - Tangent Poisson ratio constants

55-64 FF

c) Strength cards (I4, 4F10.4) (Number of cards required = NZONES)

1-4 N - Material type number

5-14 CC - Cohesion.

15-24 PHI - Angle of internal friction (degrees)

25-34 RF - Failure ratio

35-44 CODE - Code for linear or nonlinear material properties
(0 for linear, 1 for nonlinear).

CONS equals a unit constant to convert the units that one desires to use into atmospheres, assuming that one uses the modulus and Poisson ratio constants as presented in the main text.

Therefore, one of the following units combinations should be used:

GAM - ton/ft³ - kip/ft³ - lb/ft³ (etc.)

CC - ton/ft² - kip/ft² - lb/ft²

CONS - 1.058 - 2.116 - 2116.2

Since the output fields have been made small, it is best to use ton or kip units. For all of these cases, it is assumed that all dimensions are in feet.

When assigning numbers to the different material types in the embankment foundation system, note that the output contains the principal stresses / γh . Therefore the program has been set up to evaluate γh using the following values:

for a rigid foundation, $\gamma(\text{Dam}) = \gamma(\text{Shell}) = \gamma(1)$

for a flexible foundation, $\gamma(\text{Foundation}) = \gamma(1)$

and $\gamma(\text{Dam}) = \gamma(\text{Shell}) = \gamma(2)$

The numbering of the material type should conform to the above.

If NONLIN = 0 on control card 1c (all materials are linear elastic), use the following for each material type:

COEF = modulus of elasticity RF = 1.0

GG = Poisson's ratio

EXP = DD = FF = CODE = 0.0

If NONLIN = 1 on control card 1c (one or more materials are nonlinear), the tangent modulus (E_t) and the tangent Poisson ratio (ν_t) are automatically calculated after each construction layer according to the following hyperbolic relationships:

$$E_t = E_i \left[1 - \text{CODE} * \frac{(\sigma_1 - \sigma_3)}{(\sigma_1 - \sigma_3)_{fh}} \right]^2 \quad \text{and} \quad \nu_t = \nu_i / (1 - \text{DD} * \epsilon_a)^2$$

where:

$$E_i = \text{CONS COEF } (\sigma_3/\text{CONS})^{\text{EXP}}$$

$$v_i = \text{GG} - \text{FF} \log (\sigma_3/\text{CONS})$$

$$(\sigma_1 - \sigma_3)_{\text{fh}} = \text{hyperbolic strength} = (\sigma_1 - \sigma_3)_f / \text{RF}$$

The evaluation of these parameters is discussed in the main text.

If the material is nonlinear, $\text{CODE}=1$, but if the material is linear, evaluate the constants the same way as is done above for $\text{NONLIN}=0$.

If v_t becomes greater than 0.49, it is automatically reset to 0.49.

If $\text{NONLIN}=1$, the initial values of E_t and v_t in a foundation zone are calculated by assuming that $\sigma_1 = \gamma h$ and $\sigma_3 = \text{AKO } \sigma_1$. The initial values of E_t and v_t in an embankment zone are calculated by assuming that $\sigma_1 = \gamma h$ and $\sigma_1 = \sigma_3 (v_t / (1 - v_t))$. Iteration is required to assure that the value of v_t used to calculate σ_3 is equal to the value of v_t calculated in the equations above. This is done automatically.

3. Nodal Point Cards (I4, 2F8.2)

(Use as many cards as necessary to define the structure.)

- 1-4 MM - Nodal point number
- 5-12 ORD (MM,1) - X coordinate of nodal point (to right)
- 13-20 ORD (MM,2) - Y coordinate of nodal point (up)

If nodal point cards are omitted, the program generates the omitted information by incrementing MM by one and by calculating ORD (MM, 1 and 2) at equal intervals along a straight line between the two defined nodal points. The first and last nodal points must always be given.

(e.g., $\text{MM}=1$ and $\text{MM}=\text{NUMNPT}$)

Nodal points must be in numerical sequence from left to right in the finite element mesh and must increase from the foundation up in layers.

4. Constrained Boundary Cards (18I4)

(Use as many cards as required to define NUMBC nodal points.)

- | | | |
|-----|------|---|
| 1-4 | NBC | - Number of constrained nodal point |
| 5-8 | NFIX | - Code to define type of fixity at this nodal point
(NFIX = 0 for X and Y fixity.)
(NFIX = 1 for X fixity)
(NFIX = 2 for Y fixity) |

Continue across the card for the constrained nodal points at repeating eight column intervals as above for a maximum of nine alternating values of NBC and NFIX per card.

Omitted nodal points are considered as freely moving nodal points.

5. Element Cards (6I4)

(Use as many cards as necessary to define the structure)

- | | | |
|-------|----------|--|
| 1-4 | N | - Element number |
| 5-8 | NPN(N,1) | - Number of nodal point I for this element |
| 9-12 | NPN(N,2) | - Number of nodal point J for this element |
| 13-16 | NPN(N,3) | - Number of nodal point K for this element |
| 17-20 | NPN(N,4) | - Number of nodal point L for this element |
| 21-24 | NPN(N,5) | - Material type of this element |

If element cards are omitted, the program generates the omitted information by incrementing the previous N and NPN (N,1 through 4) by one while retaining the same NPN (N,5). Cards must always be supplied for the first and last elements. (e.g., N=1 and N=NUMELT)

Elements must be numbered consecutively, proceeding counterclockwise around the quadrilateral elements. Nodal point numbers within an element must be ≤ 39 .

In the finite element mesh, elements are numbered consecutively from left to right in horizontal strips, starting at the bottom of the mesh and proceeding upward.

Triangular shaped elements may be used as long as a fourth nodal point is placed in the center of the "slope side" of these elements. Care must be exercised that the diagonal from nodal point J to nodal point L is not on a straight line including either I or K. Numbering must be done in the following way.



6. Construction Layer Cards (5I4, F8.2)

(One cards is required for each layer totalling NLAY cards)

1-4	LN	-	Number of construction layer, increasing upward from the bottom.
5-8	NOMEL(LN,1)-		Smallest element number of the newly placed elements in this layer
9-12	NOMEL(LN,2)-		Largest element number of the newly placed elements in this layer
13-16	NOMNP(LN,1)-		Smallest nodal point number of the newly placed nodal points in this layer
17-20	NOMNP(LN,2)-		Largest nodal point number of the newly placed nodal points in this layer
21-28	HEIGHT	-	Surface elevation of this layer

If a foundation is included in the mesh, it must have LN=1. Therefore the first constructed layer = 2.

If NWATER=1, an additional layer card must be added to simulate added loads placed after the embankment is completed. In this case, columns 5 through 28 on the LN=NLAY card (last card) will be identical to those on the LN=NLAY-1 card (last layer of the constructed embankment).

7. Cofferdam Element and Nodal Point Cards

a) Cofferdan element cards (18I4)

(Use as many cards as required to define NUMCEL elements.)

1-4	NCEL	-	Number of cofferdam element
5-8	NCEL	-	Number of cofferdam element
			etc.

Continue across the card for all of the input cofferdam elements at repeating four column intervals for a maximum of 18 values per card.

b) Cofferdam nodal point cards (18I4)

same as 7 a using NCNP for a total of NUMCNP nodal points.

If NUMCEL = 0, these cards are omitted.

8. Force Cards (I4, 2F8.2)

(Use as many cards as necessary to define the added loads.)

1-4 MM - Nodal point number where force is applied

5-14 FX - X component of force applied at MM (+ to right)

15-24 FY - Y component of force applied at MM (+ up)

If NWATER = 0, these cards are omitted.

If NWATER = 1, these cards must be supplied, in numerical sequence, and the first and last cards must always be supplied, even if there are no forces applied at these points.

If cards, are omitted, MM is incremented by 1 and FX and FY are set equal to 0.

Care must be exercised to be sure that a force is not applied at a nodal point which is fixed in the direction of the applied force.

9. Cofferdam Existing Property Cards

a. Stress cards (I10, 5F10.3)

b) Elastic property cards (I10, 5F10.3)

c) Strain cards (I10,5F10.3)

These cards (a,b,c) are punched out properly from the auxiliary program. (FEMINT)

d) Displacement cards (I10, 4F10.3)

1-10 NCNP - Cofferdam nodal point number

11-20 ORD (N,1) - X ordinate of nodal point

21-30 ORD (N,2) - Y ordinate of nodal point

31-40 DISP (N,1) - X displacement of nodal point

41-50 DISP (N,2) - Y displacement of nodal point

When the finite element meshes for the cofferdam and the cofferdam - embankment systems are different, be sure that the nodal points are in the same locations. If this procedure is followed, only the nodal point numbers will have to be changed on the punched output from the cofferdam analysis before it is used as input in the re-numbered cofferdam-embankment system.

PROGRAM LSBUILD 74/176 OPT=0,ROUND= A/ S/ M/-D,-DS FTN 5.1+577 85/11
 -LONG/-DT,ARG=-COMMON/-FIXED,CS= USER/-FIXED,DB=-TB/-SB/-SL/ ER/-ID/-PHD/-ST,PL=500
 5,I=LSB,L=ER.

```

PROGRAM LSBUILD (INPUT,OUTPUT,TAPE1,TAPE2,TAPE4,TAPE7,TAPE8)
C*****
C FEM NON-LINEAR EMBANKMENT ANALYSIS - F.H. KULHAWY , 1968-69
C*****
COMMON /INIT/ HED(12),NUMELT,NUMNPT,NFEL,NFNP,NPUNCH
COMMON /NPEL/ NPN(275,5),ORD(300,2),XCP(275),YCP(275)
COMMON /CDAM/ NUMCEL,NUMCNP,NCEL(100),NCNP(100)
COMMON /NPBC/ NUMBC,NBC(100),NFIX(100),NKWATER,FX(300),FY(300)
COMMON /BANS/ MBAND,NUMBLK,B(160),A(160,80)
COMMON /LIFT/ NLAY,LN,NOMEL(25,2),NOMNP(25,2),HEIGHT(25),NUMIT,IT
COMMON /GEOM/ FNL(2),TL(2),CRL(2),CTR(2),CRR(2),TR(2),FNR(2)
COMMON /MAT1/ NONLIN,BULK(275),SHEAR(275),POIS(275),GAM(10),REDKOD
COMMON /MAT2/ CONS,COEF(10),EXP(10),DD(10),GG(10),FF(10),NZONES
COMMON /MAT3/ CC(10),PHI(10),RF(10),DEV1(10),DEV2(10),CODE(10),AKO
C*****
C READ AND PRINT INPUT DATA - SET UP INITIAL CONDITIONS
C*****
C
  100 CALL LAYOUT
C
C*****
C ANALYZE FOR EACH CONSTRUCTION LAYER
C*****
  DO 400 LN=1,NLAY
    PRINT 1000, HED,LN,(NOMEL(LN,N),N=1,2),(NOMNP(LN,M),M=1,2),
      1 HEIGHT(LN)
    DO 400 IT=1,NUMIT
      CALL SECOND (TIME1)
      IF (LN.GT. 1 .OR. NFEL .EQ. 0) GO TO 200
      PRINT 1005
      GO TO 300
C
C DEVELOP STIFFNESS MATRIX, SOLVE EQUATIONS, EVALUATE RESULTS
C
  200 CALL LSSTIF
    CALL BANSOL
    CALL LSRFSUL
C
  300 CALL SECOND (TIME2)
    TIME=TIME2-TIME1
  400 PRINT 1010, LN,IT,TIME
C*****
  1000 FORMAT (1H6 /// 12A6 /// 20H LAYER NO. = ,I4 //
    1 20H ADDED ELEMENTS = ,I4,6H THRU ,I4 //
    2 20H ADDED NODAL POINTS = ,I4,6H THRU ,I4 //
    3 20H SURFACE ELEVATION = ,F10.3 )
  1005 FORMAT (49H-FOUNDATION ZONE, SEE PREVIOUS PAGES FOR STRESSES )
  1010 FORMAT (7H-LAYER=,I3,5X,11H ITERATION=,I2,5X,15H TIME(SECONDS)=,
    1 F9.3)
C*****
  CALL EXIT
  END

```

ROUTINE LAYOUT 74/176 OPT=0,ROUND= A/ S/ H/-D,-DS FTN 5.1+577 85/11
 -LONG/-DT,ARG=-COMMON/-FIXED,CS= USER/-FIXED,DB=-TB/-SB/-SL/ ER/-ID/-PRD/-ST,PL=500
 5,I=LSB,L=FR.

SUBROUTINE LAYOUT

```

C*****
COMMON /INIT/ HED(12),NUMELT,NUMNPT,NFEL,NFNP,NPUNCH
COMMON /NPEL/ NPN(275,5),ORD(300,2),XCP(275),YCP(275)
COMMON /CDAM/ NUMCEL,NUMCNP,NCEL(100),NCNP(100)
COMMON /NPBC/ NUMBC,NBC(100),NFX(100),NWXTR,FX(300),FY(300)
COMMON /BANS/ MBAND,NUMBLK,B(160),A(160,80)
COMMON /LIFT/ NLAY,LN,NOMEL(25,2),NOMNP(25,2),HEIGHT(25),NUMIT,IT
COMMON /GEOH/ FNL(2),TL(2),CRL(2),CTR(2),CRR(2),TR(2),FNR(2)
COMMON /MAT1/ NONLIN,BULK(275),SHEAR(275),POIS(275),GAK(10),REDMOD
COMMON /MAT2/ CONS,COEF(10),EXP(10),DD(10),GG(10),FF(10),NZONES
COMMON /MAT3/ CC(10),PHI(10),RF(10),DEV1(10),DEV2(10),CODE(10),AKO
DIMENSION STRESS(275,3),STRAIN(275,3),DISP(300,2)
EQUIVALENCE (STRESS(1,1),A(80,13)),(STRAIN(1,1),A(160,25)),
1 (DISP(1,1),A(80,38))
C*****
C READ AND PRINT CONTROL DATA
C*****
READ 1000, HED
READ 1005, NUMELT,NUMNPT,NFEL,NFNP,NUMCEL,NUMCNP
READ 1005, NUMBC,NZONES,NLAY,NUMIT,NONLIN,NWATER,NPUNCH
READ 1010, AKO,REDMOD
READ 1010, (FNL(N),TL(N),CRL(N),CTR(N),CRR(N),TR(N),FNR(N),N=1,2)
PRINT 2000, HED
PRINT 2005, NUMELT,NUMNPT,NFEL,NFNP,NUMCEL,NUMCNP
PRINT 2010, NUMBC,NZONES,NLAY,NUMIT,NONLIN,NWATER,NPUNCH
PRINT 2015, AKO,REDMOD
PRINT 2020, TL(1),TL(2),CRL(1),CRL(2),CTR(1),CTR(2),CRR(1),CRR(2),
1 TR(1),TR(2)
IF (NFEL.EQ.0) PRINT 2021
IF (NFEL.GT.0) PRINT 2022, FNL(1),FNL(2),FNR(1),FNR(2)
C*****
C READ AND PRINT MATERIAL PROPERTY DATA
C*****
READ 1010, CONS
READ 1016, (GAK(N),COEF(N),EXP(N),DD(N),GG(N),FF(N),N=1,NZONES)
READ 1021, (CC(N),PHI(N),RF(N),CODE(N),N=1,NZONES)
PRINT 2025, CONS
PRINT 2030
PRINT 1015, (N,GAK(N),COEF(N),EXP(N),DD(N),GG(N),FF(N),N=1,NZONES)
PRINT 2035
PRINT 1020, (N,CC(N),PHI(N),RF(N),CODE(N),N=1,NZONES)
C*****
C READ AND PRINT NODAL POINT ARRAY
C*****
LL=0
100 READ 1025, MM,(ORD(MM,H),M=1,2)
DX=(ORD(MM,1)-ORD(LL,1))/(MM-LL)
DY=(ORD(MM,2)-ORD(LL,2))/(MM-LL)
110 LL=LL+1
IF (MM-LL) 140,130,120
120 ORD(LL,1)=ORD(LL-1,1)+DX
ORD(LL,2)=ORD(LL-1,2)+DY
GO TO 110
130 IF (NUMNPT-MM) 140,150,100

```

ROUTINE LAYOUT 74/176 OPT=0,ROUND= A/ S/ M/-D,-DS FTN 5.1+577 85/11

```

140 PRINT 5000, MH
    CALL EXIT
150 PRINT 2040
    CTRF=TL(2)+(TR(2)-TL(2))*(CTR(1)-TL(1))/(TR(1)-TL(1))
    DO 160 N=1,NUMNPT
    IF (ORD(N,1) .LE. CTR(1)) XDIM=(CTR(1)-ORD(N,1))/(CTR(1)-TL(1))
    IF (ORD(N,1) .GT. CTR(1)) XDIM=(ORD(N,1)-CTR(1))/(TR(1)-CTR(1))
    YDIM=(ORD(N,2)-CTRF)/(CTR(2)-CTRF)
160 PRINT 1020, N,(ORD(N,M),M=1,2),XDIM,YDIM
C
    READ 1005, (NBC(K),NFIX(K),K=1,NUMBC)
    PRINT 2045
    DO 180 K=1,NUMBC
    IF (NFIX(K) .EQ. 0) PRINT 2050,NBC(K)
    IF (NFIX(K) .EQ. 1) PRINT 2055,NBC(K)
    IF (NFIX(K) .EQ. 2) PRINT 2060,NBC(K)
180 CONTINUE
C*****
C READ AND PRINT ELEMENT ARRAY, COMPUTE PT. FOR STRESSES
C*****
    NN=0
200 READ 1005, N,(NPN(N,M),M=1,5)
210 NN=NN+1
    IF (N .LE. NN) GO TO 230
    DO 220 K=1,4
220 NPN(NN,K)=NPN(NN-1,K)+1
    NPN(NN,5)=NPN(NN-1,5)
230 IF (N .GT. NN) GO TO 210
    IF (NUMELT .GT. NN) GO TO 200
C
    PRINT 2065
    DO 250 N=1,NUMELT
    J=NPN(N,2)
    L=NPN(N,4)
    XCP(N)=0.5*(ORD(J,1)+ORD(L,1))
    YCP(N)=0.5*(ORD(J,2)+ORD(L,2))
    IF (XCP(N) .LE. CTR(1)) XDIM=(CTR(1)-XCP(N))/(CTR(1)-TL(1))
    IF (XCP(N) .GT. CTR(1)) XDIM=(XCP(N)-CTR(1))/(TR(1)-CTR(1))
    YDIM=(YCP(N)-CTRF)/(CTR(2)-CTRF)
250 PRINT 2070, N,(NPN(N,M),M=1,5),XCP(N),YCP(N),XDIM,YDIM
C*****
C READ AND PRINT CONSTRUCTION SEQUENCE INFORMATION
C*****
    READ 1030, ((NOMEL(LN,N),N=1,2),(NOMNP(LN,M),M=1,2),
1      HEIGHT(LN),LN=1,NLAY)
    PRINT 2075
    PRINT 2080, (LN,(NOMEL(LN,N),N=1,2),(NOMNP(LN,M),M=1,2),
1      HEIGHT(LN),LN=1,NLAY)
C
    IF (NUMCEL .EQ. 0) GO TO 350
    PRINT 2082
    READ 1005, (NCEL(N),N=1,NUMCEL)
    PRINT 1005, (NCEL(N),N=1,NUMCEL)
    PRINT 2083
    READ 1005, (NCNP(N),N=1,NUMCNP)
    PRINT 1005, (NCNP(N),N=1,NUMCNP)
C

```

ROUTINE LAYOUT

74/176 OPT=D,ROUND= A/ S/ M/-D,-DS

FTN 5.1+577

85/11

```

350 IF (NWATER .EQ. 0) GO TO 500
    PRINT 2085
    DO 400 NN=1,NUMNPT
        FX(NN)=0.0
400  FY(NN)=0.0
        NN=0
410  READ 1025, MM,FX(MM),FY(MM)
420  NN=NN+1
        PRINT 1025, NN,FX(NN),FY(NN)
        IF (MM .GT. NN) GO TO 420
        IF (NUMNPT .GT. NN) GO TO 410
C*****
C  DETERMINE BAND WIDTH OF STIFFNESS MATRIX, ABORT IF TOO LARGE
C*****
500  MBAND=0
    DO 510 N=1,NUMELT
        II=MAX0(NPN(N,1),NPN(N,2),NPN(N,3),NPN(N,4))
        JJ=MIN0(NPN(N,1),NPN(N,2),NPN(N,3),NPN(N,4))
        KK=2*(II-JJ+1)
        IF (KK .GT. MBAND) MBAND=KK
        IF (MBAND .LE. 80) GO TO 510
        PRINT 5005, N
        GO TO 999
510  CONTINUE
C*****
C  INITIALIZE VALUES IN FOUNDATION AND IN EMBANKMENT
C*****
    PRINT 2090
    DO 550 N=1,NUMELT
        DO 550 M=1,3
            STRESS(N,M)=0.0
550  STRAIN(N,M)=0.0
        DO 560 N=1,NUMNPT
            DO 560 M=1,2
2560  DISP(N,M)=0.0
            IF (NFEL .EQ. 0) GO TO 580
            DO 570 N=1,NFEL
                STRESS(N,2)=GAM(1)*(HEIGHT(1)-YCP(N))
570  STRESS(N,1)=STRESS(N,2)*AKO
C
580  IF (NUMCEL .EQ. 0) GO TO 600
        READ 1035, (N,XCP(N),YCP(N),(STRESS(N,M),M=1,3),J=1,NUMCEL)
        READ 1035, (N,XCP(N),YCP(N),(STRAIN(N,M),M=1,3),J=1,NUMCEL)
        READ 1035, (N,XCP(N),YCP(N),BULK(N),SHEAR(N),POIS(N),J=1,NUMCEL)
        READ 1040, (N,(ORD(N,M),M=1,2),(DISP(N,M),M=1,2),J=1,NUMCNP)
C
600  IF (NONLIN .EQ. 1) GO TO 640
        DO 620 N=1,NUMELT
            MTYPE=NPN(N,5)
            POIS(N)=GG(MTYPE)
            EMOD=COEF(MTYPE)
            SHEAR(N)=EMOD/(2.0*(1.0+POIS(N)))
620  BULK(N)=SHEAR(N)/(1.0-2.0*POIS(N))
C
640  DO 650 N=1,NZONES
            PHI(N)=PHI(N)/57.29577951
            CONST=2.0/(RF(N)*(1.0-SIN(PHI(N))))

```

ROUTINE LAYOUT

74/176 OPT=0,ROUND= A/ S/ M/-D,-DS

FTN 5.1+577

85/11

```

        DEV1(N)=CONST*CC(N)*COS(PHI(N))
650    DEV2(N)=CONST*SIN(PHI(N))
        IF (NONLIN .EQ. 0) GO TO 740
C
        DO 690 LN=1,NLAY
        IF (LN .EQ. NLAY .AND. NHATER .EQ. 1) GO TO 690
        IF (LN .GT. 1) GO TO 660
        IF (NFEL .GT. 0) GO TO 690
660    NFEL1=NDMEL(LN,1)
670    NFEL2=NDMEL(LN,2)
        DO 680 N=NFEL1,NFEL2
        MTYPE=NPN(N,5)
        HT=HEIGHT(LN)-YCP(N)
        IF (N .GT. NFEL1 .AND. N .LT. NFEL2) GO TO 680
        J=NPN(N,2)
        K=NPN(N,3)
        L=NPN(N,4)
        IF (N .EQ. NFEL1) HT=HT-0.5*(ORD(K,2)-ORD(L,2))
        IF (ORD(K,2) .EQ. ORD(L,2)) GO TO 680
        IF (N .EQ. NFEL2) HT=HT-0.5*(ORD(K,2)-ORD(J,2))
680    STRESS(N,2)=HT*GAM(MTYPE)*0.5
690    CONTINUE
C
        POIS1=GG(1)
        DO 730 N=1,NUMELT
        DO 695 M=1,NUMCEL
        IF (N .EQ. NCEL(M)) GO TO 730
695    CONTINUE
696    MTYPE=NPN(N,5)
        IF (N .LE. NFEL) GO TO 710
700    IF (POIS1 .GT. 0.490) POIS1=0.490
        STRESS(N,1)=STRESS(N,2)*POIS1/(1.0-POIS1)
710    DEVSTR=STRESS(N,2)-STRESS(N,1)
        DEVVFH=DEV1(MTYPE)+DEV2(MTYPE)*STRESS(N,1)
        EI=COEF(MTYPE)*CONS*((STRESS(N,1)/CONS)**EXP(MTYPE))
        EPS=DEVSTR/(EI*(1.0-(DEVSTR/DEVVFH)))
        POIS1=GG(MTYPE)-FF(MTYPE)*ALOG10(STRESS(N,1)/CONS)
        POIST=POIS1/((1.0-DD(MTYPE)*EPS)**2.0)
        IF (POIST .GT. 0.490) POIST=0.490
        IF (N .LE. NFEL) GO TO 720
        IF (ABS(POIS1-POIST) .LT. 0.00001) GO TO 720
        POIS1=POIS1+(POIST-POIS1)/10.0
        GO TO 700
720    POIS(N)=POIST
        STRESS(N,1)=0.0
        STRESS(N,2)=0.0
725    EMOD=EI*((1.0-(CODE(MTYPE)*DEVSTR/DEVVFH)**2.0)
        SHEAR(N)=EMOD/(2.0*(1.0+POIS(N)))
        BULK(N)=SHEAR(N)/(1.0-2.0*POIS(N))
730    CONTINUE
C
740    DO 750 N=1,NUMELT
        EMOD=2.0*SHEAR(N)*(1.0+POIS(N))
750    PRINT 2095, N, XCP(N), YCP(N), EMOD, BULK(N), SHEAR(N), POIS(N),
1      (STRESS(N,M), M=1,3)
        IF (NUMCEL .EQ. 0) GO TO 760
        PRINT 3000

```

ROUTINE LAYOUT

74/176 OPT=0,ROUND= A/ S/ M/-D,-DS

FTN 5.1+577

85/11

```

PRINT 1035, (N,XCP(N),YCP(N),(STRAIN(N,M),M=1,3),N=1,NUMELT)
PRINT 3005
PRINT 1040, (N,(ORD(N,M),M=1,2),(DISP(N,M),M=1,2),N=1,NUMNPT)
760 REWIND 4
WRITE (4) ((STRESS(N,M),M=1,3),N=1,NUMELT)
WRITE (4) ((STRAIN(N,M),M=1,3),N=1,NUMELT)
WRITE (4) ((DISP(N,M),M=1,2),N=1,NUMNPT)
RETURN
C*****
1000 FORMAT (12A6)
1005 FORMAT (18I4)
1010 FORMAT (7F10.0)
1015 FORMAT (I4,6F10.4)
1016 FORMAT (6F10.4)
1020 FORMAT (I4,4F10.4)
1021 FORMAT (4F10.4)
1025 FORMAT (I4,2F8.2)
1030 FORMAT (4I4,F8.2)
1035 FORMAT (I10,5F10.3)
1040 FORMAT (I10,4F10.4)
2000 FORMAT (1H6 /// 12A6)
2005 FORMAT(21H-TOTAL NO. ELEMENTS =,I4 / 21H TOTAL NO. NODES =,I4 /
1 21H FOUNDATION ELEMENTS=,I4 / 21H FOUNDATION NODES =,I4 /
2 21H COFFERDAM ELEMENTS =,I4 / 21H COFFERDAM NODES =,I4 )
2010 FORMAT (27H:NO. RESTRAINED NODES =,I4 /
1 27H NO. DIFFERENT MATERIALS =,I4 /
2 27H NO. CONSTRUCTION LAYERS =,I4 /
3 27H NO. ITERATIONS PER LAYER =,I4 //
4 49H NONLINEAR CODE (0=LINEAR, 1=NONLINEAR)-----,I4 /
5 49H CODE FOR PRESENCE OF WATER FORCES (0=NO,1=YES)---,I4 /
6 49H CODE FOR PUNCHING FINAL STRESSES (0=NO,1=YES)---,I4 )
2015 FORMAT (32HGEARTH PRESSURE COEF. IN FNDN. =,F6.3 /
1 32H MODULUS REDUCTION FACTOR =,F9.6 //)
2020 FORMAT (23H0EMBANKMENT COORDINATES / 5X,9H TOE LEFT,10X,
1 11H CREST LEFT,9X,11H CENTERLINE,9X,12H CREST RIGHT,9X,
2 10H TOE RIGHT / 5X,1HX,9X,1HY,9X,1HX,9X,1HY,9X,1HX,9X,1HY,
3 9X,1HX,9X,1HY,9X,1HX,9X,1HY / 10F10.3 //)
2021 FORMAT (31H FOUNDATION ASSUMED TO BE RIGID //)
2022 FORMAT (23H FOUNDATION COORDINATES / 7X,5H LEFT,15X,6H RIGHT /
1 5X,1HX,9X,1HY,9X,1HX,9X,1HY / 4F10.3 //)
2025 FORMAT (23H-MATERIAL PROPERTY DATA///17H UNITS CONSTANT =,F8.4
//)
2030 FORMAT (21X,8H MODULUS,13X,14H POISSON RATIO /
1 39H MATL UNIT WT CONSTANT EXPONENT D,9X,1HG,9X,1HF//)
2035 FORMAT (48H-MATL C PHI FAIL.RATIO NONLIN(1=YES) //)
2040 FORMAT (19H1 NODAL POINT ARRAY //
1 44H NP X-ORD Y-ORD X-ORD/W Y-ORD/H //)
2045 FORMAT (39H1 NODAL POINTS WITH GEOMETRIC RESTRAINTS //)
2050 FORMAT (12H NODAL POINT, I4 ,13H CAN NOT-MOVE)
2055 FORMAT (12H NODAL POINT, I4 ,33H CAN MOVE ONLY IN THE Y-DIRECTION)
2060 FORMAT (12H NODAL POINT, I4 ,33H CAN MOVE ONLY IN THE X-DIRECTION)
2065 FORMAT (50H1 ELEMENT ARRAY + PT. WHERE STRESSES ARE EVALUATED ///
1 50H ELE I J K L MATL X-ORD Y-ORD ,
2 20H X-ORD/W Y-ORD/H //)
2070 FORMAT (6I5,4F10.3)
2075 FORMAT (32H1 CONSTRUCTION LAYER INFORMATION // 6H LAYER,
1 48H INCLUSIVE ELEMENTS INCLUSIVE NODES ELEVATION //)

```

ROUTINE LAYOUT

74/176 OPT=0,ROUND= A/ S/ M/-D,-DS

FTN 5.1+577

85/11

```

2080 FORMAT (I5,I10,I7;I12,I6,F14.3)
2082 FORMAT (19H-COFFERDAM ELEMENTS //)
2083 FORMAT (23H-COFFERDAM NODAL POINTS //)
2085 FORMAT (20H1 NODAL POINT FORCES//20H NP X-FORCE Y-FORCE //)
2090 FORMAT (28H1 INITIAL VALUES IN ELEMENTS //)
      1 45H ELE X-ORD Y-ORD ELAS MOD BULK MOD,
      2 50H SHEAR MOD POISSON SIG-X SIG-Y TAU-XY //)
2095 FORMAT (I5,2F10.3,3F10.1,4F10.3)
3000 FORMAT (35H1 INITIAL COFFERDAM ELEMENT STRAINS // 10H ELE,
      1 50H X-ORD Y-ORD EPS-X EPS-Y GAM-XY //)
3005 FORMAT (45H1 INITIAL COFFERDAM NODAL POINT DISPLACEMENTS //)
      1 50H N.P. X-ORD Y-ORD X-DISP Y-DISP //)
5000 FORMAT (17H N.P. ERROR , N = ,I4)
5005 FORMAT (32H BAND WIDTH TOO LARGE AT ELEMENT ,I4)
C*****
999 STOP
END

```

ROUTINE LSSTIF 74/176 OPT=0,ROUND= A/ S/ M/-D,-DS FTN 5.1+577 85/11
 -LONG/-OT,ARG=-COMMON/-FIXED,CS= USER/-FIXED,DB=-TB/-SB/-SL/ ER/-IO/-PMD/-ST,PL=500
 5,I=LSB,L=ER.

```

SUBROUTINE LSSTIF
C*****
COMMON /INIT/ HED(12),NUMELT,NUMNPT,NFEL,NFNP,NPUNCH
COMMON /NPEL/ NPN(275,5),DRD(300,2),XCP(275),YCP(275)
COMMON /CDAM/ NUMCEL,NUMCNP,NCEL(100),NCNP(100)
COMMON /NPBC/ NUMBC,NBC(100),NFX(100),NHWATER,FX(300),FY(300)
COMMON /BANS/ MBAND,NUMBLK,B(160),A(160,80)
COMMON /LIFT/ NLAY,LN,NOMEL(25,2),NOMNP(25,2),HEIGHT(25),NUMIT,IT
COMMON /MAT1/ NONLIN,BULK(275),SHEAR(275),POIS(275),GAM(10),REDMOD
COMMON /LST1/ I,J,K,S(10,10),ST(3,10),C(3,3),P(10),NP(4),VOL
C*****
C INITIALIZE BLOCK CONSTANTS AND STIFFNESS ARRAY
C*****
REWIND 2
NB=40
ND=2*NB
ND2=2*ND
NUMBLK=0

C
DO 210 N=1,ND2
B(N)=0.0
DO 210 M=1,MBAND
210 A(N,M)=0.0
C*****
C FORM STIFFNESS MATRIX IN BLOCKS
C*****
300 NUMBLK=NUMBLK+1
NH=NB*(NUMBLK+1)
NM=NH-NB
NNL=NH-NB+1
KSHIFT=2*NNL-2

C
NUMEL=NUMEL(LN,2)
IF (NUMCEL .NE. 0) NUMEL=MAX0(NUMEL(LN,2),NCEL(NUMCEL))
DO 540 N=1,NUMEL
KMIN=MIN0(NPN(N,1),NPN(N,2),NPN(N,3),NPN(N,4))
IF (KMIN .LT. NNL .OR. KMIN .GT. NM) GO TO 540
CALL LSQUAD(N)
C*****
C 1. ADD ELEMENT STIFFNESS TO TOTAL STIFFNESS
C*****
DO 440 I=1,4
DO 440 K=1,2
II=2*NPN(N,I)-2+K-KSHIFT
KK=2*I-2+K
B(II)=B(II)+P(KK)
DO 440 J=1,4
DO 440 L=1,2
JJ=2*NPN(N,J)-2+L-II+1-KSHIFT
LL=2*J-2+L
IF (JJ .LE. 0) GO TO 430
IF (ND .GE. JJ) GO TO 420
PRINT 1000, MBAND,N
CALL EXIT
420 A(II,JJ)=A(II,JJ)+S(KK,LL)

```


ROUTINE LSSTIF 74/176 OPT=0,ROUND= A/ S/ M/-D,-DS FTN 5.1+577 85/11

```

430 CONTINUE
440 CONTINUE
540 CONTINUE
C*****
C      2. ADD CONCENTRATED FORCES WITHIN EACH BLOCK (IF PRESENT)
C*****
      IF (LN .NE. NLAY .OR. NWATER .EQ. 0) GO TO 600
      DD 500 N=NNL,NM
      K=2*N-KSHIFT
      B(K)=B(K)+FY(N)
500 B(K-1)=B(K-1)+FX(N)
C*****
C      3. MODIFY STIFFNESS EQUATIONS FOR BOUNDARY CONSTRAINTS
C*****
600 NUMNP=NOMNP(LN,2)
      IF (NUMCNP .NE. 0) NUMNP=MAXD(NOMNP(LN,2),NCNP(NUMCNP))
      DD 650 M=1,NUMBC
      IF (NBC(M) .LT.>NNL) GO TO 650
      IF (NBC(M) .GT. NH .OR. NBC(M) .GT. NUMNP) GO TO 700
      N=2*NBC(M)-1-KSHIFT
      IF (NFIX(M) .EQ. 0 .OR. NFIX(M) .EQ. 1) GO TO 620
610 IF (NFIX(M) .EQ. 0 .OR. NFIX(K) .EQ. 2) N=N+1
620 DD 640 MM=2,MBAND
      KK=N-MM+1
      IF (KK .LE. 0) GO TO 630
      A(KK,MM)=0.0
630 KK=N+MM-1
      IF (ND2 .LT. KK) GO TO 640
      A(N,MM)=0.0
640 CONTINUE
      A(N,1)=1.0
      B(N)=0.0
650 CONTINUE
C*****
C      4. WRITE BLOCK ON TAPE,MOVE UP LOWER BLOCK,CHECK FOR LAST BLOCK
C*****
700 WRITE (2) (B(N),(A(N,M),M=1,MBAND),N=1,ND)
      DD 710 N=1,ND
      K=N+ND
      B(N)=B(K)
      B(K)=0.0
      DD 710 M=1,MBAND
      A(N,M)=A(K,M)
710 A(K,M)=0.0
      IF (NM .LT. NUMNP) GO TO 300
      RETURN
C*****
1000 FORMAT (13H BAND WIDTH = ,I4,20H EXCEEDED AT ELEMENT ,I4)
C*****
      END

```

ROUTINE LSQUAD 74/176 OPT=0,ROUND= A/ S/ M/-D,-DS FTN 5.1+577 85/11
 -LONG/-OT,ARG=-COMMON/-FIXED,CS= USER/-FIXED,DB=-TB/-SB/-SL/ ER/-ID/-PMD/-ST,PL=500
 5,I=LSB,L=ER.

```

SUBROUTINE LSQUAD(N)
C*****
COMMON /INIT/ HED(12),NUMELT,NUMNPT,NFEL,NFNP,NPUNCH
COMMON /NPEL/ NPN(275,5),ORD(300,2),XCP(275),YCP(275)
COMMON /CDAM/ NUMCEL,NUMCNP,NCEL(100),NCNP(100)
COMMON /LIFT/ NLAY,LN,NOMEL(25,2),NOMNP(25,2),HEIGHT(25),NUMIT,IT
COMMON /MAT1/ NONLIN,BULK(275),SHEAR(275),POIS(275),GAM(10),REDMOD
COMMON /LST1/ I,J,K,S(10,10),ST(3,10),C(3,3),P(10),NP(4),VOL
DATA C(1,3),C(2,3),C(3,1),C(3,2)/0.,0.,0.,0./
C*****
C INITIALIZE AND FORM STRESS-STRAIN MATRIX
C*****
DO 100 II=1,10
P(II)=0.0
DO 100 JJ=1,10
100 S(II,JJ)=0.0
VOL=0.0
IF (N.LE. NOMEL(LN,2) .OR. NUMCEL .EQ. 0) GO TO 130
DO 120 M=1,NUMCEL
IF (N.EQ. NCEL(M)) GO TO 130
120 CONTINUE
RETURN
130 FMODET=1.0
IF (NLAY .EQ. 1 .OR. NOMEL(LN,2) .EQ. NFEL) GO TO 150
150 MTYPE=NPN(N,5)
C(1,1)=FMODET*(BULK(N)+SHEAR(N))
C(1,2)=FMODET*(BULK(N)-SHEAR(N))
C(2,1)=C(1,2)
C(2,2)=C(1,1)
C(3,3)=FMODET*SHEAR(N)
C*****
C FORM 10*10 QUAD. STIFFNESS, REDUCE TO 8*8, CALCULATE GRAVITY LOADS
C*****
I=NPN(N,1)
J=NPN(N,2)
K=NPN(N,4)
CALL LST8(1,3,7)
I=NPN(N,3)
J=NPN(N,4)
K=NPN(N,2)
CALL LST8(5,7,3)
IF (VOL .GT. 0.0) GO TO 200
PRINT 1000, N
CALL EXIT
200 DO 300 K=1,2
IH=10-K
ID=IH+1
DO 300 I=1,IH
S(ID,I)=S(ID,I)/S(ID,ID)
DO 300 J=1,IH
300 S(J,I)=S(J,I)-S(J,ID)*S(ID,I)
IF (N.LT. NOMEL(LN,1) .OR. N.GT. NOMEL(LN,2)) RETURN
IF (N.LE. NFEL) RETURN
DO 400 I=1,4
400 P(2*I)=P(2*I)-GAM(MTYPE)*VOL/4.0

```

ROUTINE LSQUAD 74/176 OPT=0,ROUND= A/ S/ H/-D,-DS FTN 5.1+577 85/11

RETURN
C*****
1000 FORMAT (34H ZERO OR NEGATIVE AREA AT ELEMENT ,I4)
C*****
END

ROUTINE LST8 74/176 OPT=0,ROUND= A/ S/ M/-D,-DS FTN 5.1+577 85/11
 -LONG/-DT,ARG=-COMMON/-FIXED,CS= USER/-FIXED,DB=-TB/-SB/-SL/ ER/-ID/-PHD/-ST,PL=500
 15,I=LSB,L=ER.

```

SUBROUTINE LST8(N1,N2,N3)
C*****
COMMON /NPCL/ NPN(275,5),ORD(300,2),XCP(275),YCP(275)
COMMON /LST1/ I,J,K,S(10,10),ST(3,10),C(3,3),P(10),NP(4),VOL
DIMENSION BA(3,2),U(3,4),V(3,4),UV(3,4,2)
EQUIVALENCE (UV(1,1,1),U(1,1)),(UV(1,1,2),V(1,1))
C*****
C DEFINE TRIANGULAR ELEMENT NODAL POINTS, GEOMETRY, AND AREA
C*****
NP(1)=N1
NP(2)=N2
NP(3)=N3
NP(4)=9
BA(1,1)=ORD(J,2)-ORD(K,2)
BA(2,1)=ORD(K,2)-ORD(I,2)
BA(3,1)=ORD(I,2)-ORD(J,2)
BA(1,2)=ORD(K,1)-ORD(J,1)
BA(2,2)=ORD(I,1)-ORD(K,1)
BA(3,2)=ORD(J,1)-ORD(I,1)
AREA=(ORD(J,1)*BA(2,1)+ORD(I,1)*BA(1,1)+ORD(K,1)*BA(3,1))/2.0
IF (AREA .LE. 0.0) GO TO 400
VOL=VOL+AREA
C*****
C SET UP TERMS FOR STRESS-STRAIN AND STRAIN-DISPLACEMENT MATRICES
C*****
AREA48=48.0*AREA
C11=C(1,1)/AREA48
C12=C(1,2)/AREA48
C13=C(1,3)/AREA48
C22=C(2,2)/AREA48
C23=C(2,3)/AREA48
C33=C(3,3)/AREA48
C
DO 200 M=1,2
UV(1,1,M)= BA(1,M)
UV(2,1,M)= BA(1,M)
UV(3,1,M)= BA(1,M)
UV(1,2,M)= BA(2,M)
UV(2,2,M)= BA(2,M)-2.0*BA(3,M)
UV(3,2,M)=-BA(2,M)
UV(1,3,M)= BA(3,M)
UV(2,3,M)=-BA(3,M)
UV(3,3,M)= BA(3,M)-2.0*BA(2,M)
UV(1,4,M)= 0.0
UV(2,4,M)= BA(3,M)*4.0
200 UV(3,4,M)= BA(2,M)*4.0
C*****
C DEVELOP CENTER N.P. STRAIN-DISP. MATRIX AND TRIANGLE STIFFNESS
C*****
AREA8=8.0*AREA
DO 300 I=1,4
II=NP(I)
C
ST(1,II) =ST(1,II) +((U(2,I)+U(3,I))/AREA8)
ST(2,II+1)=ST(2,II+1)+((V(2,I)+V(3,I))/AREA8)

```

ROUTINE LST8

74/176 DPT=0,ROUND= A/ S/ M/-D,-DS

FTN 5.1+577

85/11

```

      ST(3,II) =ST(3,II) +((V(2,I)+V(3,I))/AREA8)
      ST(3,II+1)=ST(3,II+1)+((U(2,I)+U(3,I))/AREA8)
C
      SUMU=U(1,I)+U(2,I)+U(3,I)
      SUM1=SUMU+U(1,I)
      SUM2=SUMU+U(2,I)
      SUM3=SUMU+U(3,I)
      SUMV=V(1,I)+V(2,I)+V(3,I)
      SVM1=SUMV+V(1,I)
      SVM2=SUMV+V(2,I)
      SVM3=SUMV+V(3,I)
C
      DO 300 J=1,4
      JJ=NP(J)
      UQU=U(1,J)*SUM1 + U(2,J)*SUM2 + U(3,J)*SUM3
      VQU=V(1,J)*SUM1 + V(2,J)*SUM2 + V(3,J)*SUM3
      VQV=V(1,J)*SVM1 + V(2,J)*SVM2 + V(3,J)*SVM3
      UQV=U(1,J)*SVM1 + U(2,J)*SVM2 + U(3,J)*SVM3
C
      S(II ,JJ )=S(II ,JJ ) + C11*UQU + C13*(VQU+UQV) + C33*VQV
      S(II+1,JJ+1)=S(II+1,JJ+1) + C22*VQV + C23*(VQU+UQV) + C33*UQU
      S(II ,JJ+1)=S(II ,JJ+1) + C23*VQV + C13*UQU + C12*VQU + C33*UQV
300 S(JJ+1,II )=S(II ,JJ+1)
C*****
400 RETURN
      END

```

ROUTINE BANSOL 74/176 OPT=0,ROUND= A/ S/ M/-D,-DS FTN 5.1+577 85/11
 -LONG/-OT,ARG=-COMMON/-FIXED,CS= USER/-FIXED,DB=-TB/-SB/-SL/ ER/-ID/-PHD/-ST,PL=500
 15,I=LSB,L=ER.

```

SUBROUTINE BANSOL
C*****
COMMON /BANS/ MBAND,NUMBLK,B(160),A(160,80)
C*****
C INITIALIZE
C*****
NN=80
NL=NN+1
NH=NN+NN
REWIND 1
REWIND 2
NB=0
GO TO 120
C*****
C 1. SHIFT BLOCK OF EQUATIONS AND READ NEXT BLOCK INTO CORE
C*****
100 NB=NB+1
DO 110 N=1,NN
NM=NN+N
B(N)=B(NM)
B(NM)=0.0
DO 110 M=1,MBAND
A(N,M)=A(NM,M)
110 A(NM,M)=0.0
C
IF (NUMBLK .EQ. NB) GO TO 200
120 READ (2) (B(N),(A(N,M),M=1,MBAND),N=NL,NH)
IF (NB .EQ. 0) GO TO 100
C*****
C 2. REDUCE BLOCK OF EQUATIONS , THEN WRITE THEM ON TAPE 1
C*****
200 DO 230 N=1,NN
IF (A(N,1) .EQ. 0.0) GO TO 230
B(N)=B(N)/A(N,1)
DO 220 L=2,MBAND
C=A(N,L)/A(N,1)
I=N+L-1
J=0
DO 210 K=L,MBAND
J=J+1
210 A(I,J)=A(I,J)-C*A(N,K)
B(I)=B(I)-A(N,L)*B(N)
A(N,L)=C
220 CONTINUE
230 CONTINUE
C
IF (NUMBLK .EQ. NB) GO TO 300
WRITE (1) (B(N),(A(N,M),M=2,MBAND),N=1,NN)
GO TO 100
C*****
C BACK-SUBSTITUTION
C*****
300 DO 310 M=1,NN
N=NN+1-M
DO 310 K=2,MBAND

```

ROUTINE BANSOL

74/176 OPT=0,ROUND= A/ S/ M/-D,-DS

FTN 5.1+577

85/11

```

L=N+K-1
310 B(N)=B(N)-A(N,K)*B(L)
    NM=N+NN
    B(NM)=B(N)
320 A(NM,NB)=B(N)
    NB=NB-1
    IF (NB .EQ. 0) GO TO 400
    BACKSPACE 1
    READ (1) (B(N), (A(N,M), M=2, MBAND), N=1, NN)
    BACKSPACE 1
    GO TO 300
C*****
C   ORDER UNKNOWNS IN B ARRAY
C*****
400 K=0
    DO 410 NB=1, NUMBLK
    DO 410 N=1, NN
    NM=N+NN
    K=K+1
410 B(K)=A(NM, NB)
    RETURN
C*****
END

```

ROUTINE LSRESUL 74/176 OPT=0,ROUND= A/ S/ M/-D,-DS FTN 5.1+577 85/11
 -LONG/-OT,ARG=-COMMON/-FIXED,CS= USER/-FIXED,DB=-TB/-SB/-SL/ ER/-ID/-PHD/-ST,PL=500
 15,I=LSB,L=ER.

```

SUBROUTINE LSRESUL
C*****
COMMON /INIT/ HED(12),NUMELT,NUMNPT,NFEL,NFNP,NPUNCH
COMMON /NPEL/ NPN(275,5),ORD(300,2),XCP(275),YCP(275)
COMMON /CDAM/ NUMCEL,NUMCNP,NCEL(100),NCNP(100)
COMMON /BANS/ MBAND,NUMBLK,B(160),A(160,80)
COMMON /LIFT/ NLAY,LN,NOMEL(25,2),NOMNP(25,2),HEIGHT(25),NUMIT,IT
COMMON /GEOM/ FNL(2),TL(2),CRL(2),CTR(2),CRR(2),TR(2),FNR(2)
COMMON /MAT1/ NONLIN,BULK(275),SHEAR(275),POIS(275),GAM(10),REDMOD
COMMON /MAT2/ CONS,COEF(10),EXP(10),DD(10),GG(10),FF(10),NZONES
COMMON /MAT3/ CC(10),PHI(10),RF(10),DEV1(10),DEV2(10),CODE(10),AKO
COMMON /LST1/ I,J,K,S(10,10),ST(3,10),C(3,3),P(10),NP(4),VOL
DIMENSION
  SIG(3),EPS(3),Q(5),QQ(4)
DIMENSION
  SIGIT(275,3),EPSIT(275,3),DISPIT(300,2)
DIMENSION
  STRESS(275,3),STRAIN(275,3),DISP(300,2)
EQUIVALENCE
  (STRESS(1,1),A(80,13)),(STRAIN(1,1),A(160,25)),
  1 (DISP(1,1),A(80,38))
C*****
C INITIALIZE
C*****
REWIND 4
READ (4) ((STRESS(N,M),M=1,3),N=1,NUMELT)
READ (4) ((STRAIN(N,M),M=1,3),N=1,NUMELT)
READ (4) ((DISP(N,M),M=1,2),N=1,NUMNPT)
IF (IT .GT. 1) GO TO 300
DO 100 N=1,NUMELT
DO 100 M=1,3
SIGIT(N,M)=0.0
EPSIT(N,M)=0.0
100 SIGIT(N,M)=STRESS(N,M)
EPSIT(N,M)=STRAIN(N,M)
DO 200 N=1,NUMNPT
DO 200 M=1,2
DISPIT(N,M)=0.0
200 DISPIT(N,M)=DISP(N,M)
C
CTRF=TL(2)+((TR(2)-TL(2))*(CTR(1)-TL(1))/(TR(1)-TL(1)))
EMBHT=CTR(2)-CTRF
SLL=(CRL(2)-TL(2))/(CRL(1)-TL(1))
SLR=(CRR(2)-TR(2))/(TR(1)-CRR(1))
IF (FNL(1) .EQ. TL(1) .AND. FNR(1) .EQ. TR(1)) GO TO 250
GAMF=GAM(1)
GAMD=GAM(2)
EMOD=COEF(2)
GO TO 280
250 GAMF=0.0
GAMD=GAM(1)
EMOD=COEF(1)
280 DIMEN=EMOD/(GAMD*EMBHT*EMBHT)
C*****
C CALCULATE THE DISPLACEMENTS, CORRECTING THOSE IN THE NEW LAYER
C*****
300 NUMNP=NOMNP(LN,2)
IF (NUMCNP .NE. 0) NUMNP=MAX0(NOMNP(LN,2),NCNP(NUMCNP))
DO 340 N=1,NUMNP

```


ROUTINE LSRESUL 74/176 OPT=0,ROUND= A/ S/ M/-D,-DS FTN 5.1+577 85/11

```

      IF (IT .LT. NUMIT) GO TO 310
      XN=N
      XXN=N/50
      IF (XXN .EQ. (XN/50.0) .OR. N .EQ. 1) PRINT 1000
310  FMODET=1.1
      IF (NLAY .EQ. 1 .OR. NOMNP(LN,2) .EQ. NFNP) GO TO 315
      IF (N .GE. NOMNP(LN,1) .AND. N .LE. NOMNP(LN,2)) FMODET=REDMOD
315  DX=B(2*N-1)*FMODET
      DY=B(2*N)*FMODET
      IF (NLAY .EQ. 1 .OR. N .LE. NFNP) GO TO 330
      IF (NUMCNP .EQ. 0) GO TO 325
      DO 320 M=1,NUMCNP
      IF (N .EQ. NCNP(M)) GO TO 330
320  CONTINUE
325  DX=0.0
      DY=0.0
330  DISP(N,1)=DISP(N,1)+DX
      DISP(N,2)=DISP(N,2)+DY
      IF (IT .EQ. NUMIT) DISP(N,1)=DISPIT(N,1)+DX
      IF (IT .EQ. NUMIT) DISP(N,2)=DISPIT(N,2)+DY
      TD=SQRT(DISP(N,1)**2+DISP(N,2)**2)
      IF (IT .LT. NUMIT) GO TO 340
      IF (ORD(N,1) .LE. CTR(1)) DIX=100.0*DISP(N,1)/(CTR(1)-TL(1))
      IF (ORD(N,1) .GT. CTR(1)) DIX=100.0*DISP(N,1)/(TR(1)-CTR(1))
      DIY=100.0*DISP(N,2)/EMBHT
      DJX=DISP(N,1)*DIMEN
      DJY=DISP(N,2)*DIMEN
      PRINT 1005, N,DX,DY,(DISP(N,M),M=1,2),TD,DIX,DIY,DJX,DJY,N
340  CONTINUE
C*****
C  CALCULATE THE STRESSES AND STRAINS, PRINT STRAINS
C*****
      AREATT=AREATE=AREATN=0.0
      NUMEL=NOMEL(LN,2)
      DO 450 N=1,NUMEL
      IF (IT .LT. NUMIT) GO TO 390
      YN=N
      YYN=N/50
      IF (YYN .EQ. (YN/50.0) .OR. N .EQ. 1) PRINT 1010
390  NTYPE=NP(N,5)
      FMODET=1.0
      IF (NLAY .EQ. 1 .OR. NOMEL(LN,2) .EQ. NFEL) GO TO 395
      IF (N .GE. NOMEL(LN,1) .AND. N .LE. NOMEL(LN,2)) FMODET=REDMOD
395  DO 400 I=1,3
      SIG(I)=0.0
      EPS(I)=0.0
      DO 400 J=1,10
400  ST(I,J)=0.0
C
      CALL LSQUAD(N)
C
      AREATT=AREATT+VOL
      EMOD=2.0*BULK(N)*(1.0+POIS(N))*(1.0-2.0*POIS(N))
      AREATE=AREATE+VOL*EMOD
      AREATN=AREATN+VOL*POIS(N)
      DO 410 I=1,4
      II=2*I

```

ROUTINE LSRESUL 74/176 OPT=0,ROUND= A/ S/ M/-D,-DS FTN 5.1+577 85/11

```

      JJ=2*NPN(N,I)
      P(II-1)=B(JJ-1)
410  P(II)=B(JJ)
      DO 420 I=9,10
      P(I)=0.0
      KK=I-1
      DO 420 K=1, KK
420  P(I)=P(I)-S(I,K)*P(K)
C
      DO 430 I=1,3
      DO 430 K=1,10
430  EPS(I)=EPS(I)+ST(I,K)*P(K)
      DO 440 I=1,3
      DO 440 K=1,3
440  SIG(I)=SIG(I)+C(I,K)*EPS(K)
      IF (NLAY .EQ. 1 .OR. NOHEL(LN,2) .EQ. NFEL) GO TO 442
      IF (N .LT. NOHEL(LN,1) .OR. N .GT. NOHEL(LN,2)) GO TO 442
      DO 441 I=1,3
      NUMREF=NOHEL(LN,1)+1
      FLHT=HEIGHT(LN)-YCP(NUMREF)
      SIG(2)=- (ELHT*GAH(MTYPE))
      SIG(1)=SIG(2)*POIS(N)/(1.0-POIS(N))
441  SIG(3)=0.0
442  DO 445 I=1,3
      IF (FMODET .EQ. REDMOD) EPS(I)=0.0
      IF (IT .LT. NUMIT) STRESS(N,I)=STRESS(N,I)-SIG(I)*0.5
      IF (IT .EQ. NUMIT) STRESS(N,I)=SIGIT(N,I)-SIG(I)
      IF (IT .LT. NUMIT) STRAIN(N,I)=STRAIN(N,I)-EPS(I)*100.0*FMODET
      IF (IT .EQ. NUMIT) STRAIN(N,I)=EPSIT(N,I)-EPS(I)*100.0*FMODET
445  CONTINUE
C
      E=(STRAIN(N,2)+STRAIN(N,1))/2.0
      F=(STRAIN(N,2)-STRAIN(N,1))/2.0
      G=SQRT((STRAIN(N,3)/2.0)**2+F**2)
      QQ(1)=E+G
      QQ(2)=E-G
      QQ(3)=2.0*G
      IF (IT .LT. NUMIT) GO TO 450
      PRINT 1015, N, EKOD, BULK(N), SHEAR(N), POIS(N), (STRAIN(N,M), M=1,3),
1      (QQ(L), L=1,3), N
450  CONTINUE
      EKODAV=AREATE/AREATT
      POISAV=AREATN/AREATT
      IF (IT .EQ. NUMIT) PRINT 1020, EKODAV, POISAV
C*****
C  CALCULATE PRINCIPAL STRESSES AND PRINT, CALCULATE NEW E AND NU
C*****
      DO 470 N=1, NUMEL
      IF (IT .LT. NUMIT) GO TO 455
      ZN=N
      ZZN=N/50
      IF (ZZN .EQ. (ZN/50.0) .OR. N .EQ. 1) PRINT 1025
455  CCCC=(STRESS(N,2)+STRESS(N,1))/2.0
      D=(STRESS(N,2)-STRESS(N,1))/2.0
      Q(3)=SQRT(STRESS(N,3)**2 + D**2)
      Q(1)=CCCC+Q(3)
      Q(2)=CCCC-Q(3)

```

ROUTINE LSRESUL 74/176 OPT=0,ROUND= A/ S/ K/-D,-DS FTN 5.1+577 85/11

```

Q(4)=0.0
IF (STRESS(N,3) .EQ. 0.0 .AND. D .EQ. 0.0) GO TO 456
Q(4)=90.0/3.14159265*ATAN2(-STRESS(N,3),D)
456 MTYPE=NPN(N,5)
DEVSTR=Q(1)-Q(2)
DEVFH=DEV1(MTYPE)+DEV2(MTYPE)*Q(2)
IF (DEVFH .GT. 0.0) GO TO 457
STRLFV=DEVLEV=0.0
GO TO 458
457 DEVLEV=DEVSTR/DEVFH
STRLEV=DEVLEV/RF(MTYPE)
C
458 IF (IT .LT. NUMIT) GO TO 463
IF (Q(2) .EQ. 0.0) Q(5)=999.999
IF (Q(2) .NE. 0.0) Q(5)=Q(1)/Q(2)
YHT=GHF=0.0
IF (YCP(N) .GE. FNL(2)) YHT=YCP(N)-TL(2)
IF (YCP(N) .LT. FNL(2)) GHF=GAMF*(TL(2)-YCP(N))
IF (XCP(N) .GT. TL(1)) GH=GHF+GAMD*((XCP(N)-TL(1))*SLL-YHT)
IF (XCP(N) .GT. CRL(1)) GH=GHF+GAMD*(CTR(2)-TL(2)-YHT)
IF (XCP(N) .GT. CRR(1)) GH=GHF+GAMD*((TR(1)-XCP(N))*SLR-YHT)
IF (XCP(N) .GT. TR(1)) GH=GHF
G1=Q(1)/GH
G2=Q(2)/GH
G3=Q(3)/GH
PRINT 1030, N,(STRESS(N,M),M=1,3),(Q(L),L=1,5),STRLEV,G1,G2,G3,N
C
463 IF (N .LE. NOHEL(LN,2) .OR. NUMCEL .EQ. 0) GO TO 460
DD 459 M=1,NUMCEL
IF (N .EQ. NCEL(M)) GO TO 460
459 CONTINUE
GO TO 470
460 IF (NONLIN .EQ. 0) GO TO 470
IF (Q(2) .LE. 0.0) GO TO 462
461 IF (STRLEV .LT. 1.0 .AND. SHEAR(N) .GT. 0.0) GO TO 465
462 SHEAR(N)=0.0
GO TO 470
465 EINIT=CONS*COEF(MTYPE)*((Q(2)/CONS)**EXP(MTYPE))
EMOD=EINIT*((1.0-DEVLEV*CODE(MTYPE))**2.0)
POISI=GG(MTYPE)-FF(MTYPE)*ALOG10(Q(2)/CONS)
EPSAX=DEVSTR/(EINIT*(1.0-DEVLEV))
POIS(N)=POISI/((1.0-DD(MTYPE)*EPSAX)**2.0)
IF (POIS(N) .GT. 0.490) POIS(N)=0.490
SHEAR(N)=EMOD/(2.0*(1.0+POIS(N)))
BULK(N)=SHEAR(N)/(1.0-2.0*POIS(N))
470 CONTINUE
C*****
IF (IT .LT. NUMIT) GO TO 600
NFEL=NOHEL(LN,2)
NFNP=NOXNP(LN,2)
600 REWIND 4
WRITE (4) ((STRESS(N,M),M=1,3),N=1,NUMELT)
WRITE (4) ((STRAIN(N,M),M=1,3),N=1,NUMELT)
WRITE (4) ((DISP(N,M),M=1,2),N=1,NUMNPT)
IF (LN .NE. NLAY .OR. IT .NE. NUMIT .OR. NPUNCH .NE. 1) RETURN
WRITE (7,1035) (N,XCP(N),YCP(N),(STRESS(N,K),M=1,3),N=1,NUMELT)
WRITE (7,1035) (N,XCP(N),YCP(N),(STRAIN(N,M),M=1,3),N=1,NUMELT)

```

ROUTINE LSRESUL 74/176 OPT=0,ROUND= A/ S/ K/-D,-DS FTN 5.1+577 85/11

```

WRITE(8,1035)(N,XCP(N),YCP(N),BULK(N),SHEAR(N),POIS(N),N=1,NUMELT)
WRITE(8,1040)(N,(ORD(N,M),M=1,2),(DISP(N,M),M=1,2),N=1,NUMNPT)
RETURN
C*****
1000 FORMAT (54H1 NP DELTA-X DELTA-Y X-DISP Y-DISP TOTAL,
1 48H X-DISP/W Y-DISP/H XDIMEN YDIMEN NP /)
1005 FORMAT (I4,7F10.4,2F12.8,I4)
1010 FORMAT (50H1ELE ELAS MOD BULK MOD SHEAR MOD NU EPS-X ,
1 42H EPS-Y GAM-XY EPS-1 EPS-3 GAMMAX ELE /)
1015 FORMAT (I4,3F10.1,F6.3,6F8.3,I4)
1020 FORMAT (4H AVG,F10.1,20X,F6.3)
1025 FORMAT (54H1ELE SIG-X SIG-Y TAU-XY SIG-1 SIG-3,
1 50H TAU-MAX THETA SIG1/3 LEVEL SIG1/GH SIG3/GH,
2 12H TAUW/GH ELE /)
1030 FORMAT (I4,6F10.3,6F8.3,I4)
1035 FORMAT (I10,5F10.3)
1040 FORMAT (I10,4F10.4)
C*****
END

```